SLU

Climate impacts due to albedo change in LCA of agricultural systems

Petra Sieber

Climate impacts due to albedo change in LCA of agricultural systems

Petra Sieber

Faculty of Natural Resources and Agricultural Sciences
Department of Energy and Technology
Uppsala

Acta Universitatis Agriculturae Sueciae
2021:87

Climate impacts due to albedo change in LCA of agricultural systems

Abstract

Agricultural systems for production of food, energy and materials are a major driver of climate change, due to land use and greenhouse gas (GHG) emissions along the supply chain. Crop cultivation also affects the climate by changing land surface albedo, *i.e.* the fraction of solar radiation reflected back from the ground. Increased albedo could counteract the radiative forcing and warming effect of emitted GHGs.

This thesis examined how individual crops and cultivation practices in Sweden influence albedo, and thus the climate. Field measurements and satellite data were used to analyse differences between crops, management practices and environmental conditions. Methods for assessing climate impacts due to albedo change and for comparing these impacts with those of GHGs were developed. Time-dependent life cycle assessment (LCA) was performed to obtain a perspective on the importance of albedo change for the climate impact of crop and bioenergy production, relative to life-cycle GHG emissions and carbon sequestration.

The results showed higher albedo for soil kept covered year-round, *e.g.* by perennial crops or winter varieties and by straw left in the field, combined with delayed or reduced tillage. In case studies, albedo increased by 31% under willow and 6-11% under different food or feed crops relative to unused land. This albedo increase countered the effect of GHG emissions from manufacture of inputs and fuel consumption, by 20-60% when measured as GWP_{100} and by 60-200% as GWP_{20}. Impacts assessed as global mean temperature change (ΔT) over time were dominated by albedo-induced cooling on short time scales and by the effects of emitted GHGs and carbon sequestration on longer time scales. The local, immediate effect of increased albedo could be exploited in strategies to dampen warming locally and alleviate heat stress in summer.

Author's address: Petra Sieber, Swedish University of Agricultural Sciences, Department of Energy and Technology, Uppsala, Sweden

Contents

List of publications

This thesis is based on the work contained in the following papers, referred to by Roman numerals in the text:

I. Sieber, P., Ericsson, N. & Hansson, P.-A. (2019). Climate impact of surface albedo change in Life Cycle Assessment: Implications of site and time dependence. *Environmental Impact Assessment Review, 77*, 191-200.

II. Sieber, P., Ericsson, N., Hammar, T. & Hansson, P.-A. (2020). Including albedo in time-dependent LCA of bioenergy. *GCB Bioenergy, 12*(6), 410-425.

III. Sieber, P., Ericsson, N., Hammar, T. & Hansson, P.-A. (2021). Albedo impacts of agricultural land use: crop-specific albedo from MODIS data and inclusion in LCA (submitted in revised form).

IV. Sieber, P., Böhme, S., Ericsson, N. & Hansson, P.-A. (2021). Albedo on cropland: Field-scale effects of current agricultural practices in Northern Europe (submitted).

Papers I-II are reproduced with the permission of the publishers. Electronic supplementary materials for Paper II can be found online. Supplementary materials for Papers III and IV can be provided upon request.

The contribution of Petra Sieber to the papers included in this thesis was as follows:

I. Planned the paper together with the co-authors. Developed the methods, carried out data collection, modelling and evaluation. Wrote the paper with revisions by the co-authors.

II. Planned the paper together with the co-authors. Built the model with input from the co-authors. Carried out calculations and analysis. Wrote the paper with revisions by the co-authors.

III. Planned the paper together with the co-authors. Developed the methods, carried out data collection, model building, calculations and analysis. Wrote the paper with revisions by the co-authors.

IV. Planned the paper together with the co-authors. Developed and planned the field measurements. Carried out the measurements together with the co-authors. Carried out calculations and analysis. Wrote the paper with revisions by the co-authors.

Abbreviations

AGTP	Absolute global temperature change potential
AR5	Fifth Assessment Report of the IPCC
BRDF	Bidirectional reflectance distribution function
CH_4	Methane
CO_2	Carbon dioxide
CO_2e	Carbon dioxide equivalent
GHG	Greenhouse gas
GTP	Global temperature change potential
GWP	Global warming potential
IPCC	Intergovernmental Panel on Climate Change
LCA	Life cycle assessment
LW	Longwave
MODIS	Moderate Resolution Imaging Spectroradiometer
N_2O	Nitrous oxide
RF	Radiative forcing
SRC	Short-rotation coppice
SW	Shortwave
TH	Time horizon
TOA	Top of the atmosphere

1. Introduction

Land plays a unique role in climate regulation and human livelihoods. Land ecosystems store large amounts of carbon in vegetation and soils, and these reservoirs can act as sinks or sources of carbon dioxide (CO_2), in response to natural or anthropogenic drivers. Human activities have increased fluxes of CO_2, methane (CH_4) and nitrous oxide (N_2O) from land to the atmosphere. Agricultural systems for production of food, energy and materials contribute substantially to anthropogenic greenhouse gas (GHG) emissions and are a major driver of global warming.

Climate regulation by land thus involves biogeochemical processes related to GHG fluxes. Furthermore, land surface characteristics regulate the exchange of energy and water between land and atmosphere. These biophysical processes influence the climate from local to global scale, and are in turn influenced by human land use activities. For example, crop cultivation and management alter vegetation and soil, and thereby change land surface reflectivity (albedo), emissivity and evapotranspiration of water.

Albedo, the fraction of incident solar radiation reflected from the ground, controls the amount of energy available at the surface and in the Earth system. Increased reflectivity leads to a reduction in net shortwave radiation at the surface and at the top of the atmosphere, with the potential to cool local and global mean temperatures. Increased albedo on cropland could therefore dampen warming locally and counteract the radiative forcing (RF) from emitted GHGs.

Life cycle assessment (LCA) is widely used to evaluate the climate performance of products and systems that involve land use, such as food, biofuels or alternative agricultural practices. Albedo is not usually included in LCA studies, but concerns about possible trade-offs between emissions reduction, carbon sequestration and albedo change have spurred the

development and application of methods for quantifying and comparing the effects of GHGs and albedo. Growing interest in evaluating and improving agricultural systems in light of climate change has added to this development. To support decision making, a clear understanding of potential land use effects is needed, including changes in land surface characteristics. Better knowledge about albedo could help evaluate land use practices, biomass-based systems and response options intended to mitigate and adapt to global warming.

Albedo effects are relatively well understood as regards conversion between land cover classes, *e.g.* from forest to cropland. Land use practices within land cover classes can also modify albedo and may be implemented on large areas. Many measures that can contribute to GHG mitigation concomitantly affect albedo, such as cultivation of perennial crops, new cultivars, cover cropping, bioenergy, agroforestry, improved fertilisation and harvest practices, residue retention, biochar application and restoration of degraded soils. However, it is currently unclear how each measure affects albedo, and whether albedo change makes a practice more or less favourable compared with other options. The level of understanding is generally lower about practices in agriculture than in forestry, due to regionally and temporally varying crop types, phenology, soil properties and management.

This thesis seeks to address three barriers to considering albedo effects in work to improve the climate impact of agricultural systems:

- It is not well understood how individual land use and management practices influence albedo and whether albedo change causes an appreciable effect on the overall climate impact of agricultural systems.
- There is no agreed method for quantifying climate impacts due to albedo change and for comparing these impacts with those of GHGs.
- There is no standardised way of integrating albedo effects into the methodological structure of LCA.

2. Aim and structure

2.1   Aim and objectives

The overall aim of this thesis was to improve understanding of how agricultural land use and management affect the climate via surface albedo, and to compare the effects with other climate impacts caused by crop and bioenergy production in a life cycle perspective. Specific objectives were to:

- Develop a framework for including albedo in LCA, using analytical methods to estimate RF from albedo change (**Paper I**) and a time-dependent climate metric (**Paper II**)
- Develop and apply methods to obtain albedo from field measurements (**Papers I, II** and **IV**) and satellite data (**Papers III** and **IV**)
- Analyse how common agricultural crops and practices in Sweden affect albedo, and thus climate considering local conditions (**Paper IV**) or regional conditions and inter-annual variations (**Papers III** and **IV**)
- Evaluate and compare the contribution of albedo change and GHG fluxes to the life-cycle climate impact of willow-based bioenergy (**Paper II**) and common crops produced in Sweden (**Paper III**)

2.2   Research structure

This thesis is based on the work described in **Papers I-IV** (Figure 1).

Paper I provided the methodological foundation for calculating RF from albedo change and including albedo in LCA. Appropriate methods were developed and evaluated using continuous radiation measurements from four sites in south-western Sweden. Two of the sites, under short-rotation coppice (SRC) willow and fallow, were used again in Paper II.

In **Paper II**, albedo was included in time-dependent LCA, which accounts for the timing of emissions and their impacts. Characterisation models were developed to express the climate impact of albedo change as global mean surface temperature change (ΔT) over time and as global warming potential (GWP). These models were used to evaluate the contributions of albedo change and GHG fluxes to the life-cycle climate impact of energy produced from SRC willow grown on former fallow land.
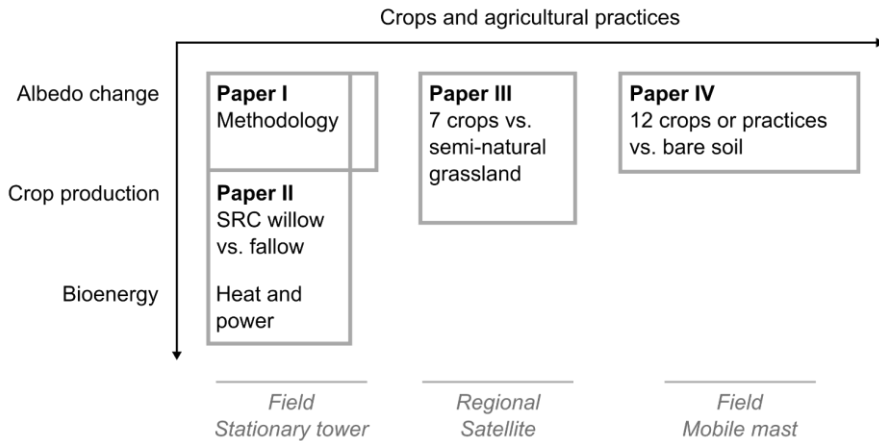
Figure 1. Structure of the work described in Papers I-IV: scope, cases and albedo data used.

Following the case study in Paper II, a need was identified to systematically evaluate the effects of agricultural land use and management practices on albedo, and thus on climate. In **Paper III**, satellite-based albedo data were combined with geodata on agricultural land use to obtain 10-year average albedo values for major crops and unimproved permanent (semi-natural) grassland under regional conditions in southern Sweden. Albedo change was included in LCA of crop production at regional level, using the methods developed in Paper II to calculate climate impacts.

In **Paper IV**, an experiment was designed to assess field-scale effects of various agricultural practices. A mobile system was developed to measure albedo on 14 plots with different crops and management. The study design relied on findings from Paper I on the effects of measurement frequency on calculated RF. The field data were used to assess the potential impacts of albedo change on local and global mean climate.

2.3 Thesis structure

The remainder of this thesis is structured as follows: Chapter 3 provides theoretical background to the work, describes the problem and presents current knowledge and methods. Chapters 4 and 5 synthesise the research in **Papers I-IV**. Data, methods, scenarios and results are presented and discussed across papers. The structure follows the objectives of this thesis:

- Methods and framework development to obtain albedo and assess impacts on climate (Chapter 4)
- Albedo under individual agricultural crops and practices and impacts on climate (Chapter 5, sections 5.1 and 5.2)
- Climate impacts in agricultural systems due to albedo change and GHG fluxes (Chapter 5, section 5.3)

Chapter 6 provides a general discussion of the research and perspectives. It reflects on the contributions of this thesis with regard to the aim and objectives, and relates them to developments in the subject area. Chapter 7 presents the conclusions drawn based on the results obtained.

3. Background

3.1 Agricultural systems and effects on climate

Land cover change and land use in agriculture affect the climate through biophysical and biogeochemical mechanisms (Mahmood *et al.*, 2014; Pielke *et al.*, 1998). Biophysical effects result from changes in land surface characteristics (*e.g.* albedo, emissivity, conductance, roughness), which alter fluxes of radiation, heat and water between land and atmosphere (Figure 2). Biogeochemical effects result mainly from changes in carbon and nitrogen cycling in land ecosystems (*e.g.* net primary productivity, soil carbon and nitrogen balance), which alter fluxes of CO_2, CH_4 and N_2O.
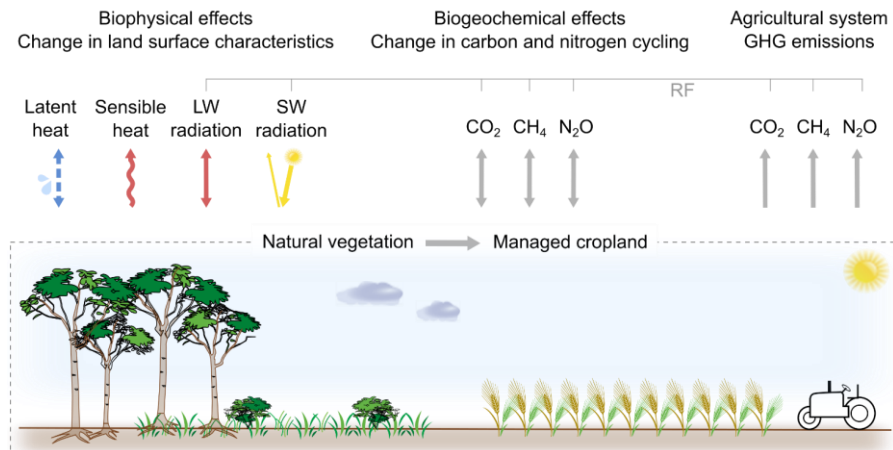

Figure 2. Impacts of agricultural systems on climate due to biophysical and biogeochemical effects of land use, and emissions from on-farm energy use and pre- and post-production processes. Perturbations to the climate system that directly act on the top of the atmosphere radiation balance can be quantified as radiative forcing (RF). GHG = greenhouse gas.

Albedo change acts directly on the shortwave (SW) radiation balance at the top of the atmosphere (TOA) and thus its effect can be compared with that of elevated GHG concentrations in terms of RF. Emissivity change leads to RF in the longwave (LW) spectrum, but this effect is omitted in this thesis. Emissivity changes are usually small and only 10-20% of upwelling LW radiation is transmitted to the TOA (Lee, 2010). Changes in land-atmosphere fluxes of sensible heat (warming the near-surface air) and latent heat (evapotranspiration cooling the surface, condensation warming the surface) affect the redistribution of heat and moisture within the Earth system. These non-radiative processes are considered important climate forcings due to land use (IPCC, 2019), but because they do not directly act on the TOA radiation balance they cannot be quantified as RF.

To understand and improve the climate performance of agricultural systems, there is a need to evaluate biophysical and biogeochemical effects of land use and GHG emissions along the supply chain. Agricultural land use mostly leads to net fluxes of GHGs from land to the atmosphere, although practices that enhance carbon sequestration in biomass and soil contribute to carbon removal. Activities in the supply chain are responsible for additional emissions from manufacture of inputs, fuel use for field operations and post-production processing and transport.

Subsections 3.1.1-3.1.3 provide the necessary background to understanding possible synergies and trade-offs between emissions reduction, carbon sequestration and albedo change in agricultural systems.

3.1.1 Land use and land cover change

Humans have transformed a large proportion of the Earth's land surface to meet the growing demands for food, energy and materials (Foley *et al.*, 2005). Since 1700, over 50% of global land surface has been affected by human activities, more than 25% of forests have been permanently cleared and at least 30% of land has been occupied by agriculture (Hurtt *et al.*, 2011). This land cover change has been dominated by conversion of natural forests, shrubland and grassland to cropland and pasture in the agricultural areas of North America, Europe and South Asia (Ghimire *et al.*, 2014).

Observed trends in land cover since 1700 have increased global annual albedo by 0.00106, resulting in RF of -0.15 Wm^{-2} and potentially cooler global mean temperature (Ghimire *et al.*, 2014). The main driver has been the shift from forests to cropland with more reflective vegetation and

enhanced snow exposure. Land use was long the major source of anthropogenic CO_2 emissions. The GHGs emitted due to land cover change and land use in the past are responsible for 40% of the present-day anthropogenic RF of 2.3 Wm^{-2} (Ward *et al.*, 2014). This land use forcing can be attributed mainly to increases in atmospheric CO_2 (0.43 Wm^{-2}) due to forest clearance, and in CH_4 (0.30 Wm^{-2}) and N_2O (0.14 Wm^{-2}) due to use of cropland and pasture (Ward *et al.*, 2014).

Anthropogenic land cover change to date has led to competing effects on global mean temperature. According to models, it has caused biophysical cooling dominated by increased albedo (-0.10 ± 0.14°C) and biogeochemical warming due to emissions of CO_2 (+0.20 ± 0.05°C) throughout the past century (IPCC, 2019). The future magnitude and net effect of biophysical and biogeochemical processes will depend on how land is allocated to production of food, biofuels and forestation to mitigate climate change (Davies-Barnard *et al.*, 2014). Management practices such as species selection, fertilisation, harvest frequency, tillage and irrigation can also have a profound influence on ecosystem productivity, biogeochemical cycles and biophysical surface properties (Erb *et al.*, 2017). Indeed, land management may have biophysical impacts of similar magnitude as land cover change and affects a much larger area (Luyssaert *et al.*, 2014). However, effects of land management are currently less well understood and insufficiently included in models (Erb *et al.*, 2017; Mahmood *et al.*, 2014).

3.1.2 Agricultural systems

Agricultural systems are currently responsible for 20-40% of total net anthropogenic GHG emissions, measured in CO_2-equivalents (IPCC, 2019; Tubiello *et al.*, 2021). The impacts comprise forest loss driven by agriculture (44%), crop and livestock production including on-farm fuel use (44%), pre- and post-production activities such as fertiliser manufacture, heating and crop drying (5%), and food supply chain processes such as processing, transport, packaging, retail, household consumption and waste disposal (30%) (FAO, 2021). Globally, farm stage emissions are dominated by CH_4 and N_2O related to livestock production, mineral and organic nitrogen fertiliser application to cropland, and rice cultivation (FAO, 2021).

Sources of impact can vary considerably among farms producing the same product under differing environmental and economic conditions (Poore & Nemecek, 2018). For example, deforestation and cultivation of drained

organic soils dominate the emissions of the highest-impact producers. On the majority of farms, emissions from crop production (except flooded rice) are dominated by manufacture of inputs, on-farm energy use and nitrogen application (Poore & Nemecek, 2018). Production of mineral nitrogen fertiliser is energy-intensive and can cause high CO_2 emissions from fossil fuel use. Application of mineral and organic nitrogen fertiliser leads to formation of N_2O, due to microbial denitrification and nitrification in the soil. Poor synchronisation of nutrient supply and crop nitrogen demand, together with high fertilisation levels, can lead to high N_2O emissions from cropland. These emissions can dominate the climate impact of crop production due to the strong climate forcing effect of N_2O. Fertilisation levels on cropland can exceed 300 kg N ha^{-1} (Poore & Nemecek, 2018), although globally most cropland receives less than 50 kg N ha^{-1} yr^{-1} (Erb *et al.*, 2017). Grassland can be equally heavily fertilised, but many pastures exclusively receive inputs from excreta of grazing animals (Erb *et al.*, 2017).

The soil carbon balance is controlled by carbon additions from plant residues and organic amendments, minus carbon losses via decomposition. Temperate cropland stores on average 30-40% less carbon in soil than natural or semi-natural ecosystems such as forests and grassland (Poeplau *et al.*, 2011). On current cropland, the effect of land use on soil carbon stocks differs depending on crop type and management practices. Practices that can contribute positively to soil carbon stocks include cultivation of crops or varieties with high root mass, residue retention, application of manure and other organic amendments, establishment of cover crops during fallow periods, adoption of crop rotations that provide high carbon inputs (*e.g.* increased productivity, inclusion of ley), reduced tillage and cultivation of perennial crops (Paustian *et al.*, 2016). Nevertheless, these practices need to be evaluated regarding effects on N_2O and CH_4 fluxes from soil, energy consumption and alternative uses of biomass and land.

Compared with forests and shrubland, cropland and grassland typically have higher albedo, leading to reduced SW absorption, and shallower roots, lower conductance and lower roughness length, leading to reduced evapotranspiration (Zhao & Jackson, 2014). Type of crop grown and management practices (*e.g.* annual vs. perennial crops, irrigation, tillage) also influence land surface characteristics (Bagley *et al.*, 2014; Bagley *et al.*, 2015). Effects of land surface changes on energy and water fluxes generally depend on temperature, water availability, incoming radiation *etc.*, and thus

impacts on local temperature can vary seasonally and geographically (Perugini *et al.*, 2017).

3.1.3   Climate change mitigation and land

The Paris Agreement (UNFCCC, 2015) put forward the target of holding the global temperature increase well below 2 °C above pre-industrial levels and pursuing efforts to limit warming to 1.5 °C. Meeting the 1.5 °C target requires stringent emissions reductions across economic sectors, including agriculture, and substantial CO_2 removal to reach net zero emissions around 2050 and net negative emissions thereafter (Rogelj *et al.*, 2018). The earlier the net emissions decline, the lower the impacts of climate change and the need for even greater CO_2 removal in the future. Carbon removal is necessary to compensate for emissions that are expensive or difficult to avoid, but many technologies are still immature or too expensive.

Research suggests that the land-based sector could sustainably contribute 30% of the mitigation required by 2050 (Roe *et al.*, 2019). Key measures include conservation and improvement of land carbon sinks, prevention of emissions from agriculture and provision of biomass to replace fossil fuels and energy-intensive products. Enhancing land-based sinks is considered the cheapest and most mature option for CO_2 removal in the near term, notably through forestation, soil carbon sequestration in cropland and grassland, and restoration of peatland (Griscom *et al.*, 2017; Minx *et al.*, 2018). Bioenergy can help reduce dependence on fossil fuels, and under ambitious climate goals, energy crops are projected to expand on agricultural land (Rogelj *et al.*, 2018). In bioenergy systems, carbon release and uptake in biomass can be balanced, but concerns have been raised about emissions from land use and the supply chain, warranting detailed assessment (Creutzig *et al.*, 2015).

Since the Paris Agreement, numerous countries have adopted or proposed targets to reach net zero emissions within the next few decades. The European Union aims to reduce net GHG emissions by 55% by 2030, and to reach climate neutrality by 2050. Sweden's national climate policy aims for net zero emissions by 2045, to be achieved by emissions reductions to at least 85% and supplementary measures to offset remaining emissions. Proposed supplementary measures rely mainly on increased carbon stocks in forests and soils, and on capture and storage of biogenic carbon. The proposed measures could affect up to 20% of current cropland in Sweden (around 600,000 ha), through increased use of cover crops, agroforestry, production

of energy crops on fallow land and rewetting of drained peatland (Inquiry SOU 2020:4, 2020). Thus, climate change mitigation will affect land use and land cover, but biophysical effects of these changes are not currently considered in the Swedish policy (May *et al.*, 2020).

Individual GHG mitigation measures can increase or decrease albedo. Cultivation of cover crops typically increases albedo compared with leaving the soil bare between main crops (Kaye & Quemada, 2017) and perennial energy crops tend to have higher albedo than annual crops or bare soil (Bagley et al., 2014; Georgescu et al., 2011). In contrast, biochar application to cropland decreases the albedo of bare soil (Smith, 2016) and forestation decreases albedo relative to open land (Bonan, 2008). The same measure can lead to different effects on global mean temperature depending on where it is implemented (*e.g.* tropical vs. boreal forestation) and to contrasting effects on global mean and local temperatures (*e.g.* global cooling vs. local warming) (Davin & de Noblet-Ducoudré, 2010; Perugini *et al.*, 2017).

Some studies have called for a comprehensive evaluation of land use effects on climate in order to avoid suboptimal or ineffective land use policies (Marland *et al.*, 2003; Pielke *et al.*, 2002). The growing awareness about biophysical effects has spurred the development of new methods within impact assessments, LCA, agroecosystem modelling, global land-climate modelling and data-driven approaches based on observations. Albedo change is increasingly considered in assessments on land use climate impacts, using the RF concept to compare impacts from albedo change and GHG fluxes. Studies included RF from albedo change either exclusively (*e.g.* Betts, 2000; Smith *et al.*, 2016) or jointly with local biophysical effects (*e.g.* Georgescu *et al.*, 2011; Zhao & Jackson, 2014).

3.2   Surface albedo

Albedo is the ratio of upwelling (reflected) to downwelling (incident) shortwave irradiance at the surface, $\alpha = SW_{Surf\uparrow}/SW_{Surf\downarrow}$. It is measured on a scale from zero to one, where zero corresponds to full absorption and one to full reflection. The word albedo means "brightness", because surfaces with high albedo appear brighter (*e.g.* snow) than surfaces with low albedo (*e.g.* asphalt). However, the visual appearance can be misleading because albedo refers to the entire SW solar spectrum (~100-5000 nm). Visible radiation (400-700 nm) accounts for less than 45% of energy reaching the surface,

while the remaining 55% is in the ultraviolet (<400 nm) and near-infrared (>700 nm) parts of the spectrum. Vegetation typically reflects three times more near-infrared than visible radiation and soils twice as much, whereas snow reflects more visible than near-infrared radiation (Dickinson, 1983).

Albedo depends on intrinsic properties of the surface, and on the angular and spectral distribution of the incident radiation (Dickinson, 1983). Both vary with solar angle and atmospheric composition, due to scattering and absorption of radiation by clouds, aerosols and gases. Consequently, albedo changes with time of day, season and latitude, even under identical surface properties. The albedo of vegetated surfaces is generally lowest under a nearly overhead sun and clear sky conditions. This is because a normal beam penetrates deeper into the surface and because the fraction of visible radiation is higher and absorbed to a large extent for photosynthesis (Dickinson, 1983). This relationship between solar angle and reflectance leads to a diurnal cycle in the albedo of cropland and grassland. This diurnal cycle can be weakened or reversed over rough surfaces (*e.g.* forests) due to shadowing and trapping of radiation.

The albedo of natural surfaces ranges from 0.03-0.10 for water to 0.45-0.70 for old snow and 0.80-0.95 for fresh snow (Bonan, 2015). Common values for major vegetation types are 0.05-0.15 for coniferous forest, 0.15-0.20 for deciduous forest, 0.16-0.26 for grassland and 0.18-0.25 for cropland (Bonan, 2015). The albedo of vegetated surfaces depends on properties of the soil (*e.g.* texture, organic matter content, moisture) and the vegetation (*e.g.* leaf and stem reflectance, orientation, density), and on the deposition of water, snow or particles (Bright *et al.*, 2015). These factors are in turn influenced by climate and weather (*e.g.* precipitation, temperature), plant phenology (*e.g.* emergence, flowering, leaf senescence) and management (*e.g.* planting, harvesting). Thus, the same vegetation type or crop can show strong albedo variations both temporally and spatially.

Albedo is particularly variable on cropland due to various agricultural practices and annual cultivation cycles with rapid changes in vegetation and the fraction of exposed soil (Cescatti *et al.*, 2012; Gao *et al.*, 2005). Growing vegetation cover can increase or decrease albedo, depending on the albedo of bare soil (~0.05-0.40) in relation to that of the vegetation and the effect of vegetation on soil moisture. Soil albedo decreases with moisture because more radiation is trapped by internal reflection (Bonan, 2015). Plant characteristics lead to variation in albedo between crop species and varieties,

depending on canopy morphology, foliage nitrogen and chlorophyll concentration, leaf trichomes, glaucousness and waxiness (Genesio *et al.*, 2021; Hollinger *et al.*, 2010; Singarayer & Davies-Barnard, 2012). Besides being influenced by the crops grown, albedo is also affected by management practices such as tillage, residue retention and fallowing (Davin *et al.*, 2014; Liu *et al.*, 2021).

3.3 Albedo measurements

Albedo can be measured directly on-site with a pair of pyranometers, one upward-facing to measure downwelling solar irradiance and one downward-facing to measure upwelling irradiance. The most accurate instruments use a thermophile detector that absorbs solar radiation and generates a small voltage in proportion to its temperature gain. The voltage signal is typically ~10 µV per Wm^{-2}, so on a clear summer day with 1000 Wm^{-2} incoming irradiance the output is around 10 mV. Each pyranometer has a unique sensitivity and calibration factor for conversion to irradiance. Thermophile pyranometers measure approximately in the 285-2800 nm solar spectrum (covering around 97% of the energy reaching the surface) over a 170-180° field of view. The area observed by the downward-facing sensor increases with height above the surface or vegetation canopy. Approximately 99% of the signal originates from an area with radius 10×height.

Albedo can also be inferred from remote sensing observations, which is particularly useful for global-scale monitoring of spatial and temporal variation. Satellite-based measurements of Earth's reflectance are obtained from above the atmosphere, at a certain view and sun angle, and in narrow spectral bands. Therefore, algorithms are needed to convert from TOA spectral reflectance to surface broadband bi-hemispherical reflectance (*i.e.* albedo). Traditional algorithms used with observations of polar-orbiting satellites comprise three steps: atmospheric correction to obtain surface reflectance, angular modelling to obtain narrowband albedo, and conversion from narrowband to broadband albedo. Alternative algorithms have been developed to estimate surface albedo directly or from geostationary satellite data, but all methods require information about how the observed reflectance depends on view and solar angles (Qu *et al.*, 2015).

Satellite-based sensors do not observe reflected radiation over the 180° hemisphere for all solar angles, but natural surfaces reflect differently in each

direction and depending on angle of incidence. The scattering properties of a surface can be described mathematically by the bidirectional reflectance distribution function (BRDF), which gives reflectance as a function of illumination and viewing geometry for each waveband. Once the surface BRDF has been estimated based on multi-angular reflectance observations, albedo under any illumination geometry can be calculated by integrating the BRDF. One model available to estimate the BRDF is the semi-empirical linear kernel-driven model used to generate the Moderate Resolution Imaging Spectroradiometer (MODIS) BRDF/Albedo products (Lucht *et al.*, 2000). This model describes reflectance as a linear combination of three kernels that characterise different scattering types: isotropic (*i.e.* even reflectance in all directions), volumetric (*i.e.* uneven reflectance by homogeneous leaf canopies) and geometric (*i.e.* uneven reflectance by vertically heterogeneous scenes with gaps and shadowing).

3.4   Energy budgets and climate impacts

Albedo acts on energy budgets at two levels, at the surface and at the TOA. The higher the albedo, the more SW radiation leaves the surface and the Earth system, so less energy is available to drive internal processes such as photosynthesis, temperature change, heat and moisture transfer, winds *etc*. Quantifying the full climate response to albedo change requires a complex model to describe interactions between land (plants, land use, physics, hydrology), atmosphere (radiation, circulation, water vapour and clouds, chemistry) and oceans (sea ice, circulation, biochemistry). Simulations with global coupled models are expensive, inherently uncertain and mostly implemented as large-scale changes to obtain strong enough effects that can be distinguished from noise. In contrast, the first-order effects of albedo change on the surface and TOA energy budgets can be estimated with relatively simple equations.

Albedo change can be linked directly to effects on local temperature by decomposing the surface energy balance (Juang *et al.*, 2007; Luyssaert *et al.*, 2014), and to effects on global mean temperature by using the RF concept (Betts, 2000; Lenton & Vaughan, 2009). These methods allow temperature impacts to be attributed directly to land use activities that modify albedo, and the effects of albedo change can be separated from those of changes in other (biophysical) variables. The results are pattern-independent and scalable.

The methods account for direct effects of albedo change, *i.e.* the temperature change that occurs due to changes in reflected and absorbed SW radiation. They do not include indirect effects via changes in atmospheric variables that in turn feed back onto surface conditions. Atmospheric feedbacks can result from changes in humidity, cloud cover, air temperature and circulation, which act on downwelling radiation and on sensible and latent heat flux (Devaraju *et al.*, 2018). Such feedbacks can affect surface climate locally and remotely due to atmospheric transport, and are commonly evaluated with global climate models (Devaraju *et al.*, 2018).

3.4.1 Surface energy balance and local temperature

Albedo determines the amount of SW radiation available at the surface. First-order local effects of albedo change can be expressed as a change in net SW radiation at the surface (*e.g.* Miller *et al.*, 2016). However, absorbed energy only partially warms the surface, and information on energy redistribution at the surface is needed to estimate the effect on surface temperature.

Energy balance decomposition can be used to quantify the effect of albedo change on surface skin temperature (Juang *et al.*, 2007). Surface skin temperature depends on how effectively energy is stored, emitted as LW radiation or transferred to the lower atmosphere as sensible heat (by conduction and convection) and latent heat (by evapotranspiration of water). This redistribution is controlled by ecosystem properties (*i.e.* biophysical surface characteristics) and meteorological conditions such as temperature, humidity and wind speed (Bright *et al.*, 2015). Thus, to evaluate the overall effect of agricultural practices on local surface temperature, changes in several biophysical variables need to be considered.

Surface skin temperature responds directly to changes in local land surface properties, and is thus convenient to estimate. It is relevant for soil organisms and agriculture, but it is not always a good proxy for the air temperature perceived by humans and considered in climate policy. Near-surface air temperature (commonly defined at 2 m height) further depends on the extent of turbulent mixing in the boundary layer and on advection. Due to atmospheric transport, air temperature is influenced by land surface properties locally and elsewhere (*i.e.* non-local or indirect effects). Thus, it depends on the pattern and scale of land surface change, which complicates assessment of impacts due to individual land use activities (Bright *et al.*, 2017; Bright *et al.*, 2015).

3.4.2   TOA energy balance and global mean temperature

Earth's mean temperature is governed by the balance between incoming SW radiation from the sun and outgoing radiation from surfaces and the atmosphere as reflected SW and emitted LW radiation. The global energy balance is commonly defined at 100 km altitude, also referred to as top of the atmosphere (TOA). Human activities and natural events (*e.g.* fires, volcanic eruptions) can disturb the TOA energy balance, forcing the planet to warm or cool towards a new steady state. For example, less outgoing LW radiation due to elevated atmospheric GHG concentrations leads to a warmer equilibrium temperature, and more outgoing SW radiation due to increased albedo leads to a cooler equilibrium temperature.

Perturbations to the Earth's energy balance are commonly expressed as RF in Wm^{-2}. Radiative forcing serves as a proxy for the potential climate response and is an important climate metric. It is easier to compute than changes in individual climate variables and allows climate change to be attributed to individual drivers (Myhre *et al.*, 2013). The Intergovernmental Panel on Climate Change (IPCC) provides widely accepted methods for calculating RF and RF-based metrics. These methods are commonly used to evaluate past and future forcing scenarios. In terms of RF, different forcing agents can be assessed and compared, *e.g.* GHGs, aerosols, albedo and natural variations in solar irradiance.

The RF concept is based on the linear relationship between sustained RF and the equilibrium response of global mean surface temperature, expressed as $\Delta T_{eq}=\lambda \times RF$, where λ is the climate sensitivity parameter in $K(Wm^{-2})^{-1}$. As the climate system responds to RF by warming or cooling, internal feedback mechanisms amplify or dampen the initial perturbation and thereby increase or decrease the ΔT_{eq} required to regain radiative equilibrium. For example, changes in atmospheric water vapour, clouds and snow/ice albedo amplify the response, while changes in outgoing LW radiation and atmospheric lapse rate dampen it (Soden & Held, 2006). These processes result from temperature changes and feed back onto RF. Feedbacks are considered part of the climate system's response and are thus included in λ, whereas RF is an imposed perturbation prior to feedbacks.

Other processes that amplify or dampen the initial perturbation but occur due to properties of the forcing itself and not due to temperature change are referred to as adjustments (Sherwood *et al.*, 2015). Adjustments can affect the stratosphere, troposphere or surface. For example, elevated CO_2

concentration induces stratospheric cooling, affects tropospheric temperature stratification and clouds, and reduces transpiration from plants due to stomatal closure (Myhre *et al.*, 2013). Depending on the definition of RF, adjustments are included either in λ together with temperature-mediated feedbacks, or in RF as a modification to the initial perturbation. Because adjustments are forcing-specific, including them in RF (termed effective RF, ERF) leads to more uniform climate sensitivity across forcing agents and thus better predictions of the long-term temperature response (Sherwood *et al.*, 2015).

Alternative definitions of RF exist, and some adjustments have long been integrated into the prevailing RF concept. Up until the Fifth Assessment Report (AR5), the IPCC conventionally used RF at the tropopause after allowing stratospheric temperatures to re-adjust to radiative equilibrium. Flux changes at the tropopause and TOA are then nearly identical. Stratospherically adjusted RF is a better predictor of ΔT_{eq} for forcing agents that substantially affect stratospheric temperatures, such as CO_2 and ozone (Myhre *et al.*, 2013). This is not the case for most forcing agents that act on SW radiation, including surface albedo, so instantaneous RF at the TOA can be used (Lenton & Vaughan, 2009). Tropospheric and surface adjustments are not readily included in the RF concept and were omitted from the IPCC's main definition of RF and RF-based metrics in AR5. For many forcing agents RF and ERF are similar, and implementing ERF increases complexity and uncertainty (Myhre *et al.*, 2013). Tropospheric adjustments are important for certain forcing agents, such as absorbing aerosols that strongly influence tropospheric temperatures and clouds. They may also be relevant for land use due to initially non-radiative processes (Andrews *et al.*, 2017). Increased albedo reduces turbulent heat fluxes, and thereby tropospheric humidity and low-altitude cloud cover (Davin *et al.*, 2007; Smith *et al.*, 2020). The resulting decreases in LW absorption and SW reflection affect the TOA energy balance, thus leading to different long-term RF and ΔT_{eq} than expected from the initial radiative perturbation.

When using the RF concept, any unit RF should ideally lead to the same ΔT_{eq}, to allow meaningful comparisons across forcing agents and scenarios. However, mean climate state, properties of the forcing agent and the vertical and latitudinal distribution of RF influence the climate response (Hansen *et al.*, 2005). The "well-mixed" GHGs CO_2, CH_4 and N_2O are sufficiently mixed throughout the troposphere, so their forcing can be assumed to be

homogeneously distributed (Myhre *et al.*, 2013). Therefore, their RF and temperature impact is commonly modelled independently of where they are emitted. Many near-term climate forcers are not homogeneously distributed, including ozone, aerosols and surface albedo. Depending on the geographical location of the forcing, they activate different climate feedbacks and can lead to stronger or weaker responses in global mean temperature per unit RF. For example, RF at middle and high latitudes of the Northern Hemisphere induces stronger snow/ice albedo feedbacks than RF at lower latitudes or in the Southern Hemisphere (Shindell *et al.*, 2015).

To provide a better estimate of the climate response, RF can be multiplied by efficacies that represent the relative effect of a forcing agent on T_{eq} compared with CO_2 (Hansen *et al.*, 2005). As originally proposed, efficacies account for both forcing-specific adjustments that are not included in RF and regional feedbacks that result from the spatial distribution of RF. For example, efficacies can be applied to the GWP of short-lived climate forcers (Tanaka *et al.*, 2010) and have been used to correct the GWP of CH_4, N_2O and snow albedo (Cherubini *et al.*, 2012). Estimates of the efficacy of biophysical RF vary widely in the literature, ranging from below 50 to over 100% (Bright *et al.*, 2015). This wide range is partly due to differences in experimental design, with some studies modelling past or future land cover change and others deforestation, resulting in different vegetation types converted, extent and spatial distribution of RF. Some studies isolated albedo change, while others perturbed all land surface properties and hence included additional biophysical mechanisms that affect the response. In fact, efficacies are highly dependent on the context in which they were derived, so it is difficult to routinely apply them as correction factors to RF or RF-based metrics in a meaningful way (Bright & Lund, 2021).

3.5   Climate metrics based on radiative forcing

The IPCC provides widely accepted methods for calculating RF and RF-based metrics for various emitted components (Myhre *et al.*, 2013). These methods avoid complex modelling by utilising linear impulse response functions to represent the cause-effect chain from emission via atmospheric concentration change to RF and climate change (*e.g.* in terms of global mean temperature). However, no such expression exists for albedo change. The RF of albedo change is a function of incoming radiation at the TOA,

transmittance of incoming radiation to the surface and transmittance of reflected radiation from the surface to the TOA. Linking albedo change to RF thus requires a model of how radiation is scattered or absorbed in the atmosphere by clouds, aerosols and gases, depending on atmospheric composition and solar angle. Models of different complexity are used in impact assessment studies, including sophisticated radiative transfer codes (*e.g.* Cai *et al.*, 2016), radiative kernels that mimic the radiative transfer scheme in global climate models (*e.g.* O'Halloran *et al.*, 2012), single-layer atmosphere models (*e.g.* Bird *et al.*, 2008) and empirical parameterisations that neglect the effect of surface albedo on radiative transfer (*e.g.* Muñoz *et al.*, 2010). Bright and O'Halloran (2019) provide a quantitative evaluation of different methods.

Metrics serve as exchange rates in multi-component assessments or policies, defining how the contributions of different forcing agents are weighted. Choosing an appropriate metric is challenging, due to the time dependence of radiative perturbations and the resulting time dependence of climate impacts (Tanaka *et al.*, 2010). The RF of albedo change lasts as long as the albedo change itself, whereas the RF of CO_2 lasts for centuries after CO_2 is emitted (Figure 3). During that time, CO_2 is redistributed among the major carbon reservoirs of the atmosphere, ocean and land biosphere. The remaining fraction can be approximated by a sum of exponentials to represent responses in ocean and land carbon sinks on different time scales. According to model experiments, an atmospheric CO_2 perturbation is reduced by 40% within the first 20 years, but it takes another 80 years to remove the next 19% and after 1000 years about a quarter of the initial perturbation is still airborne (Joos *et al.*, 2013). Most other forcing agents are removed from the atmosphere by chemical processes or deposition. The atmospheric response to perturbations of CH_4 and N_2O can be modelled by simple exponential decay with time constants of 12.4 and 121 years, respectively (Myhre *et al.*, 2013). These constants represent the mean lifetime of a perturbation, or the time it takes for a perturbation to decrease to 1/e=37% of its initial quantity. The half-life is given by mean lifetime *ln(2) and is 8.6 years for CH_4 and 84 years for N_2O.
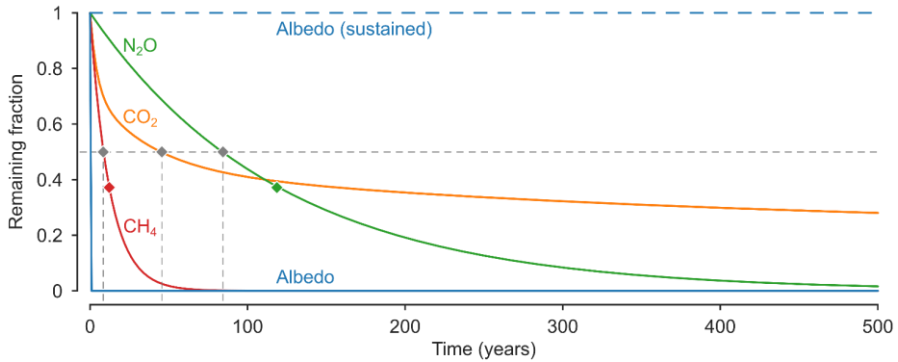
Figure 3. Reduction over time in radiative perturbations caused by different forcing agents: pulse emissions of CO_2, CH_4 and N_2O in year 0, and albedo change in year 0 or sustained. Dashed vertical lines show the point at which 50% of the initial perturbation remains. Coloured diamonds show the perturbation lifetime of CH_4 (12.4 years) and N_2O (121 years). Removal of CO_2 is represented using multiple time scales.

Global warming potential is the most widely used metric to convert emissions to the common scale of CO_2-equivalents (CO_2e). GWP gives the time-integrated RF over a chosen time horizon (TH, typically 20, 100 or 500 years) due to a pulse emission of a component, relative to that of a pulse emission of CO_2. The choice of TH involves important value judgements about short- and long-term impacts (Tanaka *et al.*, 2010). Choosing a TH of 20 instead of 100 years increases the weight of near-term climate forcers (*e.g.* CH_4, ozone, aerosols, short-term albedo change) and decreases the weight of long-lived forcers (*e.g.* CO_2, N_2O, sustained albedo change). The greater the spread in lifetime among the different forcing agents included, the more sensitive the result to the choice of TH.

The informative value of GWP for climate policy has long been debated, because time-integrated RF is (at best) indicative of cumulative warming but not of temperature change at any point in time (O'Neill, 2000). GWP with a 100-year TH (GWP_{100}) effectively indicates the relative temperature impact of long-lived and short-lived pollutants 20-40 years after emission, not in year 100 and not in the same year for all forcing agents (Allen *et al.*, 2016).

An alternative metric, global temperature change potential (GTP), defines equivalence in terms of near-surface air temperature change (ΔT) at a chosen time after emission. The climate system's response is represented by an impulse response function that accounts for climate sensitivity and gradual transfer of heat to the ocean and other sinks (Boucher & Reddy, 2008; Shine

et al., 2005). This response serves as a physical discount function, giving RF at distant (*i.e.* early) times less weight than RF closer to the target year. It also contains important inertia and prolongs the climate impact about two decades beyond the duration of the RF. Like GWP, GTP values are sensitive to the choice of TH. For near-term climate forcers, a long TH means that most of the heat gained has been removed from the atmosphere. Compared with GWP, GTP is further down the cause-effect chain from emissions to climate impacts. It involves higher uncertainty, but has greater relevance to temperature-related policy targets and an unambiguous interpretation (Shine *et al.*, 2005). The same concept can be used without normalisation, *i.e.* as absolute GTP (AGTP), to calculate the temperature response to pulse emissions or forcing scenarios (Aamaas *et al.*, 2013).

Established definitions of GWP and GTP are based on pulse emissions, with distinct radiative efficiencies and perturbation lifetimes. Albedo change does not fit into that framework. Its strength as a climate forcer is site- and time-dependent, and the duration of RF depends on the scenario. Bright and Lund (2021) reviewed methods for converting RF of albedo change to equivalents of carbon or CO_2, and found that the methods differ mainly in how they handle the time dependence of RF caused by albedo change and CO_2 fluxes.

3.6   Life cycle assessment

3.6.1   LCA methodology

Life cycle assessment is a tool for assessing the potential environmental impacts of products or services throughout their life cycle, *i.e.* from raw material acquisition, via production and use, to end of life. The aim is to provide a quantitative understanding of impacts and to avoid burden-shifting between life cycle stages, regions and environmental problems. LCA can be used to learn about systems and drivers of environmental impacts, to detect and prioritise potential for improvement, or to compare systems based on a common function that needs to be defined with regard to the purpose of the study. The function provided by a system is measured by the functional unit, which serves as the quantitative basis for the assessment.

LCA comprises four phases, as specified in the ISO standards 14040/44 (ISO, 2006a, 2006b): (1) Goal and scope definition outlines the purpose and

system boundaries of the study. (2) Inventory analysis involves data collection and modelling to quantify a system's resource use and emissions, and to relate them to the functional unit. (3) Impact assessment links resource use and emissions to environmental impacts. Characterisation factors express the relative contribution of a resource or emission to an impact category, and are used to convert the inventory results to the common unit of the category indicator. (4) Interpretation summarises the results and evaluates them in accordance with defined goal and scope of the study.

The impact category global warming accounts for the contribution of anthropogenic GHG emissions to climate change, with GWP_{100} being the most common category indicator. Use of two complementary indicators is recommended to assess different types of damage: GWP_{100} to assess shorter-term impacts associated with the rate of warming and adaptation (*e.g.* heat stress, malnutrition, changing habitats) and GTP_{100} to assess long-term temperature change in 100 years (*e.g.* future climate stabilisation, sea level rise, polar icecap melting) (Jolliet *et al.*, 2018). GWP_{20} is recommended as an indicator of very short-term climate change effects, *e.g.* to evaluate the importance of near-term climate forcers in a sensitivity analysis.

3.6.2   LCA of biomass-based systems

Life cycle assessment has been widely used to assess the climate impact of products that involve land use by agriculture or forestry. It has been endorsed as the tool of choice for assessment of bio-based commodities including food, materials, energy and waste, and has been attributed a key role in monitoring, evaluating and forecasting potential environmental impacts of bioeconomy sectors in the European Union (EU) (Giuntoli *et al.*, 2019). Bioenergy can, but does not always, reduce GHG emissions compared with fossil fuels, depending on emissions from energy consumption and land use along the life cycle (Cherubini *et al.*, 2009; Creutzig *et al.*, 2015). Policies to encourage the production of biofuels, such as the EU Renewable Energy Directive and the United States (US) Renewable Fuel Standard, rely on LCA methodology for quantifying avoided GHG emissions. LCA approaches are also commonly used to evaluate and certify sustainable production and consumption of food, which accounts for 20-30% of environmental impacts from private consumption (Notarnicola *et al.*, 2015).

The purpose of many LCA studies is to provide results that are sufficiently specific to guide decisions, but still represent a broad range of

possible production conditions. In this context, biomass-based systems are challenging to assess because they are dynamic and inherently variable. This section summarises three challenges in assessing climate impacts due to GHG fluxes in LCA of crop production. Section 3.6.3 then describes how the same challenges complicate the consideration of albedo effects.

Challenge 1: Variability in biological systems

Crop yields and field-level GHG fluxes vary substantially depending on climate, soil and management (Ceschia *et al.*, 2010; Poore & Nemecek, 2018). Because GHG fluxes are difficult and expensive to measure or model for a range of conditions, they are frequently neglected or simplified in LCAs. Soil N_2O emissions and carbon stock changes can make a large contribution to the climate impact of crop production, but LCA studies normally need to make a compromise between accuracy and feasibility (Goglio *et al.*, 2018). Moreover, in many studies inventory modelling is designed to reflect probable average effects, rather than reproducing actual fluxes in a single field and year (Cederberg *et al.*, 2013).

Soil N_2O emissions are often estimated using IPCC Tier 1 methods (IPCC, 2006), which assume a linear relationship between nitrogen inputs and emitted N_2O. The refined IPCC Tier 1 methods (Hergoualc'h, 2019) differentiate climate zones and nitrogen sources, but still involve high uncertainties. Slightly more advanced models consider site conditions, but are not necessarily better at reproducing field-level emissions (Henryson *et al.*, 2020). A comparative study has indicated that IPCC Tier 2 methods or estimates from a properly calibrated agroecosystem model can substitute for observations (Goglio *et al.*, 2018).

Similar challenges arise when estimating the effects of land use on soil carbon stocks. Methods of different complexity can be used, ranging from emission factors to observations and agroecosystem models. The choice of method is often determined by data availability and familiarity with a given tool or method (Goglio *et al.*, 2015). IPCC Tier 1 methods differentiate climate zones, basic crop types and management regimes. However, they do not consider actual carbon inputs and losses over time. Simple carbon models that are calibrated for regional conditions, *e.g.* for use as a Tier 3 method, can provide more accurate results (Goglio *et al.*, 2018).

Challenge 2: Attribution of land use effects to a product or system

Attributing land use impacts to a product or system in LCA is a fundamental conceptual challenge. A dynamic reference situation needs to be defined, which would occur in the absence of the system of interest. A suitable reference scenario could be either non-use (*e.g.* potential natural vegetation, regeneration state) or a likely alternative use (*e.g.* alternative management, business as usual), depending on the goal of the study (Cao *et al.*, 2017; Milà i Canals *et al.*, 2007). Both approaches require expert judgement and involve uncertainties due to either ecosystem dynamics or market-mediated effects (Koponen *et al.*, 2018). Assumptions regarding the reference concern land and possibly other system components (*e.g.* alternative energy supply), and several climate forcers (*e.g.* various GHGs, albedo). Many LCA studies lack a clearly and consistently defined reference scenario (Koponen *et al.*, 2018).

There is no consensus on the impacts for which one year of land use should be held accountable (Bessou *et al.*, 2020). Generally, the study system can be held responsible for any divergence from the reference. This can include GHG fluxes during cultivation and, depending on the temporal scope of the study, an initial transformation before and potential regeneration after the cultivation period (Koponen *et al.*, 2018). Some methods use carbon stock differences between two states and operate with amortisation periods to distribute carbon gains or losses over time, *e.g.* IPCC Tier 1 and the method proposed by Müller-Wenk and Brandão (2010). Thereby, hypothetical fluxes due to land transformation and/or delayed regeneration are attributed to a product or system. Other approaches use annual average sequestration based on observations or modelling (*e.g.* Brandão *et al.*, 2011; Joensuu *et al.*, 2021).

Challenge 3: Timing of GHG fluxes and climate impact

Biogenic carbon stocks can increase and decrease at different points in time during the study period, resulting in temporary CO_2 removals or emissions. The impact of biogenic CO_2 can thus differ from that of fossil CO_2, which stays in the atmosphere for centuries. The same bioenergy plantation can be considered to temporarily store or emit carbon, depending on whether the assessment started at the time of plantation or at the time of harvest. Furthermore, the timing of carbon fluxes affects the RF trajectory over time and thus the timing of climate impacts. Other GHGs may also be emitted in certain years of a crop rotation or perennial system.

There is no consensus on how to account for the timing of emissions and impacts in LCA (Brandão *et al.*, 2013; Levasseur *et al.*, 2016). The convention is to use GWP with a fixed TH regardless of when emissions occur, and to aggregate the life cycle inventory over time. All emissions are treated as pulses in year 0 and receive the same weight. Thus, temporary effects during the study period are omitted because emissions and removals of the same magnitude result in a net impact of zero. The dynamic LCA approach uses cumulative RF with a variable TH depending on the timing of emissions in relation to a fixed end-point (Levasseur *et al.*, 2010). A similar logic has been used to develop emission metrics for biogenic CO_2, which account for carbon dynamics in biomass rotations (Cherubini *et al.*, 2011). Climate impacts of an emission scenario can also be expressed as a function of time, using absolute metrics such as RF, cumulative RF or ΔT (Ericsson *et al.*, 2013; Peters *et al.*, 2011).

3.6.3 LCA including albedo

Few LCA studies to date have included albedo. Kirschbaum *et al.* (2013) assessed climate impacts due to albedo change and GHG fluxes associated with land use changes between forestry and agriculture. Agricultural LCA studies that have quantified albedo effects evaluated bioenergy crops (Cai *et al.*, 2016; Caiazzo *et al.*, 2014; Jørgensen *et al.*, 2014), biochar (Meyer *et al.*, 2012), cover crops (Guardia *et al.*, 2019) and greenhouse agriculture (Muñoz *et al.*, 2010). Forestry LCA studies have included albedo in the context of forestation (Schwaiger & Bird, 2010) and forest management including biofuels (Bright *et al.*, 2011; Cherubini *et al.*, 2012; Holtsmark, 2015).

This section summarises how the three challenges in assessing the climate impact of crop production in LCA (variability, attribution and timing) apply to albedo effects. Albedo varies between crops, management practices and environmental conditions, but albedo data are not generally available for various combinations of these factors. Previous studies have relied on generic literature values, or have obtained primary data from satellite observations, field measurements and laboratory analyses. Most albedo data represent specific local or regional conditions and practices, and are difficult to reuse for other purposes.

Albedo change results from the difference in albedo between a land use of interest and the reference. Therefore the choice of reference situation has as much influence on the result as the studied system itself. For example,

studies have found that albedo can increase or decrease for the same crop, depending on the type of land converted and its properties under regional conditions (Cai *et al.*, 2016; Caiazzo *et al.*, 2014). Albedo of the land reference is not trivial to determine, especially for a non-use situation. Temporarily set-aside agricultural land can be bare or vegetated (*i.e.* black or green fallow), and permanently unused land can be vegetated with a range of possible plant types (*e.g.* trees, shrubs, grass or a mix). As for other land use impacts, albedo effects can be considered during cultivation, due to an initial transformation or due to delayed regeneration.

Albedo can increase or decrease at different points in time during the study period, leading to temporary changes and case-specific RF trajectories that affect the climate differently over time. The radiative perturbation can be significantly shorter than that following a pulse emission of CO_2, because albedo RF lasts precisely as long as the albedo change itself (section 3.5). This poses problems when comparing the impacts of albedo change and GHG fluxes with standard metrics such as GWP_{100}. In fact, 1 kg CO_2e can have different climate impacts depending on the timing of albedo RF and emissions during the study period, and on the lifetimes of the forcing agents considered. Nevertheless, most studies to date have used GWP_{100} to assess and compare the impacts of albedo change and GHG fluxes.

Some additional challenges are specific for albedo effects. The cause-effect chain from albedo change to climate impacts is currently not well understood in the LCA community. Albedo values, radiation data and models to account for atmospheric transmittance are not well known and readily accessible. Moreover, there is a lack of consensus on how to quantify and express climate impacts of albedo change, and especially on how to compare them with those of GHG fluxes from the same system.

4. Methods and framework development

4.1 Study areas and albedo data

The systems described in **Papers I-IV** were located at different sites or regions in Sweden (Figure 4, Table 1). In **Papers I** and **II**, measurement data from stationary towers were used to calculate the albedo of green fallow, willow, coniferous forest and clear-cut forest. Data were taken from the same period for each land use change scenario, *i.e.* April 2013-March 2016 for fallow to willow, and December 2013-February 2015 for forest to clear-cut. The fallow and forest sites were part of the Skogaryd research catchment, 100 km north of Gothenburg. The willow plantation was located nearby, at Grästorp, and the clear-cut at St Olof, 300 km south of the other sites.
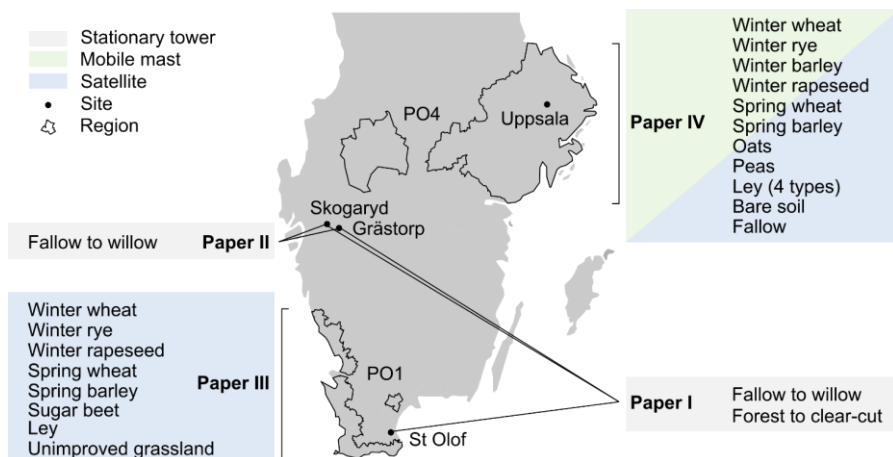

Figure 4. Study areas and albedo data used in Papers I-IV. PO = production region (*produktionsområde* in Swedish).

In **Paper III**, MODIS BRDF/Albedo products were used to calculate 10-year average albedo of seven major crops and unimproved permanent (semi-natural) grassland in Sweden's southernmost production region (PO1). MODIS data for August 2010-October 2020 were utilised for crops harvested in 2011-2020. **Paper IV** included one year (September 2019-September 2020) of mobile field measurements on 14 plots in Uppsala. MODIS albedo in the region encompassing Uppsala (PO4) was used for comparison. Regions PO1 and PO4 are two of eight production regions (*produktionsområden*) in Sweden, each of which is characterised by specific agricultural production conditions regarding topography, climate and soil type. Production regions do not necessarily coincide with administrative borders and are used as an alternative aggregation level in Swedish agricultural statistics. For example, crop yields, fertiliser use and pesticide application are reported per production region.

Table 1. Overview of land use scenarios, scope and metrics in Papers I-IV. In Paper IV, 10 years of MODIS data in region PO4 (encompassing Uppsala) were used for comparison with field-measured values.

	Paper I	Paper II	Paper III	Paper IV
Land use				
Previous	-	Green fallow	Cropland	-
Main	SRC willow or clear-cut	SRC willow	7 major crops	12 crops or practices
Reference	Green fallow or forest	Green fallow	Semi-natural grassland	Bare soil
Albedo data	Stationary tower, 3 years or 1 year	Stationary tower, 3 years	MODIS, 10 years	Mobile mast, 1 year
Scope				
Temporal	3 years or 1 year	50 years	1 year	1 year
Spatial	Field	Field	Region	Field
Location	SW Sweden	V Götaland	PO1	Uppsala
Life cycle	-	To bioenergy	To harvest	-
Agents	Albedo	Albedo, CO_2, CH_4, N_2O	Albedo, CO_2, CH_4, N_2O	Albedo
Results				
Basis	1 ha	1 ha, 1 MJ	1 ha	1 ha
Metrics	RF	RF, ΔT, GWP	RF, ΔT, GWP	RF, GWP, $\Delta SW_{Surf,net}$

4.2 Albedo measurements

4.2.1 Stationary tower measurements

Micrometeorological towers are usually equipped with an upward-facing pyranometer to measure downwelling (incoming) SW radiation. Some stations also measure upwelling (reflected) SW radiation. Thus, surface albedo can be directly calculated as the ratio of upwelling to downwelling radiation over any time interval. This is a robust way to determine site-level albedo. Continuous data from stationary towers include diurnal and seasonal variations in solar angle, atmospheric conditions and surface properties, and they often span multiple years. However, continuous measurements are expensive and only available at selected sites. Research stations belonging to national networks such as SITES (Swedish Infrastructure for Ecosystem Science), regional networks such as ICOS (Integrated Carbon Observation System) or global networks such as FLUXNET perform long-term monitoring that is representative of major ecosystem and climate types. In Sweden, only a few stations are located on agricultural land and some do not provide data on upwelling SW radiation. Even in FLUXNET, few albedo measurements are available for site pairs with similar environmental conditions, but differing management practices.

Measurements for willow used in **Papers I** and **II** were obtained from a research project on SRC willow run by the University of Gothenburg. The data covered a full three-year cutting cycle of the plantation. Albedo of the reference, long-term green fallow, was approximated by a mire vegetated with grasses and sedges, which was part of SITES. **Paper I** included a second case, comparing coniferous forest with clear-cut. Data for coniferous forest were obtained from SITES and for clear-cut from a research project on forest harvesting at Lund University.

Downwelling and upwelling SW irradiance were received as 30-min averages. Raw data were cleaned and corrected to remove instrumental noise and unrealistic values. Data gaps were usually a few hours due to instrument failure, but could be several weeks in the case of maintenance or harvesting. Gaps were filled while preserving the diurnal and seasonal cycles of SW radiation. The corrected and gap-filled time series were used to calculate hourly, daily, monthly or annual albedo. The methods were developed and described in **Paper I**, and used again in **Paper II**.

4.2.2   Mobile mast measurements

A mobile system was developed for measuring albedo on multiple plots in Uppsala on the same day throughout one year. A total of 22 plots were regularly sampled, covering common crops and management practices in Northern Europe, some less common crops (*e.g.* winter barley, maize, peas) and different cultivation intensities. The plots were located on four commercially farmed fields and at an experimental site consisting of two fields with multiple plots each. Field operations and inputs followed normal practice in conventional cropping, except for trials with low, normal and high nitrogen fertilisation of three cereal crops. **Paper IV** included 14 plots, whereof two were replicates (plots not included were maize, undersown ley with minimal management, and low and high fertilisation levels on winter rye, winter wheat and spring barley).

The mobile system consisted of a portable tripod with a vertically extendable mast and 2-m long horizontal cross-arm, a pair of thermophile pyranometers, a data logger, a Bluetooth serial adapter and a mobile app for direct data transfer and display in the field. The plots were sampled every 1-2 weeks under stable conditions. Measurements were taken for 3-5 minutes within three hours of solar noon. The sampling design was based on a previous evaluation of continuous pyranometer data in **Paper I**, which showed that selectively measured albedo on clear days around solar noon can be used to approximate seasonal albedo for energy balance calculations. Albedo for each plot and sampling day was calculated as the ratio of reflected to incoming average irradiance in a stable period. After replacing individual missing values, the sampled time series was interpolated to daily frequency. Annual albedo was calculated as the weighted mean of daily albedo, using daily incoming radiation for weighting. Weighting is necessary to handle discontinuous measurements.

4.2.3   MODIS satellite products

MODIS BRDF/Albedo products utilise reflectance observations from the MODIS instruments aboard Terra and Aqua satellites, which travel in near-polar orbits at 705 km altitude. MODIS scans a wide swath of 2300 km, so both instruments sample almost the entire surface of the Earth every day. MODIS BRDF/Albedo products are provided daily at 500 m nominal grid resolution. Because of their high temporal resolution (at the expense of spatial resolution), the products are commonly used to monitor land surface

properties over time and to characterise the albedo of contrasting land cover classes. However, the products use a spatial and temporal sampling procedure, so that the BRDF and albedo values assigned per pixel may derive from observations over a larger area and temporal interval than the product's nominal resolution suggests.

The coarser effective resolution and lack of information about the actual observational footprint of MODIS BRDF/Albedo pixels make it difficult to match the product with surface conditions. In spatially heterogeneous agricultural landscapes, many fields are smaller and differently shaped and placed than the area contributing to a pixel's signal. Thus, most BRDF and albedo values do not represent a single crop or management regime, but are composed of several crops, grassland and other landscape elements (*e.g.* hedges, trees *etc.*). Furthermore, different annual crops are grown every year and accurate maps of yearly crop cultivation are not generally available.

In **Paper III**, methods were developed to identify homogeneous pixels and to obtain representative albedo values for common crops and unimproved permanent grassland in production region PO1. Geospatial analysis was used to determine the overlap between the observational footprint of MODIS BRDF/Albedo pixels, modelled by a Gaussian function, and agricultural land use in harvest years 2011-2020, represented by annual polygon layers of individual fields. Pixels whose signal originated to at least 80% from a single land use were selected to achieve high pixel purity while maintaining a representative sample of pixels per land use and year. Blue-sky albedo, *i.e.* albedo under actual illumination conditions with a combination of diffuse and direct radiation, was calculated in two steps. First, the kernel-driven BRDF model was used with a pixel's daily BRDF parameters for the SW band (300-5000 nm) to calculate daily white-sky albedo (WSA) under completely diffuse illumination and hourly black-sky albedo (BSA) under direct illumination as a function of solar zenith angle. Second, blue-sky albedo was obtained as the average of WSA and BSA weighted by the fractions of diffuse and direct surface irradiance. As with other discontinuous albedo data, daily and annual albedo were calculated as the weighted mean, using incoming radiation for weighting.

Similar methods were employed in **Paper IV** to derive MODIS-based albedo for crops in production region PO4 (encompassing Uppsala). MODIS data were used for comparison with field-measured values and to assess variability across years and sites within a region.

4.3 Net shortwave irradiance and radiative forcing

The effect of albedo change was expressed as the difference in net SW irradiance at the surface (**Paper IV**) and at the TOA (**Papers I-IV**) between the land use of interest and a chosen reference. Calculating these values required information about the transfer of radiation through the atmosphere. Incoming radiation varies with solar angle and downward atmospheric transmittance. It is enhanced over surfaces with high albedo, due to multiple reflections between the surface and the atmosphere. Outgoing radiation is a function of incoming radiation and surface albedo. The fraction that passes from the surface to the TOA depends on upward atmospheric transmittance.

Incoming SW irradiance at the surface can be directly taken from continuous measurements. Nevertheless, it was modelled in all studies (also **Papers I** and **II** when suitable data were available) to ensure consistent atmospheric conditions on downward and upward passes of radiation through the atmosphere and at different sites. Incoming and outgoing SW radiation were calculated using a single-layer atmosphere model with isotropic properties (Figure 5).
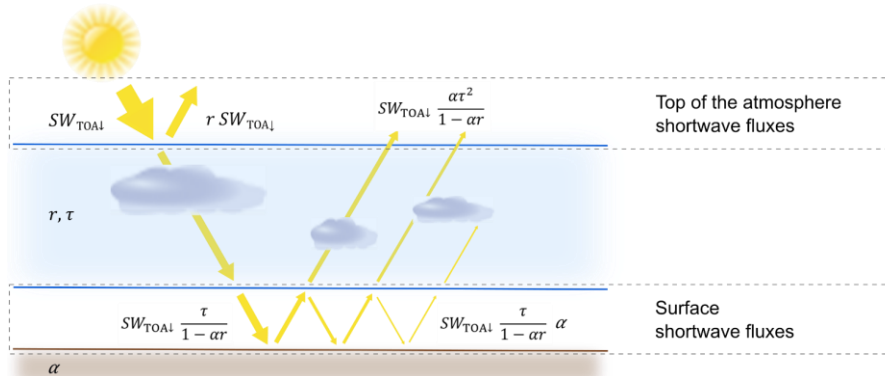
Figure 5. Radiative transfer of shortwave (SW) fluxes in the isotropic single-layer atmosphere model. Radiation travelling downwards or upwards through the atmosphere is partially reflected and transmitted on each pass, according to single-pass atmospheric reflectivity (r) and transmittance (τ). The remainder is absorbed, so that $a+r+\tau=1$. Radiation reaching the surface experiences multiple reflections between a surface with albedo α and the atmosphere.

With the simplifying assumption that atmospheric properties are isotropic (*i.e.* directionally independent and constant on all passes), single-pass transmittance (τ) and reflectivity (r) can be estimated from four boundary fluxes (Equations 1 and 2) (Winton, 2005). Data on these boundary fluxes,

i.e. downwelling and upwelling SW irradiance at surface and TOA, at a resolution of 31 km and 1 hour, were obtained from the ERA5 global reanalysis dataset (Hersbach *et al.*, 2018).

$$\tau = \frac{SW_{\text{TOA}\downarrow}\,SW_{\text{Surf}\downarrow} - SW_{\text{TOA}\uparrow}\,SW_{\text{Surf}\uparrow}}{SW_{\text{TOA}\downarrow}^{2} - SW_{\text{Surf}\uparrow}^{2}} \tag{1}$$

$$r = \frac{SW_{\text{TOA}\downarrow}\,SW_{\text{TOA}\uparrow} - SW_{\text{Surf}\downarrow}\,SW_{\text{Surf}\uparrow}}{SW_{\text{TOA}\downarrow}^{2} - SW_{\text{Surf}\uparrow}^{2}} \tag{2}$$

Net SW irradiance at surface and TOA were calculated as functions of surface albedo (α), downwelling irradiance at the TOA ($SW_{\text{TOA}\downarrow}$), τ and r (Equations 3 and 4). In both equations, the denominator ($1\text{-}\alpha r$) represents multiple reflections between surface and atmosphere. The TOA energy balance in Equation 4 consists of contributions of atmospheric reflectivity in the first term, and surface albedo in the second term.

$$SW_{\text{Surf,net}} = (1 - \alpha)\,SW_{\text{TOA}\downarrow}\,\frac{\tau}{1 - \alpha r} \tag{3}$$

$$SW_{\text{TOA,net}} = (1 - r)\,SW_{\text{TOA}\downarrow} - SW_{\text{TOA}\downarrow}\,\frac{\alpha \tau^{2}}{1 - \alpha r} \tag{4}$$

First-order radiative effects of albedo change on the local surface energy balance were expressed as $\Delta SW_{\text{Surf,net}}$ during a specified time interval (*e.g.* daily, seasonal or annual in **Paper IV**), and on the global TOA energy balance as global annual average RF ($RF = A/A_{\text{E}} \times \Delta SW_{\text{TOA,net}}$), where A is the area affected by albedo change in relation to the Earth's total surface area ($A_{\text{E}} = 5.1 \times 10^{14}$ m^{2}).

Methods for calculating RF of albedo change were evaluated in **Paper I**, including theoretical and empirical considerations about the spatial and temporal (co-)variation of albedo, irradiance and transmittance. Because of their covariation on seasonal time scales, time steps in calculation of RF should be at least monthly and preferably daily. Diurnal covariation had small effects on calculated RF in the cases evaluated in **Paper I**. Standard atmospheric conditions for a region or multi-year period were obtained by aggregating SW variables while retaining sub-annual time steps (*e.g.* to the regional or climatological daily mean) prior to using them in Equations 1-4.

4.4 Time-dependent LCA of agricultural systems

4.4.1 System boundaries and scope

Crop production in **Papers II** and **III** included manufacture of inputs, fuel consumption for field operations and land use effects due to changes in albedo, biogenic carbon stocks and soil nitrogen balance (Figure 6). **Paper II** also included transport and combustion of wood chips to produce heat and power. Results were expressed per hectare, to compare different crops or agricultural practices. In addition, the output-based functional unit 1 MJ energy was used in **Paper II** for comparison with alternative energy sources. **Paper IV** included only albedo changes due to various crops or practices.
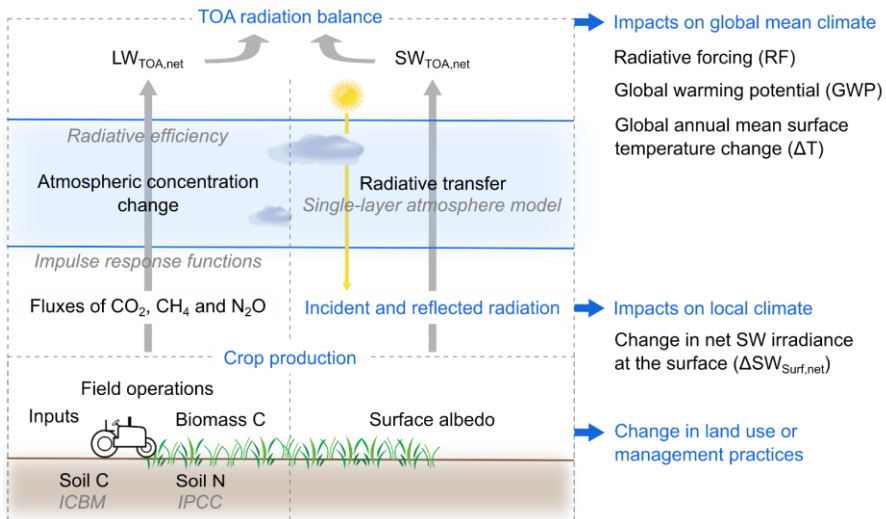
Figure 6. System components of crop production and impact pathways considered in this thesis. Several metrics were used to assess impacts on global mean and local climate. Models used in inventory analysis and impact assessment are shown in italics.

The study period in **Paper II** was 50 years, consisting of two consecutive rotations of SRC willow with harvest every third year. The reference scenario included natural gas as a fuel and continuation of the former land situation, *i.e.* green fallow with minimal management and no succession. **Paper III** included seven common crops (winter and spring wheat, winter rye, spring barley, winter rapeseed, sugar beet and ley). Crop production on current cropland was assessed relative to a situation without cultivation, *i.e.*

a semi-natural state represented by unimproved permanent grassland. **Paper IV** included 12 crops or practices (winter and spring wheat, winter rye, winter and spring barley, winter rapeseed, oats, peas and four types of ley) that were assessed relative to bare soil and relative to each other. In all studies, the temporal system boundary was limited to the period of crop production so that only land use effects in cultivation years were considered.

Land use effects were calculated as the difference between the studied crop and a dynamic reference situation. Input data for activities, albedo and radiation were chosen and aggregated temporally or spatially in accordance with the goal and scope of the study. Input data in **Paper II** represented common management of SRC willow, site-specific albedo and local conditions for radiative transfer. In **Paper III**, common crop management in PO1, regional albedo and regional average conditions for radiative transfer were used. The representativeness of field- and MODIS-based albedo regarding crops, management, soil, local or regional climate, and yearly or climatological weather was compared in **Paper IV**, and implications for the choice of LCA inventory data were discussed in **Paper III**.

4.4.2   Time-dependent LCA methodology including albedo

Time-dependent LCA methodology was used to account for the timing of inventory flows and their impacts. The methodology was originally developed for GHGs (Ericsson *et al.*, 2013) and expanded for albedo in **Paper II**. GHG fluxes and albedo RF were recorded for each year of the study period, in a time-distributed life cycle inventory. Climate impacts were expressed as a function of time from the start of the study period up to year 100, using global mean surface temperature change (ΔT) as an indicator. GWP was calculated with a TH of 100 and 20 years. Metric values were taken from IPCC AR5 (Myhre *et al.*, 2013), and included climate carbon cycle feedbacks in GWP but not in the AGTP values used to calculate ΔT. Addition of feedback to AGTP, as proposed by Gasser *et al.* (2017), had only minor effect on ΔT of non-CO_2 forcers including albedo change and was omitted for simplicity. Radiative efficiencies from AR5 were used, assuming constant atmospheric background concentrations.

To convert the inventory vector of annual albedo RF to ΔT, $AGTP_\alpha$ was formulated to give the temperature response to a unit RF that lasts on constant level for one year (**Paper II**). A temperature response function with equilibrium climate sensitivity of 1.06 K $(Wm^{-2})^{-1}$ and two time scales for

ocean heat uptake was used (Boucher & Reddy, 2008). The parameters originate from simulations with increased CO_2 concentration, but they are usually used independently of the emitted species (Aamaas *et al.*, 2013). Differences in climate sensitivity between albedo and CO_2 can be expressed by the efficacy factor included in the formulation of $AGTP_\alpha$. The default assumption was that it is unity, because appropriate values for specific scenarios of albedo change are currently not available.

CO_2-equivalents were calculated as the sum of annual albedo RF relative to the time-integrated RF of a 1 kg pulse emission of CO_2. Characterisation factors per unit (1 Wm^{-2}) and year albedo RF were thus $GWP_{100}=10.9\times10^{12}$ kg CO_2e and $GWP_{20}=40.1\times10^{12}$ kg CO_2e. These methods treat albedo RF during the study period as annual pulse emissions with one year perturbation lifetime. If the TH is shorter than the study period (*e.g.* using GWP_{20} to assess crop cultivation for 50 years), equal weight is given to albedo RF in all 50 years and no cut-off is applied after reaching the 20-year TH.

Considerations when integrating albedo in time-dependent LCA

Radiative forcing of albedo change was treated as an inventory element, not albedo or albedo change. Every land use scenario has unique seasonal albedo dynamics, and albedo co-varies with solar irradiance and atmospheric transmittance. Consequently, the relationship between albedo change and (annual mean) RF is not linear, and the cause-effect pathway from albedo change via RF to climate impacts cannot be expressed by a site- or case-generic linear characterisation model. The model evaluation performed in **Paper I** showed that temporal simplifications by pre-aggregating albedo, irradiance and transmittance affect estimations of RF. Temporal and spatial aggregation of inventory results is possible with RF, but not with albedo or albedo change. By modelling albedo RF in the inventory phase, generic characterisation methods can be developed and applied. Other approaches use site- and case-specific GWP_α (Bright *et al.*, 2012; Cherubini *et al.*, 2012).

Considerations when attributing albedo effects to crop production

Climate impacts from albedo change considered in this thesis resulted from perturbations to the Earth's radiative balance in specific years during the study period. Annual flows recorded in the life cycle inventory (*i.e.* annual albedo RF) were calculated relative to a land reference, which can be an alternative use or business-as-usual situation (**Paper II**), a semi-natural or

regeneration state (**Paper III**), potential natural vegetation (*e.g.* forest) or a theoretical "zero" reference with no emissions and albedo of 0 (**Paper III**).

Other approaches interpret albedo change as a consequence of land transformation, *i.e.* a one-time intervention with lasting effect (Muñoz *et al.*, 2010). Thus, albedo RF is treated as a one-off pulse with infinite lifetime that lasts until it is cut off at the TH, regardless of the study period. In a study by Muñoz *et al.* (2010), this led to the counterintuitive result that the magnitude of the albedo effect increased as the TH was extended from 20 to 100 or 500 years. Albedo change can also be interpreted as a consequence of land occupation, *i.e.* of preventing the land from reverting back to the reference state (Bright *et al.*, 2012). Impacts due to occupation are numerically equivalent to those obtained with the time-dependent method for albedo with GWP. However, the approach is conceptually different, and results would differ for soil carbon changes and a time-dependent indicator such as ΔT.

Considerations in choice of climate metric

Results with the time-dependent metric ΔT reflect the timing of GHG fluxes and albedo RF during the study period, and the timing of RF depending on the perturbation lifetime of each forcing agent. Explicit consideration of time in inventory and impact assessment can be useful to evaluate dynamic systems (*e.g.* 50 years of willow production) and to compare climate forcers with widely differing perturbation lifetimes (*e.g.* short-term albedo change and CO_2). Presenting ΔT over time avoids the value-laden choice of a single TH or end-point and provides additional information (Peters *et al.*, 2011).

GWP has merit as a widely used, well-known and simple climate metric. However, the relative importance of near-term climate forcers such as short-term albedo change is difficult to interpret when measured in GWP. GWP obscures the immediate temperature effect of short-term albedo change, of which only 10% remains after 20 years and 1% after 100 years (Figure 7A). While the temperature effect of albedo change is largely realised within about 25 years, the effect of a CO_2 pulse emission only peaks at that time and lasts long afterwards (Figure 7B). GWP_{100} for albedo RF effectively indicates the temperature impact of an equivalent CO_2 pulse 22 years after emission (Figure 7B). Thus, the importance of albedo relative to CO_2 is understated on time scales shorter than 22 years, and overstated on longer time scales. The correspondence to the temperature response of a CO_2 pulse emission is better for sustained albedo change (Figure 7C). This applies to near-term climate forcers in general (Allen *et al.*, 2016).
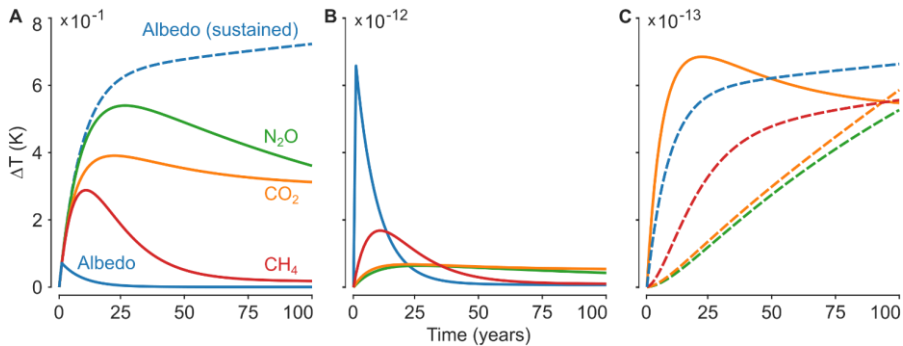
Figure 7. Effect of timing and perturbation lifetime on the temperature response to different forcing agents. The perturbations considered are: **A** Initial radiative forcing (RF) of 1 Wm^{-2} resulting from emission pulses of 570 Pg CO_2, 4.7 Pg fossil CH_4 or 2.8 Pg N_2O in year 0; from temporary albedo change in year 0; or from sustained albedo change in years 0-100. **B** 1 Mg CO$_2$e with GWP$_{100}$ resulting from emission pulses of 1 Mg CO_2, 27.8 kg fossil CH_4 or 3.4 kg N_2O, or from albedo RF of 9.2×10^{-11} Wm^{-2} in year 0 [quantities corrected compared with the caption of Figure 7 in Paper II]. **C** 1 Mg CO$_2$e with GWP$_{100}$ resulting from sustained emissions at constant rate or sustained albedo RF over 100 years. The response to the CO_2 pulse (solid orange line in panel C) is reproduced from panel B for comparison.

4.4.3 Modelling of activities and GHG emissions

In **Papers II** and **III**, yields, inputs and field operations per crop were obtained from Swedish agricultural statistics, reported common practice and recommended production methods. Fuel use was calculated based on machine passes and energy consumption. Swedish and European emissions data on production of mineral fertilisers, pesticides and fuels were used.

Biogenic carbon stocks were determined for each year of the study period and used to calculate annual net fluxes of CO_2 from or to the atmosphere. Biomass carbon was modelled by plant compartment, and only accumulating biomass such as willow stems and coarse roots was considered in terms of carbon stock change. Residues left in the field were recorded as input to the soil carbon pool.

Accumulation or loss of carbon in the topsoil (25 cm) was estimated using the ICBMr model, a version of the Introductory Carbon Balance Model that accepts annual inputs per production region, soil type and crop type (Andrén *et al.*, 2004). Soil carbon stocks under the previous land use were used as a starting condition, *i.e.* simulated equilibrium stocks of 58 Mg C ha^{-1} under long-term green fallow in Västra Götaland (**Paper II**) and measured average stocks of 71 Mg C ha^{-1} in arable soils in PO1 (**Paper III**). For each crop, the

soil carbon balance was simulated with crop-specific inputs over 100 years. Mean annual changes over the 100-year period were used when assessing a single cultivation year (**Paper III**). In the reference scenarios, stable soil carbon stocks were assumed.

Additions of nitrogen to soil were calculated annually, considering application of mineral fertiliser and above- and belowground crop residues. Direct and indirect emissions of N_2O were modelled using the refined IPCC Tier 1 methods (Hergoualc'h, 2019) and country-specific values for Sweden (Swedish EPA, 2019).

5. Results and discussion

5.1 Albedo on cropland

Field and satellite data obtained in this thesis confirmed that albedo on cropland is influenced by environmental conditions (climate, yearly and seasonal weather, soil type), agricultural land use (cultivated crop, crop rotation, fallow) and management practices (timing and intensity of tillage, fertilisation, harvest, residue retention). These factors introduced spatial, seasonal and inter-annual variation in albedo. Extensive data were needed to obtain robust albedo values for specific crops or management practices.

5.1.1 Daily albedo at field level and influencing factors

Field-measured albedo in Uppsala ranged from 0.05 on moist bare soil in autumn to 0.95 on snow cover in winter (**Paper IV**). Frequent observations were needed to capture natural and management-induced variations during the year. The seasonal course of albedo was influenced by crop, phenology, precipitation, temperature, harvest and tillage (Figure 8).

Albedo was low when the dark clay soil was exposed. Soil albedo varied depending on surface soil moisture, from 0.05-0.11 for moist clay soil to 0.13-0.16 for harrowed and dry clay soil. Albedo increased with growing vegetation density and plateaued at full plant cover. This effect was strongest during green-up of most crops in spring. Only two winter crops, rapeseed and to a smaller extent barley, developed substantial vegetation cover before winter dormancy. During the growing season, differences between crops were highest in autumn and spring, when ley and winter-sown varieties had 0.05-0.2 higher albedo due to better soil coverage than spring-sown varieties. Full canopy albedo in early summer was more similar across crops (0.21-

0.25), but ripening led to contrasting effects. These observations were in good agreement with findings in other studies (Monteith & Unsworth, 2013; Piggin & Schwerdtfeger, 1973; Zhang *et al.*, 2013).
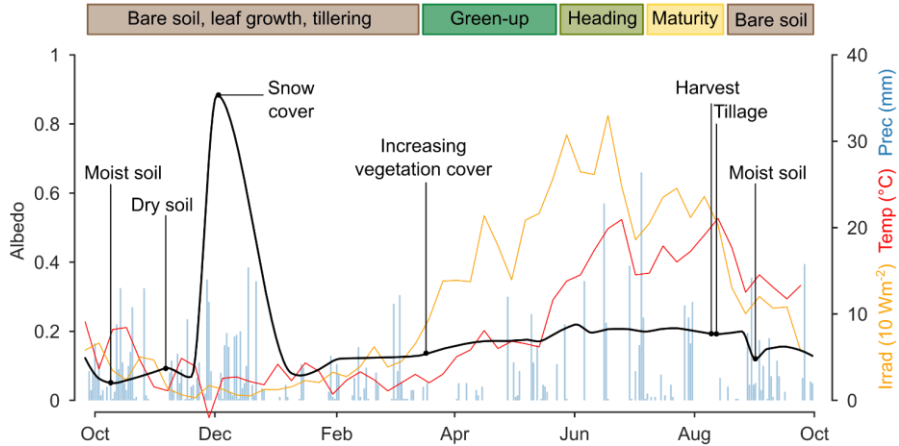

Figure 8. Daily albedo of winter wheat in Uppsala 2019-2020 (black line) and meteorological conditions at the field site (yellow line = 7-day mean surface irradiance, red line = 7-day mean temperature, blue bars = daily precipitation). Influences of phenology, soil moisture, harvest and tillage are shown.

Influencing factors at the field level were related (*e.g.* weather and timing of harvest) or unrelated (*e.g.* weather and cultivated crop), and led to inter-dependent effects on albedo. For example, the effect of residue retention on albedo depended on harvested crop, tillage, weather and soil type. Reflective plant debris increased albedo on dark clay soil, especially when the soil was moist, but this effect diminished quickly if harvest was followed by early tillage or rainfall. These factors led to different seasonal and annual albedo on adjacent plots cultivated with cereals in the same year (**Paper IV**). Winter wheat was followed by an early-sown crop (winter rapeseed), and spring cereals were harvested late in August, with rainfall soon afterwards. Residue retention thus had a smaller effect than on other plots, despite identical environmental conditions and similar crops grown.

One aim of this thesis was to analyse how common crops and agricultural practices in Sweden affect albedo. In general, disentangling the multiple factors influencing albedo is inherently difficult and requires observations from many fields (with different crops, crop rotations and management), years and regions. Field measurements in **Paper IV** represented pedo-

climatic conditions in Uppsala, weather in 2019-2020, and crops and management practices on specific fields in that year. The experimental design using paired plots enabled robust identification of land use effects under the given environmental conditions. However, the albedo values were context-specific and cannot be generalised to other sites.

5.1.2 Daily albedo at regional level and sources of variation

MODIS-derived albedo for harvest years 2011-2020 enabled a more general characterisation of albedo per crop under regional conditions. **Papers III** and **IV** included 3263 and 1567 crop-specific pixels in regions PO1 and PO4, respectively, covering a range of field conditions in terms of weather, soil type and management. Ten-year average albedo values were produced for major crops, without differentiating management practices. High numbers of pixels improved the representation of various prevalent field conditions in the regional average albedo. Pure pixels consisted of large contiguous or adjacent fields (at least 50 ha, often 65-85 ha depending on position and shape). Thus, the method was suitable for crops cultivated on a large scale in major agricultural areas (Figure 9), *e.g.* winter wheat in PO1.
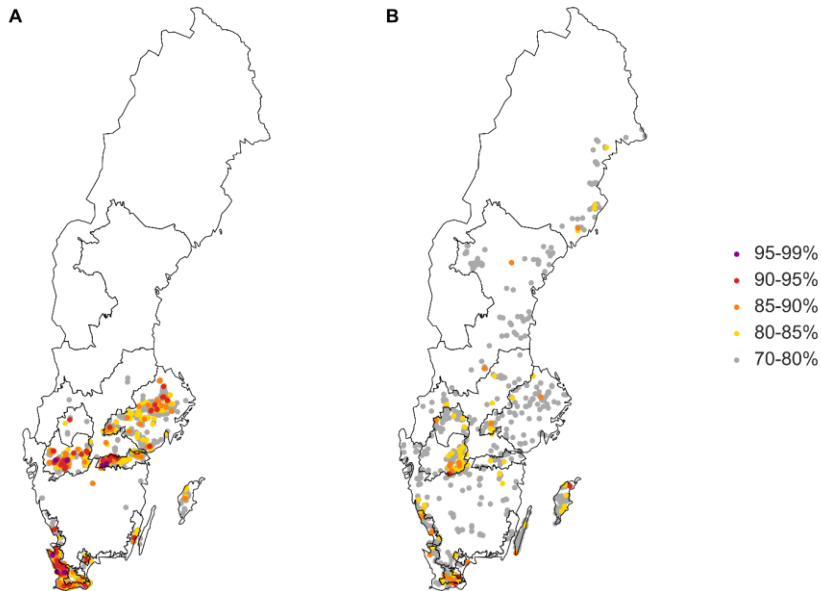

Figure 9. Pixels whose signal originated mainly from **A** winter wheat or **B** ley harvested in 2020. Only pixels with at least 80% purity were utilised.

Further development of satellite products with high spatial and temporal resolution will improve the possibilities to produce crop- or management-specific albedo using the methods presented here, or similar approaches (Liu *et al.*, 2021; Starr *et al.*, 2020).

Comparison of albedo obtained from field measurements in Uppsala and MODIS products in PO4 for the same crop and year showed that the site-specific data fell into the range of values resulting from regionally varying field conditions (Figure 10). For annual crops, regional variation was small during the main growing season (*i.e.* late green-up to harvest), and increased due to differences in timing of harvest, post-harvest management (*e.g.* timing and intensity of tillage, residue retention, soil preparation for the next crop) and snow cover. The representation of snow cover in the MODIS data was compromised by cloudiness and low solar angle in the high-latitude winter, leading to uncertainty about the timing, duration and magnitude of snow effects (Figure 10, data gaps in December filled by linear interpolation at pixel level). Snow albedo was higher and confined to fewer days in the field data. However, discontinuous sampling in mobile field measurements could lead to short-term effects being over- or under-represented. For example, no measurements were taken in early March and hence two days with snow cover (as indicated by the MODIS data) were not captured (Figure 10).
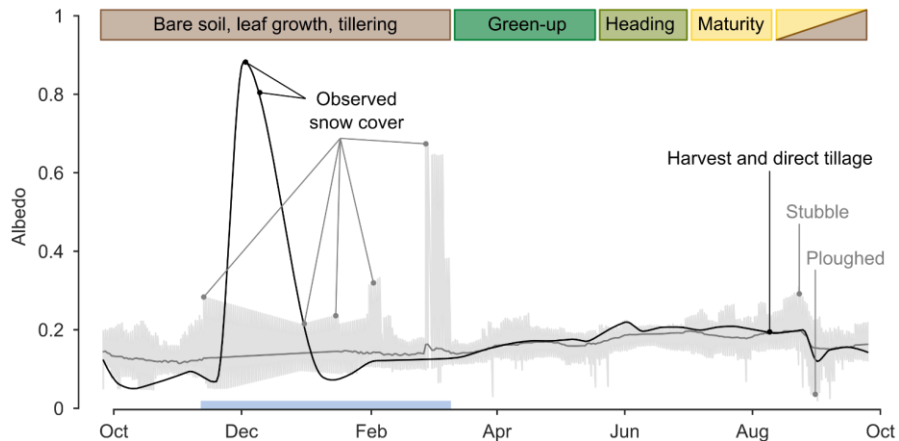

Figure 10. Daily albedo of winter wheat in 2019-2020 based on mobile field measurements in Uppsala (black line) and MODIS products in Swedish production region PO4 encompassing Uppsala (grey line = mean, grey shade = 142 individual pixels). The snow period in the region is shown in blue.

5.1.3   Annual albedo under different land uses and crops

Analysis of the field and satellite data obtained in this thesis indicated that crops with a long growing season (*i.e.* perennial and winter-sown crops) had higher annual albedo than spring-sown crops, unimproved grassland, bare soil and coniferous forest (Figure 11). Climatological (10-year average) MODIS albedo in PO1 was highest with ley (0.19) and winter crops (0.18-0.19), followed by spring crops (0.18) and unimproved grassland (0.17) (**Paper III**). Similarly, field-measured albedo in Uppsala 2019-2020 was highest with ley (0.20-0.22) and winter crops (0.18-0.22), followed by spring crops (0.16-0.18) and bare soil (0.13) (**Paper IV**). Differences in the albedo of winter cereals (barley > rye > wheat) resulted from faster development of barley and rye plants in spring and early ploughing in the wheat plot.
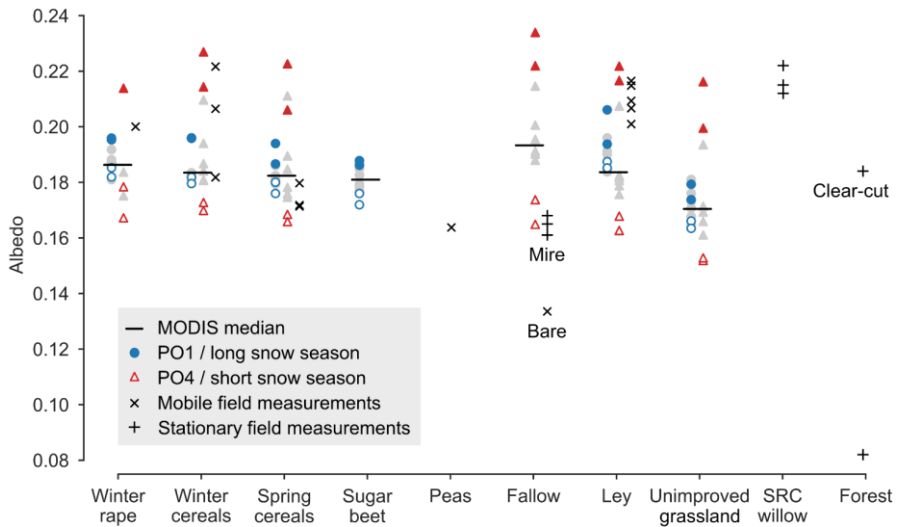
Figure 11. Annual albedo of different land uses or crop types, based on mobile field measurements in Uppsala 2019-2020 (x), stationary field measurements in south-western Sweden 2013-2016 (+), and MODIS products in Swedish production regions PO1 (o) and PO4 (Δ) in 2010-2020. The snow season was long in harvest years 2013 and 2018 (filled markers) and short in 2014 and 2020 (empty markers).

In stationary field measurements in south-western Sweden 2013-2016, albedo was higher on SRC willow (0.21-0.22) than on fallow (0.16-0.17), and higher on clear-cut (0.18) than on coniferous forest (0.08) (**Paper I**). Fallow refers to temporarily set-aside land, which can be vegetated or bare. Albedo of fallow can thus be as high as that of ley or as low as that of bare

soil, covering the full range of values found on agricultural land in this thesis (Figure 11). This can introduce great uncertainty to LCA studies that use fallow as a reference situation. Studies do not always define whether unused land is assumed to be vegetated or not. Moreover, the albedo of green fallow can vary depending on the vegetation present. The mire used as a proxy for green fallow in **Papers I** and **II** had relatively low albedo.

Inter-annual variations in albedo were partly explained by differences in the timing and duration of snow cover. Abundant snowfall increased winter albedo, while prolonged snow cover in spring shifted annual albedo upward across crops compared with the climatological average (Figure 11, filled markers). The effect was stronger in PO4, which generally receives more snow during a longer period than PO1. Snow-free albedo was lower in PO4 with dark clay soil than in PO1 with sandy loam soil (Figure 11, empty markers). Effects of rainfall and temperature were mainly important on seasonal time scales and differed between crops. For instance, the severe growing season drought in 2018 increased summer albedo (July until harvest in early August) on cereals and rapeseed and decreased summer albedo on ley. In fact, drought gives rise to several opposing mechanisms which can cause contrasting albedo anomalies for various vegetation types, soil types and regions (Sütterlin *et al.*, 2016).

Overall, the results obtained in this thesis suggest that albedo observations from different regions and years might not be comparable. Assessments of albedo at crop level should be made considering annual weather, particularly anomalies in seasonal snow cover and possibly precipitation.

5.2 Effects of albedo change on climate

Climate impacts per unit (0.01) albedo increase ($\Delta\alpha$) can be expressed as a function of incoming SW irradiance at the TOA, atmospheric transmittance and reflectivity, and reference surface albedo (α_{ref}). The impact of a unit $\Delta\alpha$ was higher in PO1 than PO4, due to higher $SW_{TOA\downarrow}$ and τ at lower latitude (Table 2). Impacts per unit $\Delta\alpha$ generally increase with α_{ref}, due to multiple reflections and higher incident irradiance at the surface. In the example provided here, α_{ref} taken from ERA5 was slightly higher in PO1. Impacts were higher in Uppsala 2019-2020 than in PO4 2010-2020 due to higher τ in the study period and higher α_{ref} in the area.

Results for a unit $\Delta\alpha$ can be used to understand the parameters of the single-layer atmosphere model and the potential magnitude of impacts. Annual albedo of the agricultural land uses studied in **Papers I-IV** differed by less than 0.1. Based on Table 2, the expected impacts in the study areas per hectare and year are thus lower than 9 Wm^{-2} $\Delta SW_{Surf,net}$, 12×10^{-11} Wm^{-2} RF and 1300 kg CO_2e with GWP_{100}. Over a 20-year TH the impact of albedo change would generally be 3.7 times as high, *i.e.* 5000 kg CO_2e with GWP_{20}.

Table 2. Annual conditions for radiative transfer (α_{ref} = reference albedo, τ = transmittance, r = reflectivity) in Swedish production regions PO1 and PO4 2010-2020 and in Uppsala 2019-2020. Climate impacts of 0.01 albedo increase during one year, per hectare. Shortwave (SW) irradiance and radiative forcing (RF) are in Wm^{-2} and global warming potential (GWP) is in kg CO_2e.

	Conditions for radiative transfer				Climate impacts of 0.01 albedo increase			
	$SW_{TOA\downarrow}$	τ	r	α_{ref}	$\Delta SW_{Surf,net}$	RF $\times10^{-11}$	GWP_{100}	GWP_{20}
PO1	255	0.460	0.308	0.124	-0.89	-1.18	-128	-472
PO4	239	0.456	0.315	0.121	-0.82	-1.08	-118	-432
Upp	238	0.469	0.305	0.128	-0.89	-1.23	-134	-492

To assess scenarios with seasonally varying albedo change ($\Delta\alpha=\alpha_{new}-\alpha_{ref}$), conditions for radiative transfer should be modelled with daily or monthly time steps (**Paper I**). Albedo has a self-reinforcing effect by increasing surface irradiance, such that higher α_{ref} and α_{new} result in higher impacts per unit $\Delta\alpha$. This effect is in the order of a few percent on annual time scales for typical albedo values on agricultural land. More importantly, α_{ref} and α_{new} co-vary with solar irradiance and conditions for radiative transfer on seasonal time scales (Figure 12A). Consequently, climate impacts of albedo change are not linearly related to $\Delta\alpha$. For example, among the scenarios studied in Uppsala (**Paper IV**), impacts per unit $\Delta\alpha$ were 0.21-1.13 Wm^{-2} $\Delta SW_{Surf,net}$, $0.8\text{-}1.8\times10^{-11}$ Wm^{-2} RF and 87-196 kg CO_2e with GWP_{100}.

The seasonal timing of $\Delta\alpha$ was important for potential impacts on global mean and local climate. Albedo change was most effective when it coincided with high solar irradiance and atmospheric transmittance, *e.g.* a unit $\Delta\alpha$ in June compared with December had 22 (35) times the impact on $\Delta SW_{Surf,net}$, and 30 (48) times the impact on RF and GWP in PO1 (PO4) (Figure 12B).
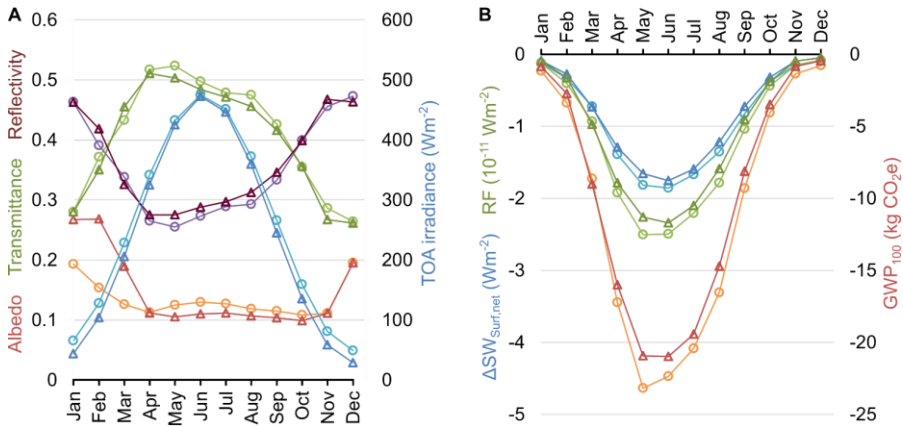
Figure 12. **A** Monthly conditions for radiative transfer and **B** monthly climate impact of 0.01 albedo increase per hectare. Values are climatological (2010-2020) averages in Swedish production regions PO1 (circles) and PO4 (triangles) based on ERA5 data.

Radiative kernels from global climate models were used as an alternative method to calculate RF. Monthly kernels per grid cell describe how a 0.01 change in surface albedo affects the TOA energy balance, and can be used for linearly relating $\Delta\alpha$ to RF. In **Paper II**, kernels derived from the CAM3, ECHAM6, CAM5 and HadGEM2 climate models were higher than the equivalent calculated with the single-layer atmosphere model in most months. However, differences between the lowest kernels and the single-layer atmosphere model were smaller than the spread between the kernels considered. The kernel method is associated with other uncertainties, *e.g.* the climatological state of a climate model may not be representative of the studied surface and atmospheric conditions. A recently developed monthly kernel based on observations provides a temporally explicit characterisation with higher spatial resolution (Bright & O'Halloran, 2019). In addition, considering co-variation of albedo and atmospheric properties on sub-monthly time scales could be relevant in periods with strong and rapid surface changes, *e.g.* due to harvest and varying snow cover on cropland.

5.3 Climate impacts in agricultural systems

In this thesis, the importance of albedo change for the climate impact of agricultural systems was evaluated primarily relative to GHG emissions from production processes, *i.e.* for crop production manufacture of inputs and fuel use by machinery (**Papers II** and **III**) and for bioenergy production also transport and combustion of wood chips (**Paper II**). Land use-related GHG fluxes (*i.e.* soil N_2O and biogenic CO_2 from and to biomass and soil) were less certain, considering actual variability in field-level emissions (section 3.6.2, Challenge 1) and uncertainty in input data and models used.

5.3.1 Production of bioenergy from SRC willow

The bioenergy system in **Paper II**, *i.e.* heat and power production from SRC willow grown on former fallow land, had a net cooling effect on global mean climate. The impact per MJ energy was -12 g CO_2e with GWP_{100}, thus fulfilling the EU sustainability criteria for solid biomass fuels and reducing emissions compared with the reference scenario (Figure 13, Table 3).
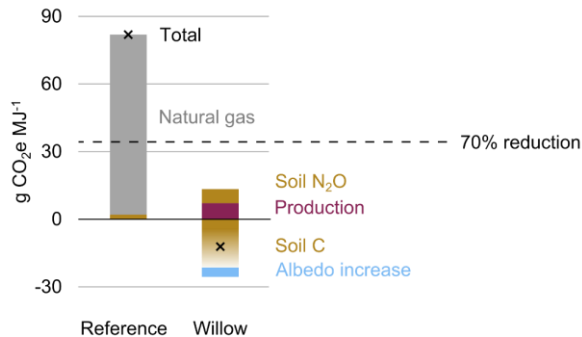
Figure 13. Climate impact of energy produced from short-rotation coppice willow and from natural gas in the reference scenario where land remained fallow, expressed as GWP_{100}. The dashed line shows the EU Renewable Energy Directive emissions savings threshold for heat and electricity produced from biomass fuels in installations starting operation in 2021-2025.

The net cooling effect in the willow scenario resulted mainly from increased soil carbon stocks under willow compared with the former fallow, owing to high carbon inputs from roots and litter. The increase was 41 Mg C ha^{-1} after 50 years, corresponding to an average uptake of 0.83 Mg C ha^{-1} yr^{-1}. The effect of soil carbon sequestration alone was sufficient to offset emissions from production (*i.e.* manufacture of inputs, field operations, transport and

combustion) and soil N_2O. The plantation stored 0-45 Mg C ha^{-1} in biomass during the study period, and captured or released high amounts of CO_2 in different years. Temporary carbon storage in biomass gave zero impact with GWP, but a cooling or warming temperature response at different times with ΔT (Table 3, Figure 14A).

Albedo was 31% higher under willow (0.216) than fallow (0.165). Increased albedo countered the GHG impact from production by around 60% measured with GWP$_{100}$, 200% with GWP$_{20}$, 10% with $\Delta T[100]$ and 120% with $\Delta T[50]$ (Table 3). Thus, the cooling effect from increased albedo was of similar magnitude to the warming effect from production during the study period. Considering all system components, albedo change dominated the short-term temperature response (<20 years) but became less important over time in relative terms, owing to accumulation of soil carbon under sustained production and the longer perturbation lifetime of GHGs (Figure 14A).

Table 3. Climate impact in the willow and reference scenarios with alternative functional units (1 MJ energy, 1 ha and yr, 1 ha) and metrics (global warming potential (GWP) with a 100 and 20 year time horizon in CO_2e and global mean surface temperature change (ΔT) in year 100 and 50). Results can be converted between functional units based on energy output (7072 GJ ha^{-1} during the 50-year study period). Production includes manufacture of inputs and field operations and for willow also transport and combustion of wood chips. Natural gas includes life-cycle greenhouse gas emissions from production, distribution and combustion.

	GWP$_{100}$ g MJ^{-1}	GWP$_{100}$ kg ha^{-1} yr^{-1}	GWP$_{100}$ Mg ha^{-1}	GWP$_{20}$ Mg ha^{-1}	$\Delta T[100]$ 10^{-11} K ha^{-1}	$\Delta T[50]$ 10^{-11} K ha^{-1}
Willow	-12.2	-1,723	-86	-165	-3.8	-10.1
Production	7.1	1,003	50	53	2.6	3.0
Biomass C	0	0	0	0	0.3	-3.2
Soil C	-21.5	-3,034	-152	-152	-8.7	-8.7
Soil N_2O	6.3	886	44	40	2.2	2.4
Albedo	-4.1	-578	-29	-106	-0.2	-3.7
Reference	81.9	11,582	579	688	30.0	37.3
Production	0.1	18	1	1	0.1	0.1
Biomass C	0	0	0	0	0	0
Soil C	0	0	0	0	0	0
Soil N_2O	1.9	263	13	12	0.7	0.7
Albedo	0	0	0	0	0	0
Natural gas	79.9	11,301	565	675	29.3	36.5
Net impact	-94.1	-13,305	-665	-853	-33.9	-47.4
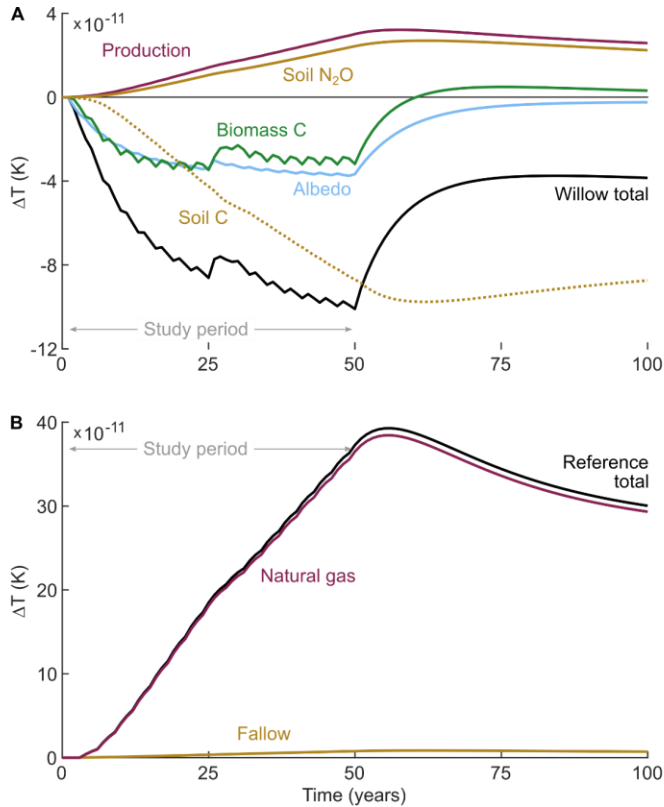
Figure 14. Climate impact per hectare as global mean surface temperature change (ΔT) in **A** the willow scenario, where production includes manufacture of inputs, field operations, transport and combustion of wood chips, and **B** the reference scenario, where fallow summarises diesel production and use for field operations and soil N_2O. Natural gas includes life-cycle greenhouse gas emissions from production, distribution and combustion.

The reference scenario had a warming effect, mainly due to the use of natural gas and to a small extent due to fallow land (Table 3). The impact was of opposite sign and with GWP_{100} nearly seven times that of the willow scenario. Thus, avoiding emissions gave the greatest mitigation potential in the case study, particularly by substituting bioenergy for natural gas.

The choice of metric did not change the overall conclusions regarding the willow and reference scenarios, but it critically affected the relative importance of forcing agents. Expressing impacts as a function of time, as with ΔT in Figure 14, provided additional information about the timing, magnitude and rate of change caused by GHG emissions, biogenic carbon fluxes and albedo change.

5.3.2 Production of crops

Production of different crops on current cropland in PO1 relative to a situation without cultivation (**Paper III**) had a net warming effect on global mean climate (Table 4). Formation of N_2O from applied mineral fertiliser and crop residues led to high impacts for crops with high fertilisation levels (*e.g.* winter wheat) or high inputs of N-rich residues (*e.g.* sugar beet). Mineral nitrogen fertiliser was also responsible for 90% of emissions from manufacture of inputs. Soil acted as a carbon sink under ley and winter rapeseed due to high productivity and carbon inputs, particularly from roots. Under all other crops, the long-term soil carbon balance was negative, *i.e.* mineralisation outweighed carbon inputs over a 100-year period, when assuming that 45% of cereal straw was removed on average in PO1.

The potential for albedo-related cooling was highest with ley, winter rapeseed and winter wheat. Albedo increased by 6-11% under different crops relative to the semi-natural reference and countered the GHG impact from production (*i.e.* manufacture of inputs and field operations) by 17-47%, measured in GWP_{100}. Total net GHG emissions were 7-20 times higher than under the semi-natural reference, thus explaining the overall warming effect, which ranged from ~500 kg CO_2e ha^{-1} for ley to ~2500 kg CO_2e ha^{-1} for spring wheat with GWP_{100} (Table 4).

Table 4. Climate impact of production of different crops relative to the land reference, expressed as global warming potential (GWP_{100}, kg CO_2e ha^{-1} yr^{-1}). Impacts are presented relative to a theoretical reference with no emissions and albedo of 0, to show the influence of the chosen reference situation on the result, and relative to a situation without cultivation (semi-natural grassland). Inputs include manufacture of mineral fertilisers, pesticides and seeds. Field operations include production and use of diesel. W = winter, S = spring.

| | Theoretical "zero" reference | | | | | Semi-natural | |
	Albedo	Inputs	Field ops	Soil N_2O	Soil C	ΔAlb	ΔGHGs
W wheat	-2495	784	172	1680	182	-232	2676
W rye	-2407	560	167	1236	258	-144	2081
W rapeseed	-2513	514	145	1322	-126	-250	1715
S wheat	-2416	730	164	1479	379	-153	2612
S barley	-2437	417	171	943	323	-174	1713
Sugar beet	-2398	336	290	1414	395	-135	2293
Ley	-2541	494	96	1099	-758	-278	791
Semi-natural	-2263	0	0	140	0	0	0

Even small changes in albedo led to considerable RF at the field scale and quantifiable climate impacts with GWP_{100}, *e.g.* 0.009 (6%) albedo increase under sugar beet resulted in -135 kg CO_2e ha^{-1} (Table 4). Thus, robust data are needed to establish representative albedo values that can be used for modelling albedo change (*e.g.* 10 years as in this thesis or a typical year) and potential impacts on climate.

When using GWP_{20} as a metric, impacts of albedo change were generally 3.7 times as high with as with GWP_{100} (section 5.2), whereas net GHG impacts were slightly lower due to the dominance of long-lived GHGs (N_2O and CO_2) in the scenarios studied. With GWP_{20}, increased albedo countered 59-160% of the GHG impact from production. The overall effect was then net cooling for ley (around -300 kg CO_2e ha^{-1}), but still net warming for other crops, ranging from ~700 kg CO_2e ha^{-1} for winter rapeseed to ~2000 kg CO_2e ha^{-1} for spring wheat. In all crop production scenarios, increased albedo was able to offset a substantial proportion of the RF deriving from field-level GHG emissions on short time scales. Thus, when using ΔT, individual crops gave a net cooling effect for 3-12 years due to increased albedo, but a net warming effect on longer time scales due to GHG emissions.

5.3.3 Choice of crop and cultivation practices

Comparison of various crops and cultivation practices in Uppsala 2019-2020 showed that keeping the dark clay soil covered year-round was a crucial factor for reducing annual mean net SW irradiance (**Paper IV**). Among the different measures to improve soil coverage evaluated, avoiding black fallow by growing grass had the greatest effect, because albedo was significantly higher during the entire year (Figure 15). Annual albedo increased by 0.07 (55%), leading to -6.6 Wm^{-2} $\Delta SW_{Surf,net}$, -9.0×10^{-11} Wm^{-2} RF and -1000 kg CO_2e with GWP_{100} (and 3.7 times higher values with GWP_{20}).

Other measures increased albedo in autumn and spring, *e.g.* growing ley or winter-sown varieties instead of spring crops, and generated at least half the cooling effect (Figure 15). Measures related to residue management and tillage after harvest affected albedo during a short period in late summer and autumn and had a smaller impact on annual mean climate. For example, termination of ley later in autumn increased albedo by 0.014 (7%) and led to -1.3 Wm^{-2} $\Delta SW_{Surf,net}$, -1.7×10^{-11} Wm^{-2} RF and -200 kg CO_2e with GWP_{100}. Effects of similar magnitude have been reported by Liu *et al.* (2021).
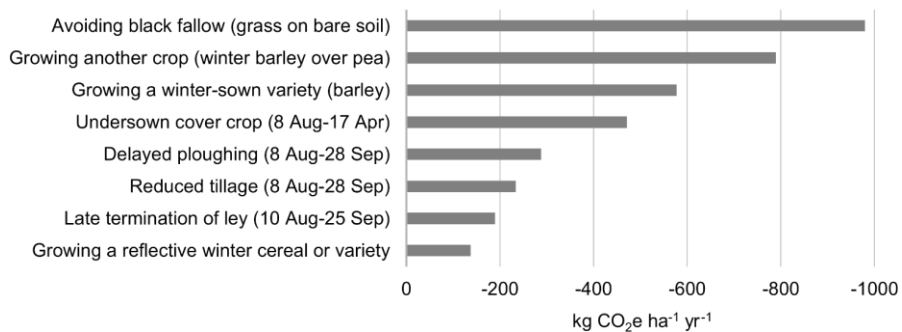
Figure 15. Climate impact of different measures to increase albedo on cropland per hectare and year, expressed as GWP_{100}.

Field-measured albedo values for bare soil and extensive ley were used to estimate the potential benefit of cultivating a cover crop undersown into a winter cereal and covering the soil from harvest of the winter cereal until sowing of the next crop in the following spring. The estimated cooling potential was -500 kg CO_2e with GWP_{100}, which was in agreement with previous findings (Kaye & Quemada, 2017). Among the winter and spring cereals studied, barley had the highest albedo. Measured albedo values could be used to estimate the potential benefit of an early-establishing, reflective cereal cultivar, *e.g.* by comparing winter barley with winter rye, while accounting for differences in post-harvest management. In that case, the estimated cooling potential was -140 kg CO_2e with GWP_{100}.

Locally, albedo increases in early spring, when soil temperature and moisture restrict tillage and plant growth, might not be desirable. Albedo increases could be most effective at reducing hot temperatures in summer. For example in June-July, oats reduced $SW_{Surf,net}$ by 0.8-5.8 Wm^{-2} compared with other cereals, ley, peas and rapeseed. Delayed or reduced tillage between early-harvested winter cereals and spring-sown crops had high cooling potential in late summer (up to -9.5 Wm^{-2} in August-September).

Overall, these examples illustrate that agricultural practices may differ in terms of albedo-related effects on global mean climate and on seasonal or peak temperatures at the local scale. To evaluate local or regional impacts, additional factors such as changes in soil moisture, evapotranspiration and cloud cover need to be considered (Bagley *et al.*, 2015; Davin *et al.*, 2014; Doughty *et al.*, 2011). Some of the shifts in crops and varieties evaluated here may be encouraged by longer and warmer growing seasons in Northern Europe due to climate change (Peltonen-Sainio & Jauhiainen, 2020).

6. General discussion and perspectives

Improving the climate performance of agricultural systems requires tools to assess and prioritise options to reduce emissions and enhance carbon sinks, while considering the biophysical effects of individual practices. The data presented in this thesis improve understanding of albedo on cropland, considering individual crops, agricultural practices and environmental conditions. Seasonal patterns in albedo and variability across years and sites were analysed. Such data have a range of scientific applications, notably to assess albedo-related effects of agricultural land use on different climate variables at local or global scale.

In this thesis, direct effects of albedo change on net SW irradiance at the surface and TOA were assessed. Changes in $SW_{Surf,net}$ were analysed on sub-annual time scales, to consider potential effects on seasonal and peak temperatures, which might be most relevant at the local scale. Annual RF at the TOA was converted to global mean temperature change (ΔT) over time and to GWP, for comparison with the effects of GHG fluxes. This information can be used to evaluate the importance of albedo change for the climate impact of agricultural systems and of future responses to global warming, *e.g.* land-based mitigation measures or zonal and temporal shifts in crops and varieties due to changing growing seasons in Northern Europe.

6.1 Methodological aspects

In this thesis, LCA was performed to obtain a perspective on the importance of albedo change for the climate impact of agricultural systems, relative to GHG emissions and carbon sequestration in biomass and soil. Time-dependent LCA methodology provided a useful framework for assessing biomass-based systems relative to a consistently defined reference, and to

compare climate impacts considering the time dependence of RF caused by albedo change and GHG fluxes. Evaluating climate impacts by system component and over time generated information about the drivers behind impacts and when impacts occur. This is one approach to gain a better understanding of albedo-related effects in agricultural systems. Other methods are needed to account for non-radiative effects and to assess changes in local temperature and moisture regimes.

LCA studies offer a systemic understanding of potential environmental impacts at comparatively low complexity. LCA is useful as a screening tool, to detect hotspots and identify strategies for improvement without burden shifting (Hellweg & Milà i Canals, 2014). In contrast to observations and land-climate models, LCA extends the scope from field to systems level, to include processes along the life cycle irrespective of timing and location (Finnveden *et al.*, 2009). In the LCA in this thesis, field-level effects were captured (*e.g.* biogenic CO_2, N_2O and radiation fluxes) and also emissions from the manufacture of inputs, fuel consumption, processing and transport.

Inclusion of albedo in LCA could have various applications. LCA is widely used to evaluate the climate performance of products and systems that involve land use, such as biofuels, food or materials. Land use effects are increasingly being considered in LCA studies, especially in the context of growing biofuel production. In this context, researchers have also advocated evaluating biophysical effects, in particular due to albedo change (Creutzig *et al.*, 2015). The methods presented in this thesis could support such increasingly comprehensive assessments. Adopting a systems perspective on agricultural practices could also be useful to explore how *e.g.* increased residue utilisation, integration of cover crops or ley in crop rotations or agroforestry affect the climate due to albedo change and GHG fluxes.

This thesis demonstrated that robust quantification of albedo change requires extensive data and modelling. Inclusion of albedo in LCA might therefore not be feasible as a routine application. Moreover, for a meaningful interpretation of potential climate impacts due to albedo change, a good understanding of the climate system and climate metrics is needed.

6.2   Role of albedo for climate mitigation and adaptation

Albedo change is playing an increasing role in discussions on land-based climate change mitigation and adaptation. In this context, it is important to

consider that land use effects via albedo change and carbon sequestration act on different temporal and spatial scales (Erb *et al.*, 2017). As new management practices are implemented, albedo change can take immediate effect and persist over time, whereas carbon stocks respond slowly and reach a new equilibrium. Moreover, albedo change imposes immediate effects on local and global radiation balances, whereas carbon fluxes invoke a slow response in the global carbon cycle and lead to delayed climate forcing. These differences have consequences for the timing of impacts, and also for the permanence and reversibility of RF. For example, maintaining elevated soil carbon stocks requires continued inputs, but the net uptake of carbon ceases once a new equilibrium has been reached. Terminating the management regime could result in re-emission of carbon and thus warming, whereas albedo might be restored with no further impact.

The local, immediate effect of albedo changes makes them an attractive option for adaptation to climate change. Albedo increase on cropland could dampen warming at local to regional scale and alleviate extreme heat (Davin *et al.*, 2014; Seneviratne *et al.*, 2018; Singarayer & Davies-Barnard, 2012). Such adaptation strategies could prioritise albedo increase in summer, and not necessarily those agricultural practices which provide the highest annual mean albedo or lowest RF.

6.3 Agricultural practices and albedo effects

Agricultural practices can strongly influence field-level albedo on seasonal and annual time scales. Under the conditions studied in this thesis, choosing crops with a long growing season gave increased albedo in spring and autumn. SRC willow, perennial ley and winter crops also had higher annual albedo than spring-sown crops and bare soil. This agrees with previous findings showing benefits of growing perennials or cover crops, especially on dark soil types (Lugato *et al.*, 2020; Miller *et al.*, 2016). Further research is needed to confirm the observed albedo increases under specific crop species, such as winter rapeseed and winter barley. Recent work indicates progress on characterising albedo for a range of individual crops at regional level based on satellite observations (Starr *et al.*, 2020).

Field measurements made in Uppsala showed that management practices affected the albedo of unvegetated fields. Between harvest and sowing of the next crop, residue retention and delayed or reduced tillage increased albedo

compared with direct ploughing. Similar observations have been made elsewhere (Davin *et al.*, 2014; Liu *et al.*, 2021). However, the effect is likely to be smaller in Northern Europe, due to later harvest dates and low incoming radiation in the period September-March.

Albedo increase on cropland may conflict with other objectives of agricultural systems. Nevertheless, farmers have several opportunities to increase albedo while contributing to crop production and soil quality. These include:

- Selection of winter varieties over spring varieties
- Selection of perennial over annual energy crops
- Residue retention and reduced or delayed tillage
- Growing cover crops between winter and spring crops
- Inclusion of ley in crop rotations
- Planting unused cropland or field margins
- Cultivation of SRC willow on fallow land

Some of these measures could provide co-benefits for soil fertility and carbon stocks, reduced leaching and erosion and biodiversity. However, trade-offs could arise, relating to soil N_2O emissions, alternative uses of straw, workload, cost and additional inputs such as herbicides and fuel.

6.4   Outlook and future research

The methods developed in this thesis could contribute to systematic and increasingly comprehensive assessments of climate impacts in agricultural systems. This work addressed the effects of individual agricultural practices on albedo, included carbon stocks and life-cycle GHG emissions and evaluated climate impacts based on radiative mechanisms. The radiation balance is the fundamental driver of the climate system and linked to global mean temperature, but the RF concept has specific limitations for land use climate impacts (Betts *et al.*, 2007; Davin & de Noblet-Ducoudré, 2010). Future work could consider the effects of non-radiative processes, rapid adjustments and spatial distribution of the forcing on the global mean temperature response (Bright & Lund, 2021).

Locally, changes in net SW irradiance driven by albedo may not be a good proxy for the effects of land use on surface temperature. Albedo change itself can affect the partitioning of available energy into sensible and latent heat

flux, while agricultural practices most likely alter several surface properties jointly. The radiative effects of albedo change quantified in this thesis could be combined with measures of energy redistribution at the surface, or of the relative contribution of non-radiative mechanisms to the local surface temperature response. Such measures have been mapped globally for conversions between major vegetation cover types (Bright *et al.*, 2017), but are currently not available at the level of individual crops or practices addressed here.

Future research could integrate different methods and provide practical guidance at the level of agricultural land use and management practices, considering effects through the surface and TOA energy balances. For example, Duveiller *et al.* (2020) proposed a tiered approach, similar to the IPCC methodology for GHG accounting (IPCC, 2006), to assess the biophysical effects of land use on local near-surface air temperature. A prototype and data for Tier 1-2 at the level of major vegetation cover types are provided in Duveiller *et al.* (2020), but methods with finer granularity in terms of land use and management, spatial and temporal resolution need to be developed. The proposed method improves consideration of biophysical mechanisms, but not their effect on local moisture regimes, other climate variables (*e.g.* precipitation) or seasonal temperatures and extremes. Further research is needed to integrate various effects of land use on climate and direct and indirect consequences from a systems perspective.

Finally, land use and agricultural practices need to be evaluated in a broader environmental and societal context. Land has a range of regulating, provisioning and cultural functions (IPCC, 2019), which are related to *e.g.* biodiversity, food and energy security, income, health and recreation. For example, the results showing benefits of SRC willow on former green fallow (**Paper II**) need to be balanced against the potential value of extensive grassland for biodiversity and recreation, and the cost of willow production relative to market prices for wood chips. The crops and practices evaluated in **Papers III** and **IV** represented possible management options rather than alternatives, because they were not functionally equal. Agronomic factors also need to be considered, such as cost, yield, synergistic effects in crop rotations and interdependencies with food, livestock and energy systems.

7. Conclusions

When evaluating climate impacts of agricultural systems, LCA has merits as a relatively fast and flexible screening tool which allows hotspots or trade-offs in complex systems to be identified. In this thesis, LCA methodology also aided the attribution of impacts to individual drivers.

In this work, potential impacts of albedo change on global mean climate were assessed based on first-order radiative effects. This allowed the impact of albedo change to be related to that of GHG fluxes in agricultural systems, and potential trade-offs or synergies between emissions reduction, carbon sequestration and albedo change to be evaluated. Impacts of albedo change on net SW irradiance at the surface were also analysed, to consider potential effects at the local scale. However, complementary methods are needed to account for non-radiative processes and to assess effects on local temperature and moisture regimes.

Time-dependent LCA methods can improve comparison of climate forcers with different perturbation lifetimes. Explicit consideration of time allows temporally varying emissions, removals and RF to be represented. In this thesis, time-dependent methods proved useful for comparing the impacts of temporary albedo change and long-lived GHGs, and for assessing multi-year dynamic systems such as bioenergy production from SRC willow.

Crop production can cause similar quantifiable impacts from albedo change and GHG fluxes. When using GWP as a metric in case studies, impacts of albedo RF were generally 3.7 times as high when assessed over a 20-year TH instead of the more common 100-year TH. In contrast, impacts of GHGs were slightly lower with GWP_{20}, due to the dominance of long-lived GHGs

(N_2O and CO_2) in the systems studied. Using ΔT, albedo change dominated the short-term temperature response but became less important over time in relative terms, due to the longer perturbation lifetime of GHGs.

Albedo on cropland is influenced by the crops grown, management practices, soil type, climate and weather. Thus, it can vary strongly between fields, regions and observation times. In this thesis, field-measured albedo proved useful for analysing differences between crops and management practices in specific fields and years. Crop-specific albedo obtained from MODIS products enabled estimation of the variation in a large number of fields and years, resulting from differing site characteristics, management practices and weather (*e.g.* precipitation and snow cover). The MODIS-based methods developed proved useful for deriving representative albedo values of crops cultivated on a large scale, and for systematically assessing albedo effects of crop production at regional level.

The strength of albedo change as a climate forcer depends on where and when it occurs. Analysis of geographical and seasonal variations in albedo, solar irradiance and atmospheric transmittance helped anticipate the potential magnitude of effect on global mean and local climate. The results can be used to guide efforts to model climate impacts in more detail. In the Swedish case studies in this thesis, high albedo changes due to snow in November-February had small effects, whereas small changes in summer sometimes had a high impact.

A significant finding was that bioenergy produced from SRC willow grown on former fallow land had a net cooling effect on global mean climate (-12 g CO_2e MJ^{-1} with GWP_{100}). This effect resulted from soil carbon sequestration and 31% higher albedo under willow than fallow. Even greater mitigation potential derived from the substitution of natural gas (-80 g CO_2e MJ^{-1} with GWP_{100}). In the willow scenario, increased albedo countered the calculated GHG impact from production (*i.e.* total GHGs excluding land use effects) by ~60% with GWP_{100} and ~200% with GWP_{20}. These results reflect the strong influence of choice of TH on the relative importance of albedo change. The timing of impacts was explicit with ΔT, showing that the cooling effect from increased albedo was of similar magnitude to the warming effect from production emissions during the study period, but smaller afterwards.

A further major finding was that production of different crops, relative to a situation without cultivation, led to competing effects on global mean temperature with cooling from increased albedo and warming from increased GHG emissions. Measured in GWP_{100}, this resulted in an overall warming effect ranging from ~500 kg CO_2e ha^{-1} for ley to ~2500 kg CO_2e ha^{-1} for spring wheat. Albedo increased by 6-11% under different crops and countered the effect of production emissions by 17-47% when using GWP_{100}. When using GWP_{20}, increased albedo countered 59-160% of the GHG impact from production. The overall effect was then net cooling for ley (around -300 kg CO_2e ha^{-1}), but still net warming for other crops. Choice of TH did not change the ranking of crops in terms of climate impact, but it affected whether ley had a net warming or cooling impact. When using ΔT, individual crops gave a cooling effect for 3-12 years due to increased albedo, but a net warming effect on longer time scales due to GHG emissions.

Field measurements performed in Uppsala 2019-2020 showed that annual albedo was higher with perennial ley (0.20-0.22) and winter-sown crops (0.18-0.22), which have a long growing season, than with spring-sown crops (0.16-0.18) and bare soil (0.13). Potential benefits for the global mean climate, expressed as GWP_{100} per hectare and year, could reach around -1000 kg CO_2e for avoiding black fallow, -600 kg CO_2e for growing a winter-sown variety and -300 kg CO_2e for delayed or reduced tillage. In summer, when increased albedo could alleviate local heat stress, oats reduced $\Delta SW_{Surf,net}$ by 0.8-5.8 Wm^{-2} compared with other cereals, ley, peas or rapeseed. Delayed or reduced tillage gave high local cooling potential (up to -9.5 Wm^{-2}) in late summer.

Overall, this thesis showed that small changes in annual albedo can lead to considerable RF at the field scale and to similar quantifiable climate impacts as production emissions (*i.e.* life-cycle GHG emissions excluding land use-related fluxes of N_2O and biogenic CO_2), measured in GWP, although the choice of metric may critically affect the outcome. It also showed that using ΔT can provide new insights on the magnitude and timing of impacts.

References

Aamaas, B., Peters, G. P., & Fuglestvedt, J. S. (2013). Simple emission metrics for climate impacts. *Earth Syst. Dynam., 4*(1), 145-170. doi:10.5194/esd-4-145-2013

Allen, M. R., Fuglestvedt, J. S., Shine, K. P., et al. (2016). New use of global warming potentials to compare cumulative and short-lived climate pollutants. *Nature Climate Change, 6*(8), 773-776. doi:10.1038/nclimate2998

Andrén, O., Kätterer, T., & Karlsson, T. (2004). ICBM regional model for estimations of dynamics of agricultural soil carbon pools. *Nutrient Cycling in Agroecosystems, 70*(2), 231-239. doi:10.1023/B:FRES.0000048471.59164.ff

Andrews, T., Betts, R. A., Booth, B. B. B., et al. (2017). Effective radiative forcing from historical land use change. *Climate Dynamics, 48*(11), 3489-3505. doi:10.1007/s00382-016-3280-7

Bagley, J. E., Davis, S. C., Georgescu, M., et al. (2014). The biophysical link between climate, water, and vegetation in bioenergy agro-ecosystems. *Biomass and Bioenergy, 71*, 187-201. doi:10.1016/j.biombioe.2014.10.007

Bagley, J. E., Miller, J., & Bernacchi, C. J. (2015). Biophysical impacts of climate-smart agriculture in the Midwest United States. *Plant, cell & environment, 38*(9), 1913-1930. doi:10.1111/pce.12485

Bessou, C., Tailleur, A., Godard, C., et al. (2020). Accounting for soil organic carbon role in land use contribution to climate change in agricultural LCA: which methods? Which impacts? *The International Journal of Life Cycle Assessment, 25*(7), 1217-1230. doi:10.1007/s11367-019-01713-8

Betts, R. A. (2000). Offset of the potential carbon sink from boreal forestation by decreases in surface albedo. *Nature, 408*(6809), 187-190. doi:10.1038/35041545

Betts, R. A., Falloon, P. D., Goldewijk, K. K., & Ramankutty, N. (2007). Biogeophysical effects of land use on climate: Model simulations of radiative forcing and large-scale temperature change. *Agricultural and Forest Meteorology, 142*(2-4), 216-233. doi:10.1016/j.agrformet.2006.08.021

Bird, D. N., Kunda, M., Mayer, A., et al. (2008). Incorporating changes in albedo in estimating the climate mitigation benefits of land use change projects. *Biogeosciences Discussions, 5*(2), 1511-1543.

Bonan, G. (2008). Forests and climate change: Forcings, feedbacks, and the climate benefits of forests. *Science, 320*(5882), 1444-1449. doi:10.1126/science.1155121

Bonan, G. (2015). *Ecological Climatology: Concepts and Applications* (3 ed.). Cambridge: Cambridge University Press.

Boucher, O., & Reddy, M. S. (2008). Climate trade-off between black carbon and carbon dioxide emissions. *Energy Policy, 36*(1), 193-200. doi:10.1016/j.enpol.2007.08.039

Brandão, M., Levasseur, A., Kirschbaum, M. U. F., et al. (2013). Key issues and options in accounting for carbon sequestration and temporary storage in life cycle assessment

and carbon footprinting. *International Journal of Life Cycle Assessment, 18*(1), 230-240. doi:10.1007/s11367-012-0451-6

Brandão, M., Milà i Canals, L., & Clift, R. (2011). Soil organic carbon changes in the cultivation of energy crops: Implications for GHG balances and soil quality for use in LCA. *Biomass and Bioenergy, 35*(6), 2323-2336. doi:10.1016/j.biombioe.2009.10.019

Bright, R. M., Cherubini, F., & Stromman, A. H. (2012). Climate impacts of bioenergy: Inclusion of carbon cycle and albedo dynamics in life cycle impact assessment. *Environmental Impact Assessment Review, 37*, 2-11. doi:10.1016/j.eiar.2012.01.002

Bright, R. M., Davin, E., O'Halloran, T., et al. (2017). Local temperature response to land cover and management change driven by non-radiative processes. *Nature Climate Change, 7*(4), 296-302. doi:10.1038/nclimate3250

Bright, R. M., & Lund, M. T. (2021). CO2-equivalence metrics for surface albedo change based on the radiative forcing concept: a critical review. *Atmos. Chem. Phys., 21*(12), 9887-9907. doi:10.5194/acp-21-9887-2021

Bright, R. M., & O'Halloran, T. L. (2019). Developing a monthly radiative kernel for surface albedo change from satellite climatologies of Earth's shortwave radiation budget: CACK v1.0. *Geosci. Model Dev., 12*(9), 3975-3990. doi:10.5194/gmd-12-3975-2019

Bright, R. M., Stromman, A. H., & Peters, G. P. (2011). Radiative Forcing Impacts of Boreal Forest Biofuels: A Scenario Study for Norway in Light of Albedo. *Environmental Science & Technology, 45*(17), 7570-7580. doi:10.1021/es201746b

Bright, R. M., Zhao, K. G., Jackson, R. B., & Cherubini, F. (2015). Quantifying surface albedo and other direct biogeophysical climate forcings of forestry activities. *Global Change Biology, 21*(9), 3246-3266. doi:10.1111/gcb.12951

Cai, H., Wang, J., Feng, Y., et al. (2016). Consideration of land use change-induced surface albedo effects in life-cycle analysis of biofuels. *Energy & Environmental Science, 9*(9), 2855-2867. doi:10.1039/c6ee01728b

Caiazzo, F., Malina, R., Staples, M. D., et al. (2014). Quantifying the climate impacts of albedo changes due to biofuel production: a comparison with biogeochemical effects. *Environmental Research Letters, 9*(2). doi:10.1088/1748-9326/9/2/024015

Cao, V., Margni, M., Favis, B. D., & Deschênes, L. (2017). Choice of land reference situation in life cycle impact assessment. *The International Journal of Life Cycle Assessment, 22*(8), 1220-1231. doi:10.1007/s11367-016-1242-2

Cederberg, C., Henriksson, M., & Berglund, M. (2013). An LCA researcher's wish list – data and emission models needed to improve LCA studies of animal production. *Animal, 7*, 212-219. doi:10.1017/S1751731113000785

Cescatti, A., Marcolla, B., Santhana Vannan, S. K., et al. (2012). Intercomparison of MODIS albedo retrievals and in situ measurements across the global FLUXNET network. *Remote Sensing of Environment, 121*, 323-334. doi:10.1016/j.rse.2012.02.019

Ceschia, E., Béziat, P., Dejoux, J. F., et al. (2010). Management effects on net ecosystem carbon and GHG budgets at European crop sites. *Agriculture, Ecosystems & Environment, 139*(3), 363-383. doi:10.1016/j.agee.2010.09.020

Cherubini, F., Bird, N. D., Cowie, A., et al. (2009). Energy- and greenhouse gas-based LCA of biofuel and bioenergy systems: Key issues, ranges and recommendations. *Resources Conservation and Recycling, 53*(8), 434-447. doi:10.1016/j.resconrec.2009.03.013

Cherubini, F., Bright, R. M., & Stromman, A. H. (2012). Site-specific global warming potentials of biogenic CO2 for bioenergy: contributions from carbon fluxes and albedo dynamics. *Environmental Research Letters, 7*(4). doi:10.1088/1748-9326/7/4/045902

Cherubini, F., Peters, G. P., Berntsen, T., et al. (2011). CO2 emissions from biomass combustion for bioenergy: atmospheric decay and contribution to global warming. *GCB Bioenergy, 3*(5), 413-426. doi:10.1111/j.1757-1707.2011.01102.x

Creutzig, F., Ravindranath, N. H., Berndes, G., et al. (2015). Bioenergy and climate change mitigation: an assessment. *GCB Bioenergy, 7*(5), 916-944. doi:10.1111/gcbb.12205

Davies-Barnard, T., Valdes, P. J., Singarayer, J. S., et al. (2014). Full effects of land use change in the representative concentration pathways. *Environmental Research Letters, 9*(11). doi:10.1088/1748-9326/9/11/114014

Davin, E. L., & de Noblet-Ducoudré, N. (2010). Climatic Impact of Global-Scale Deforestation: Radiative versus Nonradiative Processes. *Journal of Climate, 23*(1), 97-112. doi:10.1175/2009JCLI3102.1

Davin, E. L., de Noblet-Ducoudré, N., & Friedlingstein, P. (2007). Impact of land cover change on surface climate: Relevance of the radiative forcing concept. *Geophysical Research Letters, 34*(13). doi:10.1029/2007gl029678

Davin, E. L., Seneviratne, S. I., Ciais, P., et al. (2014). Preferential cooling of hot extremes from cropland albedo management. *Proceedings of the National Academy of Sciences of the United States of America, 111*(27), 9757-9761. doi:10.1073/pnas.1317323111

Devaraju, N., de Noblet-Ducoudré, N., Quesada, B., & Bala, G. (2018). Quantifying the Relative Importance of Direct and Indirect Biophysical Effects of Deforestation on Surface Temperature and Teleconnections. *Journal of Climate, 31*(10), 3811-3829. doi:10.1175/jcli-d-17-0563.1

Dickinson, R. E. (1983). Land surface processes and climate - Surface albedos and energy balance. *Advances in Geophysics, 25*, 305-353. doi:10.1016/S0065-2687(08)60176-4

Doughty, C. E., Field, C. B., & McMillan, A. M. S. (2011). Can crop albedo be increased through the modification of leaf trichomes, and could this cool regional climate? *Climatic Change, 104*(2), 379-387. doi:10.1007/s10584-010-9936-0

Duveiller, G., Caporaso, L., Abad-Viñas, R., et al. (2020). Local biophysical effects of land use and land cover change: towards an assessment tool for policy makers. *Land Use Policy, 91*, 104382. doi:10.1016/j.landusepol.2019.104382

Erb, K.-H., Luyssaert, S., Meyfroidt, P., et al. (2017). Land management: data availability and process understanding for global change studies. *Global Change Biology, 23*(2), 512-533. doi:10.1111/gcb.13443

Ericsson, N., Porsö, C., Ahlgren, S., et al. (2013). Time-dependent climate impact of a bioenergy system - methodology development and application to Swedish conditions. *GCB Bioenergy, 5*(5), 580-590. doi:10.1111/gcbb.12031

FAO. (2021). FAOSTAT Emissions Totals. Retrieved 2021-11-06, from Food and Agriculture Organization of the United Nations (FAO) https://www.fao.org/faostat/en/#data/GT

Finnveden, G., Hauschild, M. Z., Ekvall, T., et al. (2009). Recent developments in Life Cycle Assessment. *Journal of Environmental Management, 91*(1), 1-21. doi:10.1016/j.jenvman.2009.06.018

Foley, J. A., DeFries, R., Asner, G. P., et al. (2005). Global Consequences of Land Use. *Science, 309*(5734), 570. doi:10.1126/science.1111772

Gao, F., Schaaf, C. B., Strahler, A. H., et al. (2005). MODIS bidirectional reflectance distribution function and albedo Climate Modeling Grid products and the variability of albedo for major global vegetation types. *Journal of Geophysical Research: Atmospheres, 110*(D1). doi:10.1029/2004JD005190

Gasser, T., Peters, G. P., Fuglestvedt, J. S., et al. (2017). Accounting for the climate–carbon feedback in emission metrics. *Earth Syst. Dynam., 8*(2), 235-253. doi:10.5194/esd-8-235-2017

Genesio, L., Bassi, R., & Miglietta, F. (2021). Plants with less chlorophyll: A global change perspective. *Global Change Biology, 27*(5), 959-967. doi:10.1111/gcb.15470

Georgescu, M., Lobell, D. B., & Field, C. B. (2011). Direct climate effects of perennial bioenergy crops in the United States. *Proceedings of the National Academy of Sciences of the United States of America, 108*(11), 4307-4312. doi:10.1073/pnas.1008779108

Ghimire, B., Williams, C. A., Masek, J., et al. (2014). Global albedo change and radiative cooling from anthropogenic land cover change, 1700 to 2005 based on MODIS, land use harmonization, radiative kernels, and reanalysis. *Geophysical Research Letters, 41*(24), 9087-9096. doi:10.1002/2014GL061671

Giuntoli, J., Bulgheroni, C., Marelli, L., et al. (2019). *Brief on the use of Life Cycle Assessment (LCA) to evaluate environmental impacts of the bioeconomy*. Publications Office of the European Union. Luxembourg.

Goglio, P., Smith, W. N., Grant, B. B., et al. (2018). A comparison of methods to quantify greenhouse gas emissions of cropping systems in LCA. *Journal of Cleaner Production, 172*, 4010-4017. doi:10.1016/j.jclepro.2017.03.133

Goglio, P., Smith, W. N., Grant, B. B., et al. (2015). Accounting for soil carbon changes in agricultural life cycle assessment (LCA): a review. *Journal of Cleaner Production, 104*, 23-39. doi:10.1016/j.jclepro.2015.05.040

Griscom, B. W., Adams, J., Ellis, P. W., et al. (2017). Natural climate solutions. *Proceedings of the National Academy of Sciences, 114*(44), 11645-11650. doi:10.1073/pnas.1710465114

Guardia, G., Aguilera, E., Vallejo, A., et al. (2019). Effective climate change mitigation through cover cropping and integrated fertilization: A global warming potential assessment from a 10-year field experiment. *Journal of Cleaner Production, 241*, 118307. doi:10.1016/j.jclepro.2019.118307

Hansen, J., Sato, M., Ruedy, R., et al. (2005). Efficacy of climate forcings. *Journal of Geophysical Research-Atmospheres, 110*(D18). doi:10.1029/2005jd005776

Hellweg, S., & Milà i Canals, L. (2014). Emerging approaches, challenges and opportunities in life cycle assessment. *Science, 344*(6188), 1109-1113. doi:10.1126/science.1248361

Henryson, K., Kätterer, T., Tidåker, P., & Sundberg, C. (2020). Soil N2O emissions, N leaching and marine eutrophication in life cycle assessment – A comparison of modelling approaches. *Science of The Total Environment, 725*, 138332. doi:10.1016/j.scitotenv.2020.138332

Hergoualc'h, K., Akiyama, H., Bernoux, M., Chirinda, N., Prado, A.D., Kasimir, Å., MacDonald, D., Ogle, S.M., Regina, K. & Weerden, T.v.d. (2019). N2O Emissions from Managed Soils, and CO2 Emissions from Lime and Urea Application. In *2019 Refinement to the 2006 IPCC Guidelines for National Greenhouse Gas Inventories* (pp. 11.11-11.48). Geneva: IPCC.

Hersbach, H., Bell, B., Berrisford, P., et al. (2018). *ERA5 hourly data on single levels from 1979 to present* [Online dataset]. Copernicus Climate Change Service (C3S) Climate Data Store (CDS). doi:10.24381/cds.adbb2d47

Hollinger, D. Y., Ollinger, S. V., Richardson, A. D., et al. (2010). Albedo estimates for land surface models and support for a new paradigm based on foliage nitrogen concentration. *Global Change Biology, 16*(2), 696-710. doi:10.1111/j.1365-2486.2009.02028.x

Holtsmark, B. (2015). A comparison of the global warming effects of wood fuels and fossil fuels taking albedo into account. *GCB Bioenergy, 7*(5), 984-997. doi:10.1111/gcbb.12200

Hurtt, G. C., Chini, L. P., Frolking, S., et al. (2011). Harmonization of land-use scenarios for the period 1500–2100: 600 years of global gridded annual land-use transitions, wood harvest, and resulting secondary lands. *Climatic Change, 109*(1), 117. doi:10.1007/s10584-011-0153-2

Inquiry SOU 2020:4. (2020). *Vägen till en klimatpositiv framtid (The pathway to a climate positive future)*. Stockholm: Government Offices of Sweden.

IPCC. (2006). *2006 IPCC Guidelines for National Greenhouse Gas Inventories*. Japan: IGES.

IPCC. (2019). *Climate Change and Land: an IPCC special report on climate change, desertification, land degradation, sustainable land management, food security, and greenhouse gas fluxes in terrestrial ecosystems*. In P. R. Shukla, J. Skea, E. Calvo Buendia, et al. (Eds.).

ISO. (2006a). *ISO 14040:2006: Environmental management – Life Cycle Assessment – principles and framework*. Geneva: International Organizational for Standardization.

ISO. (2006b). *ISO 14044:2006: Environmental management – Life Cycle Assessment – requirements and guidelines*. Geneva: International Organizational for Standardization.

Joensuu, K., Rimhanen, K., Heusala, H., et al. (2021). Challenges in using soil carbon modelling in LCA of agricultural products—the devil is in the detail. *The*

International Journal of Life Cycle Assessment, 26(9), 1764-1778. doi:10.1007/s11367-021-01967-1

Jolliet, O., Antón, A., Boulay, A.-M., et al. (2018). Global guidance on environmental life cycle impact assessment indicators: impacts of climate change, fine particulate matter formation, water consumption and land use. *The International Journal of Life Cycle Assessment, 23*(11), 2189-2207. doi:10.1007/s11367-018-1443-y

Joos, F., Roth, R., Fuglestvedt, J. S., et al. (2013). Carbon dioxide and climate impulse response functions for the computation of greenhouse gas metrics: a multi-model analysis. *Atmospheric Chemistry and Physics, 13*(5), 2793-2825. doi:10.5194/acp-13-2793-2013

Juang, J.-Y., Katul, G., Siqueira, M., et al. (2007). Separating the effects of albedo from eco-physiological changes on surface temperature along a successional chronosequence in the southeastern United States. *Geophysical Research Letters, 34*(21). doi:10.1029/2007GL031296

Jørgensen, S. V., Cherubini, F., & Michelsen, O. (2014). Biogenic CO2 fluxes, changes in surface albedo and biodiversity impacts from establishment of a miscanthus plantation. *Journal of Environmental Management, 146*, 346-354. doi:10.1016/j.jenvman.2014.06.033

Kaye, J. P., & Quemada, M. (2017). Using cover crops to mitigate and adapt to climate change. A review. *Agronomy for Sustainable Development, 37*(1), 4. doi:10.1007/s13593-016-0410-x

Kirschbaum, M. U. F., Saggar, S., Tate, K. R., et al. (2013). Quantifying the climate-change consequences of shifting land use between forest and agriculture. *Science of the Total Environment, 465*, 314-324. doi:10.1016/j.scitotenv.2013.01.026

Koponen, K., Soimakallio, S., Kline, K. L., et al. (2018). Quantifying the climate effects of bioenergy – Choice of reference system. *Renewable and Sustainable Energy Reviews, 81*, 2271-2280. doi:10.1016/j.rser.2017.05.292

Lee, X. (2010). Forests and Climate: A Warming Paradox. *Science, 328*(5985), 1479. doi:10.1126/science.328.5985.1479-a

Lenton, T. M., & Vaughan, N. E. (2009). The radiative forcing potential of different climate geoengineering options. *Atmospheric Chemistry and Physics, 9*(15), 5539-5561. doi:10.5194/acp-9-5539-2009

Levasseur, A., Cavalett, O., Fuglestvedt, J. S., et al. (2016). Enhancing life cycle impact assessment from climate science: Review of recent findings and recommendations for application to LCA. *Ecological Indicators, 71*, 163-174. doi:10.1016/j.ecolind.2016.06.049

Levasseur, A., Lesage, P., Margni, M., et al. (2010). Considering Time in LCA: Dynamic LCA and Its Application to Global Warming Impact Assessments. *Environmental Science & Technology, 44*(8), 3169-3174. doi:10.1021/es9030003

Liu, J., Worth, D. E., Desjardins, R. L., et al. (2021). Influence of two management practices in the Canadian Prairies on radiative forcing. *Science of The Total Environment, 765*, 142701. doi:10.1016/j.scitotenv.2020.142701

Lucht, W., Schaaf, C., & Strahler, A. H. (2000). An algorithm for the retrieval of albedo from space using semiempirical BRDF models. *IEEE Transactions on Geoscience and Remote Sensing, 38*(2), 977-998. doi:10.1109/36.841980

Lugato, E., Cescatti, A., Jones, A., et al. (2020). Maximising climate mitigation potential by carbon and radiative agricultural land management with cover crops. *Environmental Research Letters, 15*(9), 094075. doi:10.1088/1748-9326/aba137

Luyssaert, S., Jammet, M., Stoy, P. C., et al. (2014). Land management and land-cover change have impacts of similar magnitude on surface temperature. *Nature Climate Change, 4*(5), 389-393. doi:10.1038/nclimate2196

Mahmood, R., Pielke, R. A., Hubbard, K. G., et al. (2014). Land cover changes and their biogeophysical effects on climate. *International Journal of Climatology, 34*(4), 929-953. doi:10.1002/joc.3736

Marland, G., Pielke, R. A., Apps, M., et al. (2003). The climatic impacts of land surface change and carbon management, and the implications for climate-change mitigation policy. *Climate Policy, 3*(2), 149-157. doi:10.3763/cpol.2003.0318

May, W., Miller, P., & Smith, B. (2020). *The importance of land-atmosphere biophysical interactions for regional climate and terrestrial ecosystem change. Improved understanding to inform Swedish national climate action*. Lund: Centre for Environmental and Climate Research (CEC), Lund University.

Meyer, S., Bright, R. M., Fischer, D., et al. (2012). Albedo Impact on the Suitability of Biochar Systems To Mitigate Global Warming. *Environmental Science & Technology, 46*(22), 12726-12734. doi:10.1021/es302302g

Milà i Canals, L., Bauer, C., Depestele, J., et al. (2007). Key Elements in a Framework for Land Use Impact Assessment Within LCA. *The International Journal of Life Cycle Assessment, 12*(1), 5-15. doi:10.1065/lca2006.05.250

Miller, J. N., VanLoocke, A., Gomez-Casanovas, N., & Bernacchi, C. J. (2016). Candidate perennial bioenergy grasses have a higher albedo than annual row crops. *GCB Bioenergy, 8*(4), 818-825. doi:10.1111/gcbb.12291

Minx, J. C., Lamb, W. F., Callaghan, M. W., et al. (2018). Negative emissions-Part 1: Research landscape and synthesis. *Environmental Research Letters, 13*(6). doi:10.1088/1748-9326/aabf9b

Monteith, J. L., & Unsworth, M. H. (2013). Chapter 6 - Microclimatology of Radiation: (i) Radiative Properties of Natural Materials. In J. L. Monteith & M. H. Unsworth (Eds.), *Principles of Environmental Physics (Fourth Edition)* (pp. 81-93). Boston: Academic Press.

Muñoz, I., Campra, P., & Fernández-Alba, A. R. (2010). Including CO2-emission equivalence of changes in land surface albedo in life cycle assessment. Methodology and case study on greenhouse agriculture. *The International Journal of Life Cycle Assessment, 15*(7), 672-681. doi:10.1007/s11367-010-0202-5

Myhre, G., Shindell, D., Breón, F.-M., et al. (2013). Anthropogenic and Natural Radiative Forcing. In T. F. Stocker, D. Qin, G.-K. Plattner, et al. (Eds.), *Climate Change 2013: The Physical Science Basis. Contribution of Working Group I to the Fifth Assessment Report of the Intergovernmental Panel on Climate Change* (pp. 659–740). Cambridge and New York, NY: Cambridge University Press.

Müller-Wenk, R., & Brandão, M. (2010). Climatic impact of land use in LCA—carbon transfers between vegetation/soil and air. *The International Journal of Life Cycle Assessment, 15*(2), 172-182. doi:10.1007/s11367-009-0144-y

Notarnicola, B., Tassielli, G., Renzulli, P. A., & Lo Giudice, A. (2015). Life Cycle Assessment in the agri-food sector: an overview of its key aspects, international initiatives, certification, labelling schemesand methodological issues. In B. Notarnicola, R. Salomone, L. Petti, et al. (Eds.), *Life Cycle Assessment in the Agri-food Sector: Case Studies, Methodological Issues and Best Practices* (pp. 1-56). Cham: Springer International Publishing.

O'Halloran, T. L., Law, B. E., Goulden, M. L., et al. (2012). Radiative forcing of natural forest disturbances. *Global Change Biology, 18*(2), 555-565. doi:10.1111/j.1365-2486.2011.02577.x

O'Neill, B. C. (2000). The Jury is Still Out on Global Warming Potentials. *Climatic Change, 44*(4), 427-443. doi:10.1023/A:1005582929198

Paustian, K., Lehmann, J., Ogle, S., et al. (2016). Climate-smart soils. *Nature, 532*(7597), 49-57. doi:10.1038/nature17174

Peltonen-Sainio, P., & Jauhiainen, L. (2020). Large zonal and temporal shifts in crops and cultivars coincide with warmer growing seasons in Finland. *Regional Environmental Change, 20*(3), 89. doi:10.1007/s10113-020-01682-x

Perugini, L., Caporaso, L., Marconi, S., et al. (2017). Biophysical effects on temperature and precipitation due to land cover change. *Environmental Research Letters, 12*(5). doi:10.1088/1748-9326/aa6b3f

Peters, G. P., Aamaas, B., Lund, M. T., et al. (2011). Alternative "Global Warming" Metrics in Life Cycle Assessment: A Case Study with Existing Transportation Data. *Environmental Science & Technology, 45*(20), 8633-8641. doi:10.1021/es200627s

Pielke, R. A., Avissar, R., Raupach, M., et al. (1998). Interactions between the atmosphere and terrestrial ecosystems: influence on weather and climate. *Global Change Biology, 4*(5), 461-475. doi:10.1046/j.1365-2486.1998.t01-1-00176.x

Pielke, R. A., Marland, G., Betts, R. A., et al. (2002). The influence of land-use change and landscape dynamics on the climate system: relevance to climate-change policy beyond the radiative effect of greenhouse gases. *Philosophical Transactions of the Royal Society of London Series a-Mathematical Physical and Engineering Sciences, 360*(1797), 1705-1719. doi:10.1098/rsta.2002.1027

Piggin, I., & Schwerdtfeger, P. (1973). Variations in the albedo of wheat and barley crops. *Archiv für Meteorologie, Geophysik und Bioklimatologie, Serie B, 21*(4), 365-391. doi:10.1007/BF02253314

Poeplau, C., Don, A., Vesterdal, L., et al. (2011). Temporal dynamics of soil organic carbon after land-use change in the temperate zone - carbon response functions as a model approach. *Global Change Biology, 17*(7), 2415-2427. doi:10.1111/j.1365-2486.2011.02408.x

Poore, J., & Nemecek, T. (2018). Reducing food's environmental impacts through producers and consumers. *Science, 360*(6392), 987-+. doi:10.1126/science.aaq0216

Qu, Y., Liang, S., Liu, Q., et al. (2015). Mapping Surface Broadband Albedo from Satellite Observations: A Review of Literatures on Algorithms and Products. *Remote Sensing, 7*(1), 990-1020. doi:10.3390/rs70100990

Roe, S., Streck, C., Obersteiner, M., et al. (2019). Contribution of the land sector to a 1.5 °C world. *Nature Climate Change, 9*(11), 817-828. doi:10.1038/s41558-019-0591-9

Rogelj, J., Popp, A., Calvin, K. V., et al. (2018). Scenarios towards limiting global mean temperature increase below 1.5 °C. *Nature Climate Change, 8*(4), 325-332. doi:10.1038/s41558-018-0091-3

Schwaiger, H. P., & Bird, D. N. (2010). Integration of albedo effects caused by land use change into the climate balance: Should we still account in greenhouse gas units? *Forest Ecology and Management, 260*(3), 278-286. doi:10.1016/j.foreco.2009.12.002

Seneviratne, S. I., Phipps, S. J., Pitman, A. J., et al. (2018). Land radiative management as contributor to regional-scale climate adaptation and mitigation. *Nature Geoscience, 11*(2), 88-96. doi:10.1038/s41561-017-0057-5

Sherwood, S. C., Bony, S., Boucher, O., et al. (2015). Adjustments in the Forcing-Feedback Framework for Understanding Climate Change. *Bulletin of the American Meteorological Society, 96*(2), 217-228. doi:10.1175/bams-d-13-00167.1

Shindell, D. T., Faluvegi, G., Rotstayn, L., & Milly, G. (2015). Spatial patterns of radiative forcing and surface temperature response. *Journal of Geophysical Research: Atmospheres, 120*(11), 5385-5403. doi:10.1002/2014JD022752

Shine, K. P., Fuglestvedt, J. S., Hailemariam, K., & Stuber, N. (2005). Alternatives to the Global Warming Potential for Comparing Climate Impacts of Emissions of Greenhouse Gases. *Climatic Change, 68*(3), 281-302. doi:10.1007/s10584-005-1146-9

Singarayer, J. S., & Davies-Barnard, T. (2012). Regional climate change mitigation with crops: context and assessment. *Philosophical Transactions of the Royal Society A: Mathematical, Physical and Engineering Sciences, 370*(1974), 4301-4316. doi:10.1098/rsta.2012.0010

Smith, C. J., Kramer, R. J., Myhre, G., et al. (2020). Effective radiative forcing and adjustments in CMIP6 models. *Atmos. Chem. Phys., 20*(16), 9591-9618. doi:10.5194/acp-20-9591-2020

Smith, P. (2016). Soil carbon sequestration and biochar as negative emission technologies. *Global Change Biology, 22*(3), 1315-1324. doi:10.1111/gcb.13178

Smith, P., Davis, S. J., Creutzig, F., et al. (2016). Biophysical and economic limits to negative CO2 emissions. *Nature Climate Change, 6*(1), 42-50. doi:10.1038/nclimate2870

Soden, B. J., & Held, I. M. (2006). An assessment of climate feedbacks in coupled ocean-atmosphere models. *Journal of Climate, 19*(14), 3354-3360. doi:10.1175/jcli3799.1

Starr, J., Zhang, J., Reid, J. S., & Roberts, D. C. (2020). Albedo Impacts of Changing Agricultural Practices in the United States through Space-Borne Analysis. *Remote Sensing, 12*(18), 2887. doi:10.3390/rs12182887

Swedish EPA. (2019). *National Inventory Report Sweden 2020. Greenhouse Gas Emission Inventories 1990-2018. Submitted under the United Nations Framework*

Convention on Climate Change and the Kyoto Protocol. Retrieved from https://unfccc.int/documents/224123

Sütterlin, M., Stöckli, R., Schaaf, C. B., & Wunderle, S. (2016). Albedo climatology for European land surfaces retrieved from AVHRR data (1990–2014) and its spatial and temporal analysis from green-up to vegetation senescence. *Journal of Geophysical Research: Atmospheres, 121*(14), 8156-8171. doi:10.1002/2016JD024933

Tanaka, K., Peters, G. P., & Fuglestvedt, J. S. (2010). Multicomponent climate policy: why do emission metrics matter? *Carbon Management, 1*(2), 191-197. doi:10.4155/cmt.10.28

Tubiello, F. N., Rosenzweig, C., Conchedda, G., et al. (2021). Greenhouse gas emissions from food systems: building the evidence base. *Environmental Research Letters, 16*(6). doi:10.1088/1748-9326/ac018e

UNFCCC. (2015). *Adoption of the Paris Agreement*. United Nations Framework Convention on Climate Change. Retrieved from https://unfccc.int/resource/docs/2015/cop21/eng/l09r01.pdf.

Ward, D. S., Mahowald, N. M., & Kloster, S. (2014). Potential climate forcing of land use and land cover change. *Atmos. Chem. Phys., 14*(23), 12701-12724. doi:10.5194/acp-14-12701-2014

Winton, M. (2005). Simple optical models for diagnosing surface-atmosphere shortwave interactions. *Journal of Climate, 18*(18), 3796-3805. doi:10.1175/jcli3502.1

Zhang, Y.-f., Wang, X.-p., Pan, Y.-x., & Hu, R. (2013). Diurnal and seasonal variations of surface albedo in a spring wheat field of arid lands of Northwestern China. *International Journal of Biometeorology, 57*(1), 67-73. doi:10.1007/s00484-012-0534-x

Zhao, K., & Jackson, R. B. (2014). Biophysical forcings of land-use changes from potential forestry activities in North America. *Ecological Monographs, 84*(2), 329-353. doi:10.1890/12-1705.1

Popular science summary

Background and motivation

Agricultural systems for production of food, bioenergy and materials are among the greatest contributors to global warming. Significant emissions of greenhouse gases (GHGs) arise, due *e.g.* to the manufacture of inputs, fuel consumption by machinery and management-dependent processes in the soil. By altering vegetation and soil, agricultural practices change the amount of solar radiation reflected from the land surface. The more reflective a surface, the higher its albedo and the greater the share of energy sent directly back into space. Bright materials such as straw usually have high albedo and absorb less energy than dark materials. Agricultural practices that increase albedo, such as cultivation of reflective crops or leaving straw in the field after harvest, can provide a cooling effect on temperature and counteract the effects of GHG emissions.

Agriculture can thus play a crucial role in limiting global warming. There is currently a strong focus in society on reducing emissions from food production, increasing carbon storage in soils and providing biomass to replace fossil fuels. Life cycle assessment (LCA) is widely used as a tool for assessing the climate performance of food or bioenergy. LCA results are used *e.g.* for providing guidance to farmers and consumers who want to reduce their environmental impact, and in legislation and standards aiming to ensure sustainable production. Considering changes in albedo could be important when seeking to improve the climate performance of agricultural systems. However, there is a lack of knowledge on the albedo change caused by individual crops and cultivation practices and there is no agreed method for comparing albedo-related effects with the climate impacts of GHG emissions.

Research in this thesis

The overall aim of this thesis was to improve understanding of how different crops and cultivation practices affect the climate via albedo, and to compare the effects with other climate impacts caused by agricultural systems. The work included method development and case studies covering three areas: (1) quantifying albedo, (2) assessing effects of albedo change on climate, and (3) evaluating the importance of albedo change for the climate impact of production of crops or bioenergy.

The effect of individual crops and cultivation practices on albedo was examined under Swedish conditions. Field and satellite data were used to analyse differences between sites and years due to crop, management, soil type, climate and weather. The results indicated clear benefits of keeping the soil covered year-round, *e.g.* by growing perennial crops or winter-sown varieties. Some practices increased the albedo of unvegetated fields after harvest compared with direct ploughing, *e.g.* leaving straw in the field combined with later ploughing or reduced tillage.

The case studies showed that crop cultivation can increase albedo relative to unused land and thus provide a cooling effect, but uncertainty about the vegetation present on unused land needs to be considered. Cultivation of willow on former fallow increased both albedo and soil carbon storage, and thereby improved the overall climate benefit of bioenergy produced from willow. Cultivation of food and feed crops such as wheat, rapeseed and ley also increased albedo relative to a situation without cultivation, where a darker mix of grass, shrubs and trees covered the land. This albedo increase counteracted the warming effect of GHG emissions from manufacture of inputs, fuel consumption and soil.

The importance of albedo change for the climate impact of crop or bioenergy production was shown to be greatest on short time scales. Albedo change influenced the global mean temperature for about 20 years after cultivation, whereas the impact of emitted GHGs lasted for centuries. The local, immediate effect of increased albedo could be exploited in strategies for adaptation to climate change, to dampen warming locally and alleviate heat stress in summer. Beyond the case studies, data and methods presented in this thesis could help evaluate possible consequences of global warming, such as zonal and temporal shifts in crops and varieties due to changing growing seasons.

Populärvetenskaplig sammanfattning

Bakgrund och motivering

Jordbrukets system för produktion av livsmedel, bioenergi och material har en omfattande påverkan på den globala uppvärmningen. Betydande utsläpp av växthusgaser uppstår bland annat på grund av tillverkning av insatsvaror, arbetsmaskinernas bränsleförbrukning samt olika insatsberoende processer i marken. Genom att förändra växtlighet och markens utseende påverkar odlingssystemen mängden solstrålning som reflekteras från markytan. Ju mer reflekterande en yta är, desto högre är dess albedo och desto större andel energi skickas direkt tillbaka ut ur atmosfären. Ljusa material som halm har vanligtvis hög albedo och absorberar mindre energi än mörka material. Grödval och odlingsteknik som ökar albedo, såsom odling av reflekterande grödor eller att lämna halm på åkern efter skörd, kan ha en kylande effekt på temperaturen och motverka effekterna av växthusgasutsläpp.

Jordbruket kan alltså spela en viktig roll för att begränsa den globala uppvärmningen. För närvarande finns det i samhället ett starkt fokus på att minska utsläppen från livsmedelsproduktionen, öka kolinlagringen i marken och tillhandahålla biomassa för att ersätta fossila bränslen. Livscykelanalys (LCA) är ett vanligt verktyg för att bedöma klimatprestanda för livsmedel och bioenergi. LCA-resultat används till exempel för att ge vägledning till lantbrukare och konsumenter som vill minska sin miljöpåverkan, och till lagstiftning och standarder som syftar till att säkerställa hållbar produktion. Att ta hänsyn till förändringar i albedo kan vara viktigt när man försöker förbättra jordbrukets klimatprestanda. Men det saknas mycket kunskap om hur individuella grödor och odlingsmetoder påverkar albedo och därmed klimatet, och det finns ingen konsensus över metod för att jämföra albedoeffekten med klimatpåverkan av växthusgasutsläpp.

Forskningen i denna avhandling

Det övergripande syftet med denna avhandling är att förbättra förståelsen för hur olika grödval och odlingstekniker påverkar klimatet via albedo, och att jämföra effekterna med annan klimatpåverkan orsakad av odlingssystem. Arbetet omfattade metodutveckling och fallstudier inom tre områden: (1) att kvantifiera albedo, (2) att bedöma effekterna på klimatet av förändringar i albedo, och (3) att utvärdera betydelsen av albedoförändringar på klimatpåverkan från produktion av grödor eller bioenergi.

Effekten av enskilda grödor och odlingsteknik på albedo undersöktes under svenska förhållanden. Fält- och satellitdata användes för att analysera skillnader mellan platser och år beroende på gröda, skötsel, jordtyp, klimat och väder. Resultaten indikerar tydliga fördelar med att hålla jorden täckt året runt, t.ex. genom att odla fleråriga grödor eller höstsådda sorter. Vissa metoder ökade albedo för obevuxen mark jämfört med direkt plöjning efter skörd, t.ex. att lämna halm kvar i fältet i kombination med senare plöjning eller minskad jordbearbetning.

Fallstudierna visade att odling av grödor kan öka albedo i förhållande till outnyttjad mark och därmed ge en kylande effekt, men osäkerheten om vegetationen som finns på outnyttjad mark bör beaktas. Odling av Salix på tidigare träda ökade både albedo och kolinlagring i marken och förbättrade därmed den övergripande klimatnyttan av bioenergi från Salix. Odling av mat- och fodergrödor som vete, raps och vall ökade också albedo i förhållande till en situation utan odling, där en mörkare blandning av gräs, buskar och träd täckte marken. Denna albedoökning motverkade den uppvärmande effekten av växthusgasutsläpp från tillverkning av insatsvaror, bränsleförbrukning och mark.

Betydelsen av albedoförändringar på klimatpåverkan från produktion av grödor eller bioenergi visade sig vara störst på korta tidsskalor. Förändringar i albedo påverkade den globala medeltemperaturen i cirka 20 år efter odling, medan växthusgasutsläpp påverkade temperaturen i århundraden. Den lokala, omedelbara effekten av ökad albedo skulle kunna utnyttjas i strategier för klimatanpassning, för att dämpa uppvärmningen lokalt och lindra värmestress på sommaren. Utöver fallstudierna kan data och metoder som presenteras i avhandlingen hjälpa till att utvärdera möjliga konsekvenser av den globala uppvärmningen, exempelvis växtzons- och årstidsförskjutningar av grödor och sorter på grund av förändrade växtsäsonger.

Acknowledgements

I would like to express my gratitude to my main supervisor Per-Anders Hansson for his trust, patience and invaluable experience. The opportunity to develop and follow my own ideas made my doctoral studies an immense learning journey, while his guidance helped me stay on track. I would also like to thank my co-supervisor Niclas Ericsson for various practical tips and critical discussions that incentivised me to see things from different angles and to re-evaluate my work. Serina Ahlgren and Torun Hammar acted as co-supervisors during parts of my journey and I am grateful for their support and encouragement. Cecilia Sundberg provided insightful comments on a draft of this thesis and during my pre-dissertation seminar.

Colleagues at SLU took the time to share their valuable expertise on specific topics and thereby contributed to the work presented in this thesis: Martin Bolinder, Thomas Kätterer, Anders Larsolle, Claudia von Brömssen and Achim Grelle. Thanks to Sepp Böhme for the good collaboration on field measurements. Related to field data and trails, I would like to acknowledge Per Weslien, Patrik Vestin, Åsa Myrbeck, Håkan Andersson, John Löfkvist and Jarl Ryberg. Thanks to Mary McAfee for brilliant work.

I am grateful to colleagues and friends at the department for making SLU such an enjoyable workplace. Special thanks to fellow PhD students and my "office family" for the good times, creative ideas, help in various situations and new expressions contributing to my Swedish.

Warm thanks to friends and family in Sweden, Austria and elsewhere for supporting me in all possible ways along this journey and contributing to Uppsala feeling like home. I am so grateful for all the cheerful and motivating words recently, the inspiration shared regarding writing a thesis, and occasional getaways in lovely company.

Climate impact of surface albedo change in Life Cycle Assessment: Implications of site and time dependence

Petra Sieber*, Niclas Ericsson, Per-Anders Hansson

Department of Energy and Technology, Swedish University of Agricultural Sciences (SLU), Uppsala SE750 07, Sweden

A R T I C L E   I N F O

A B S T R A C T

Land use affects the global climate through greenhouse gas and aerosol emissions, as well as through changes in biophysical properties of the surface. Anthropogenic land use change over time has caused substantial climate forcing related to albedo, i.e. the share of solar radiation reflected back off the ground. There is growing concern that albedo change may offset climate benefits provided by afforestation, bioenergy or other emission reduction measures that affect land cover. Conversely, land could be managed actively to increase albedo as a strategy to combat global warming.

Albedo change can be directly linked to radiative forcing, which allows its climate impact to be compared with that of greenhouse gases in Life Cycle Assessment (LCA). However, the most common LCA methods are static and linear and thus fail to account for the spatial and temporal dependence of albedo change and its strength as a climate forcer. This study sought to develop analytical methods that better estimate radiative forcing from albedo change by accounting for spatial and temporal variations in albedo, solar irradiance and transmission through the atmosphere. Simplifications concerning the temporal resolution and aggregation procedures of input data were evaluated.

The results highlight the importance of spatial and temporal variations in determining the climate impact of albedo change in LCA. Irradiance and atmospheric transmittance depend on season, latitude and climate zone, and they co-vary with instantaneous albedo. Ignoring these dependencies led to case-specific errors in radiative forcing. Extreme errors doubled the climate cooling of albedo change or resulted in warming rather than cooling in two Swedish cases considered. Further research is needed to understand how different land use strategies affect the climate due to albedo, and how this compares to the effect of greenhouse gases. Given that albedo change and greenhouse gases act on different time scales, LCAs can provide better information in relation to climate targets if the timing of flows is considered in life cycle inventory analysis and impact assessment.

1. Introduction

Land ecosystems are an important component of the climate system. Vegetation and soil store large amounts of carbon, and regulate the exchange of energy, water, trace gases, aerosols and momentum between surface and atmosphere (Pielke et al., 1998). Human land use interferes with the coupled land-atmosphere system. Land conversion and management affect the climate by greenhouse gas (GHG) and aerosol emissions, and by changes in biophysical properties of the surface. Albedo, the share of solar radiation reflected back off the ground, acts directly on the Earth's radiation budget. A perturbation to the global radiation budget resulting from surface albedo change can be expressed as radiative forcing (RF) and can be compared with the RF of GHGs (Betts, 2001).

Agriculture and forestry are recognised for their climate change mitigation potential (Smith et al., 2014). Afforestation, management options and biomass production for energy have been widely evaluated based on GHG emissions and carbon sequestration. Surface albedo is not generally considered in climate impact assessments, although the RF from albedo change can be of the same magnitude as that of GHGs. In some cases, albedo change counteracts or even offsets the benefit of carbon sequestration (Arora and Montenegro, 2011; Betts, 2000; Schaeffer et al., 2006). Moreover, land cover could be managed actively towards higher albedo to combat global warming (Carrer et al., 2018). A growing body of literature advocates accounting for surface biophysical variables, in particular albedo, in order to avoid suboptimal or counterproductive land-based mitigation measures (Bright et al., 2015; Creutzig et al., 2015; Smith et al., 2014).

---

* Corresponding author at: Department of Energy and Technology, Swedish University of Agricultural Sciences (SLU), PO Box 7032, SE-750 07 Uppsala, Sweden.
E-mail addresses: petra.sieber@slu.se (P. Sieber), niclas.ericsson@slu.se (N. Ericsson), per-anders.hansson@slu.se (P.-A. Hansson).

Life Cycle Assessment (LCA) is a standardised methodology for quantifying the potential environmental impacts of a product or service. It has been widely applied to agricultural and forestry products to support decision making (Hellweg and Milà i Canals, 2014). There are growing efforts to extend the framework of LCA from resource use and emissions to albedo, so that GHGs and albedo change can be compared on a common basis. LCA studies that include albedo have found important implications of the choice of site, crop, production system and land management (Bright et al., 2012; Cai et al., 2016; Caiazzo et al., 2014; Cherubini et al., 2012; Muñoz et al., 2010; Schwaiger and Bird, 2010). These studies agree on the impact pathway, i.e. that the RF caused by albedo change depends on solar irradiance and transmission through the atmosphere. However, the temporal and spatial inter-dependence of these variables pose challenges for inclusion of albedo in LCA.

LCA has been developed as a static and site-generic tool (Finnveden et al., 2009). This is reflected in its traditional methodological structure. Inventory analysis and impact assessment are not linked by information about the timing and geographical location of emissions. Instead, flows from and to the environment are summed over the temporal and spatial extent of the system. This approach to assessing land use in LCA has been debated for two reasons: (1) land use is defined to begin and end at the temporal system boundaries, so that an initial transformation of land is exactly compensated for by the relaxation to its natural state, with a net effect of zero; and (2) environmental processes and impacts of land use depend on biogeographical factors that vary over space and time, such as climate, soil type and vegetation (Finnveden et al., 2009; Milà i Canals et al., 2007). To account for spatial and temporal differences in LCA, disaggregated inventories have been suggested in combination with regional or time-dependent impact assessment methods (Ericsson et al., 2013; Levasseur et al., 2010; Roy et al., 2014). However, temporal disaggregation is usually on annual timescales thus leaving diurnal or seasonal variations in insolation, climate or presence of species unconsidered.

The static and site-generic framework of LCA is problematic for modelling the climate impact of albedo change, for the same reasons as for land use in general. Methods to include temporary albedo change in LCA have been suggested, assuming that albedo change is constant after land transformation (Muñoz et al., 2010), or changes during land occupation based on a decay function (Bright et al., 2012). The temporal and spatial dependence of albedo change and its ability to cause RF have received little attention in LCA. It is common to approximate annual or monthly albedo by instantaneous values, and to model transmission of reflected radiation through the atmosphere based on a global constant for clear-sky conditions. However, the albedo of old and new land cover, solar irradiance and atmospheric transmittance depend on solar zenith angle (SZA), which varies on diurnal and seasonal time scales. Clouds, aerosols and gases attenuate the reflected radiation, and cause substantial differences in atmospheric transmittance. Ignoring the temporal and spatial dependence of albedo, irradiance and transmittance may therefore introduce bias in RF calculations.

Few of the LCAs performed to date have included land surface albedo change as a climate forcer. Static and linear LCA methods generally reduce complexity and may facilitate the consideration of albedo. However, there is a risk of the climate impact of albedo change being under- or overestimated to the extent that the results do not support better decision making. Therefore, this study aimed to advance the quantification of climate impacts due to albedo change in LCA. The objectives were (1) to analyse spatial and temporal variations in albedo and its strength as a climate forcer; (2) to develop analytical methods that better estimate RF from albedo change by accounting for spatial and temporal variations in albedo, irradiance and atmospheric transmittance; and (3) to evaluate how simplifications concerning the temporal resolution and aggregation procedures of input data may affect estimations of RF from albedo change. Radiative forcing was calculated at hourly resolution before balancing accuracy, robustness and data requirements.

Section 2 of this paper provides theoretical background on determinants of albedo and on site- and time-dependent factors that control the impact of albedo change on the global climate. Methods to calculate RF under consideration of spatial and temporal variations are introduced in Section 3. Temporal variations were studied based on radiation measurements at four sites with differing land cover in south-western Sweden. Albedo patterns were analysed on diurnal, seasonal and inter-annual time scales, along with variations in local solar irradiance and atmospheric transmittance. The effect of resolution and aggregation procedures on annual mean RF was illustrated using two cases of albedo change in south-western Sweden: cultivating short-rotation coppice (SRC) willow on long-term fallow land, and clear-cutting a coniferous forest. The results are presented in Section 4 and evaluated in an LCA context in Section 5.

2. Theoretical background

Common climate metrics in LCA such as the Global Warming Potential are based on RF, which is a proxy for the potential response of the climate system. Annual mean RF from albedo change has been widely calculated by multiplication of the difference in instantaneous albedo, mean local irradiance and a global transmittance factor. However, individual aggregation of these variables over different spatial and temporal scales omits their dependence. Albedo, irradiance and transmittance are controlled by solar position and atmospheric composition, leading to geographical, diurnal and seasonal co-variation of their instantaneous values.

2.1. Site and time dependence of albedo

Instantaneous albedo is determined by (1) surface properties resulting from vegetation physiology and structure, soil geology and moisture, management interventions and deposition of snow, water or particles (Bright et al., 2015); and (2) the angular and spectral distribution of incident radiation (Dickinson, 1983). The latter depends on SZA, as well as on scattering and absorption in the atmosphere due to clouds, aerosols and gases. In combination, variations in surface properties, SZA and atmospheric composition render albedo site- and time-dependent. The geographical location determines the range of SZA between sunrise/sunset and local noon, and hence controls diurnal and seasonal patterns. The following analysis focuses on albedo for the shortwave solar spectrum, while differences by wavelength were outside the scope of the study.

Albedo varies between land cover types, and is generally lower for dark vegetation canopies of evergreen coniferous forests (8–12%) and deciduous broadleaf forests (13–18%) than for light-coloured open land such as cropland (19%), grassland (15–23%), desert (27–43%) or snow and ice (70–87%) (Briegleb et al., 1986; Hollinger et al., 2010; Schaeffer et al., 2006). However, the actual value is sensitive to properties of vegetation and underlying soil, local climate and management.

Natural surfaces reflect anisotropically, which means that they respond unequally to radiation coming from different directions. Depending on the angular distribution of incident radiation, the same surface can reflect more or less, and in different directions (Dickinson, 1983). Surface irradiance is a combination of direct beam radiation coming from the direction of the sun and diffuse radiation that has been scattered and can come from any direction. The direct proportion dominates under clear-sky conditions and overhead sun, whereas the diffuse proportion increases with clouds and SZA, since a longer path through the atmosphere gives more opportunity for scattering (Yang et al., 2008).

Albedo increases with SZA under direct insolation. On a clear summer day with large SZA variation, albedo at sunrise/sunset can be 2–3 times the albedo at local noon (Yang et al., 2008). As the diffuse proportion increases, the diurnal pattern of albedo becomes weaker. This is because diffuse albedo is not sensitive to SZA, and is assumed to

be similar to direct beam albedo at the average incidence angle of 60°. When clouds augment the share of diffuse radiation, they increase albedo at low SZA and decrease albedo at high SZA (Lyapustin, 1999). Under overcast conditions, albedo does not exhibit a diurnal cycle (Yang et al., 2008).

The variation in albedo with SZA depends on land cover, geographical location and season. Several attempts have been made to parameterise the relationship between direct beam albedo and SZA (Briegleb et al., 1986; Wang et al., 2007; Yang et al., 2008), with markedly different findings regarding the strength of dependence and how land cover classes compare. Yang et al. (2008) conclude that that direct beam albedo is predominantly a function of SZA when normalised by its value at 60° and that albedo at 60° SZA can adequately represent surface type and season in such a model. Assuming that direct beam albedo increases with SZA proportionally to its value at 60°, light-coloured surfaces generally exhibit larger albedo variations in absolute terms. This causes greater differences in albedo from land use change at high SZA. The resulting angular dependence of albedo change has two implications for the assessment of its climate impact.

First, it leads to systematic underestimation of albedo change when daily albedo is replaced by direct beam albedo at local noon. This replacement is often used because direct beam albedo at local noon is readily available in public datasets derived from satellite observations, such as the MODIS albedo product. However, it has been shown to cause a negative bias in the surface energy balance (Wang et al., 2015).

Second, it leads to a negative correlation of instantaneous albedo change with surface irradiance and atmospheric transmittance, which both generally decrease with SZA. The correlation can be addressed by calculating albedo from the total upwelling and downwelling short-wave fluxes during the aggregation interval. However, this requires continuous radiation measurements. Using discontinuous observations, the same can be achieved by calculating the weighted mean of instantaneous albedo values, thereby giving higher weight to periods with greater surface irradiance (Winton, 2005).

2.2. Site and time dependence of atmospheric transmittance

Solar position and atmospheric composition determine the strength of albedo change as a climate forcer by regulating surface irradiance and atmospheric transmittance. Clouds, aerosols and gases limit the transmission of radiation through the atmosphere, and thereby control how much energy reaches the surface and how much energy reaches back to the top of the atmosphere (TOA) after reflection. Atmospheric attenuation of upwelling radiation has been represented by the global annual mean clear-sky transmittance ($T_c = 0.854$) in several LCAs accounting for albedo. This factor is based on cloud-free conditions and 60° mean SZA, and is therefore not appropriate for characterising "latitudinally and seasonally biased" albedo change (Lenton and Vaughan, 2009). When albedo change occurs in a confined region and varies with season, spatial and temporal differences in atmospheric properties may be important.

The atmosphere attenuates the surface contribution by 69% on average (Donohoe and Battisti, 2011). Atmospheric scattering differs by geographical location and season, owing to changes in (1) water vapour and ozone concentrations determining absorption; (2) effective cloud amount and aerosols determining reflection; and (3) SZA determining atmospheric path length. Absorptivity has a latitudinal gradient, ranging from 15% or less at high latitudes to 25% in the tropics; atmospheric reflectivity is low in the drier subtropics and high over the cloud band of the Intertropical Convergence Zone, in Southeast Asia and over polar regions (Donohoe and Battisti, 2011). Consequently, attenuation of surface albedo can vary geographically between 60 and 85%. Seasonal variation results mainly from atmospheric path length at high latitudes, whereas the seasonal cycle of cloudiness has a major effect at low latitudes (Stephens et al., 2015).

3. Methods and data

3.1. Impact assessment approach

Surface albedo change causes RF by increasing or decreasing the upwelling shortwave flux at the Earth's surface. The effect on the TOA energy balance is masked by clouds, aerosols and gases, which attenuate solar radiation on its way through the atmosphere. Instantaneous RF from a change in surface albedo (RF_α in Wm^{-2}) is given by:

$$RF_\alpha = \frac{A}{A_E} R_{\text{TOA}\downarrow} \left(\alpha_{S,\text{ref}} f_{A,\text{ref}} - \alpha_{S,\text{new}} f_{A,\text{new}} \right) \tag{1}$$

where A denotes the affected area, A_E the Earth's total surface area ($A_E = 5.1 \cdot 10^{14}\,\text{m}^2$) and $R_{\text{TOA}\downarrow}$ the downwelling solar irradiance at the TOA. For reference and new land cover, α_S is surface albedo and f_A represents downward and upward radiative transfer between TOA and surface (Lenton and Vaughan, 2009). The parameter f_A includes atmospheric scattering and absorption, as well as multiple reflections between surface and atmosphere:

$$f_A = \frac{\tau_\downarrow \tau_\uparrow}{1 - \alpha_S \alpha_{A\uparrow}} \tag{2}$$

where τ is atmospheric transmittance, i.e. the fraction of radiation remaining after absorption and reflection during a single downward or upward pass through the atmosphere. The denominator represents an infinite number of reflections between the surface with albedo α_S and the atmosphere with upward reflectivity $\alpha_{A\uparrow}$ (Winton, 2005). Combining Eqs. (1) and (2), instantaneous RF_α can be rewritten as:

$$RF_\alpha = \frac{A}{A_E} R_{\text{TOA}\downarrow} \tau_\downarrow \tau_\uparrow \left[\frac{\alpha_{S,\text{ref}}}{1 - \alpha_{S,\text{ref}} \alpha_{A\uparrow}} - \frac{\alpha_{S,\text{new}}}{1 - \alpha_{S,\text{new}} \alpha_{A\uparrow}} \right] \tag{3}$$

Eq. (3) highlights that surface albedo controls multiple reflection, which increases solar irradiance at the surface, i.e. $R_{S\downarrow} = R_{\text{TOA}\downarrow} \tau_\downarrow / (1 - \alpha_S \alpha_{A\uparrow})$, and thereby reinforces RF_α. This effect is negligible for albedo levels and albedo changes typically occurring in agriculture and forestry. For a change in albedo from 0.1 to 0.2, additional multiple reflection increases RF_α by 1–6%, taking a range of 0.1–0.3 for $\alpha_{A\uparrow}$ (Winton, 2005) and the old or new albedo for α_S. Ignoring this effect, we assume $f_{A,\text{ref}} = f_{A,\text{new}}$ and obtain:

$$RF_\alpha = \frac{A}{A_E} R_{\text{TOA}\downarrow} \Delta\alpha_S f_A = \frac{A}{A_E} R_{S\downarrow} \Delta\alpha_S \tau_\uparrow \tag{4}$$

Atmospheric transmittance can be calculated with a simple model that consists of a single atmospheric layer which scatters and absorbs radiation over a reflecting surface. The atmospheric layer is typically assumed to have the same optical properties on any pass in the downward and upward direction so that $\tau_\downarrow = \tau_\uparrow$ (Stephens et al., 2015). Using this simplification, atmospheric transmittance can be computed from four fluxes (Winton, 2005):

$$\tau = \frac{R_{\text{TOA}\downarrow} R_{S\downarrow} - R_{\text{TOA}\uparrow} R_{S\uparrow}}{R_{\text{TOA}\downarrow}^2 - R_{S\uparrow}^2} \tag{5}$$

The term transmittance refers to the transmission property of the atmospheric layer throughout this study. This should not be confused with the transmission property of the surface-atmosphere system which includes multiple reflection, i.e. $T_\downarrow = R_{S\downarrow}/R_{\text{TOA}\downarrow} = \tau_\downarrow/(1 - \alpha_S\alpha_{A\uparrow})$. The approximation $\tau = T_\downarrow$ has been made for clear-sky conditions (Lenton and Vaughan, 2009) when $\alpha_{A\uparrow}$ is small.

Annual mean RF_α can be calculated according to Eq. (6) where y denotes the year and T is the number of sub-annual time steps t:

$$\overline{RF_\alpha}(y) = \frac{A}{A_E} \frac{1}{T} \sum_{t=1}^{T} R_{S\downarrow}(y,t) \, \Delta\alpha_S(y,t) \, \tau(y,t) \tag{6}$$

Radiative kernels were used to verify Eq. (6) as it contains

simplifications related to multiple reflection (Eq. (4)) and isotropic transmittance (Eq. (5)). A kernel K_α describes how a constant 0.01 change in surface albedo affects the TOA energy balance (Soden et al., 2008), and can be used to linearly relate $\Delta\alpha_S$ to RF_α (e.g. Ghimire et al., 2014). Radiative kernels depend on the radiative properties and base state of the model they are derived from (Shell et al., 2008). The monthly kernels used in this study were generated from the offline versions of CAM3 (Shell et al., 2008), ECHAM6 (Block and Mauritsen, 2013), CAM5 (Pendergrass et al., 2018) and HadGEM2 (Smith et al., 2018).

Radiative forcing is the basis for other climate metrics such as the Global Warming Potential (GWP), which is most commonly used in LCA. The GWP allows to compare emissions of different GHGs by converting them to a pulse emission of carbon dioxide that exerts the same cumulative RF over a given time horizon (*TH*). Similarly, the climate impact of albedo change can be expressed in kg carbon dioxide equivalents (CO_2e):

$$GWP_\alpha^{TH} = \frac{\sum_{y=1}^{TH} \overline{RF_\alpha}(y)}{AGWP_{CO2}^{TH}}$$

(7)

The Absolute Global Warming Potential of carbon dioxide ($AGWP_{CO2}$) was determined based on metric values from Myhre et al. (2013), resulting in $91.7 \cdot 10^{-15}$ $Wm^{-2}yrkg^{-1}$ for $TH = 100$.

3.2. Surface albedo data

In the first case considered in this study, SRC willow was compared with an area vegetated by sedges and grasses, serving as a proxy for long-term fallow land. On two closely located sites in south-western Sweden, downwelling and upwelling shortwave irradiance was measured using pairs of Hukseflux NR-01 pyranometers (285–3000 nm). Irradiance was sampled at 30-min intervals over 3 years to cover a full cutting cycle of the willow plantation, starting in April. In the second case considered, a coniferous forest and a clear-cut were compared. Shortwave irradiance was measured with Kipp & Zonen CNR4 pyranometers (300–2800 nm) over 1 year. The clear-cut was located 300 km south of the other sites. The measurement periods of the two cases overlapped.

The measurements were used without pre-selection of clear-sky observations. Raw data were corrected for likely measurement errors. Irradiance was set to zero in intervals with SZA > 85° to remove instrumental noise at night-time and to limit directional error and interference with reflection at high incidence angles. The cut-off affected < 2% of incident radiation, while removing 99.97% of negative values. Remaining negative values were discarded.

Positive irradiance was checked according to recommendations of the Baseline Surface Radiation Network (Roesch et al., 2011). Observations exceeding the "extremely rare" upper bound for downwelling or upwelling shortwave irradiance were discarded ($R_{S\downarrow}^{max} = 1.2\ S_a\ \mu^{1.2} + 50\ Wm^{-2}$ or $R_{S\uparrow}^{max} = S_a\ \mu^{1.2} + 50\ Wm^{-2}$, respectively, where S_a is the solar constant adjusted for Earth-Sun distance and μ is the cosine of SZA). Discarded observations were treated as gaps for both downwelling and upwelling irradiance at the same interval and site. Larger gaps of several hours to up to 40 consecutive days occurred due to instrument failure.

Observations of $R_{S\uparrow} > R_{S\downarrow}$ can result from multiple reflections and are an indication of high reflectivity. In order to avoid albedo > 1, upwelling irradiance was not allowed to exceed downwelling irradiance in the same interval in the present analysis. Corrections were required predominantly in winter months with snow.

The corrected 30-min data were aggregated to hourly means. Data gaps are usually not distributed homogeneously between years, seasons and times of day. This affects the results when calculating RF_α, and it affected the result of our models in different ways. To avoid this, gaps were filled with the closest 15-day mean of available data for the same hour, aiming to preserve the diurnal and seasonal cycle of shortwave fluxes.

3.3. Irradiance and transmittance data

Surface solar irradiance and atmospheric transmittance were derived from shortwave fluxes of the ERA5 global reanalysis dataset (ECMWF, 2018). These data are available at a horizontal resolution of 31 km and at hourly frequency when combining analyses and short 12-h forecasts. Downwelling and net shortwave fluxes were retrieved at the surface and the TOA for all-sky conditions. Clear-sky fluxes from simulations of a cloud-free atmosphere were used for comparison. Night-time noise was removed by setting irradiances < 1^{-10} Wm^{-2} to zero. Surface irradiance was used directly, whereas atmospheric transmittance was computed according to Eq. (5). The data were retrieved to match the period and location of the albedo measurements in the case studies.

3.4. Resolution and aggregation methods

Annual mean RF_α was calculated according to Eq. (6) with different resolutions and aggregation methods. Mean RF_α from hourly albedo, irradiance and transmittance was used as a benchmark. This model was compared against models with reduced resolution, where the variables were aggregated according to the following four methods.

In method 1, albedo change, irradiance and transmittance were determined from total fluxes per day, month or year (models D, M and Y, respectively). This is the logical approach when continuous radiation measurements are available. Method 1 is sensitive to data gaps and requires adequate gap-filling.

In method 2, albedo change, irradiance and transmittance were aggregated to monthly mean diurnal cycles, i.e. means by month and hour (model MH). This nested form of aggregation was used to preserve diurnal and seasonal patterns while reducing day-to-day variability. Method 2 does not require data for every day of the month and is not sensitive to non-homogeneously distributed gaps. It was evaluated with gap-filled data as in all methods, and tested additionally with the corrected dataset with gaps.

In method 3, 1 day per month was selected to determine albedo from total fluxes (model Mc) and from hourly fluxes at local noon (model Mnc). These values were used as proxies for monthly albedo. Days with minimum cloudiness were chosen, as clouds are a common cause of instrument failure and error. Daily cloudiness was evaluated based on the ratio of downwelling shortwave fluxes measured in the field, and ERA5 clear-sky fluxes. This approach mimics a situation where field data are collected selectively to save costs.

In method 4, albedo at local noon was used as a proxy for daily albedo (model Dn), and aggregated to the arithmetic mean to use as monthly albedo (model Mn) and annual albedo (model Yn). Local noon was approximated by the hourly time step with the lowest average SZA per day. Time-dependent transmittance was compared to the global constant $T_c = 0.854$ (Lenton and Vaughan, 2009). This approach is similar to methods suggested for LCA, which are based on the MODIS albedo product and do not consider the site and time dependence of transmission for upwelling radiation.

4. Results

4.1. Time dynamics in the case studies

Albedo was higher for willow (0.216) than for fallow (0.165), and higher at the clear-cut (0.184) than at the forest site (0.082) when calculated from total fluxes over the entire study period. Instantaneous observations at the four sites differed in terms of dispersion (Table 1). Hourly albedo of fallow land usually fell within a narrow range, but had many outliers due to high reflectivity of snow in winter. Willow had a

Table 1

Summary statistics for hourly surface albedo (α_S), surface irradiance ($R_{S\downarrow}$) and atmospheric transmittance (τ): arithmetic mean, median, first quartile (Q1), third quartile (Q3) and quartile coefficient of dispersion CD = (Q3-Q1)/(Q1+Q3).

	Mean	Median	Q1	Q3	CD
α_S willow [−]	0.219	0.211	0.180	0.238	0.14
α_S fallow [−]	0.185	0.153	0.140	0.171	0.10
α_S clear-cut [−]	0.193	0.172	0.145	0.200	0.16
α_S forest [−]	0.079	0.081	0.070	0.089	0.12
$R_{S\downarrow}$ [Wm^{-2}]	115	4	0	167	1.00
τ [−]	0.38	0.37	0.23	0.53	0.40

Note that the arithmetic mean of hourly albedo is not the same as albedo calculated from total fluxes. Data are based on the 3-year study period except for α_S clear-cut and α_S forest.

broad distribution of albedo values, owing to seasonal changes in phenology. Snow effects were less pronounced on willow, resulting in fewer and less extreme outliers. The hourly albedo of the clear-cut showed a broad distribution and increased considerably due to snow deposition. The albedo of forest varied little and was almost unaffected by snow.

Surface irradiance reached up to 800 Wm^{-2} around local noon on clear summer days. Irradiance was on average 115 Wm^{-2}, with median value of only 4 Wm^{-2} due to night-time zeros (Table 1). Atmospheric transmittance was symmetrically distributed. It fell below 10% under overcast conditions and reached up to 75% under clear sky. Over the study period, transmittance was 45% when calculated from total fluxes. This is higher than the arithmetic mean as calculation based on total fluxes gives higher weight to clear-sky observations.

Regular patterns in albedo, surface irradiance and atmospheric transmittance were found on two time scales: (1) seasonal, resulting from vegetation phenology, atmospheric conditions and mean SZA; and (2) diurnal, resulting mainly from SZA.

On seasonal time scales, monthly albedo was higher for willow than for fallow from April to October in all study years (Fig. 1a). The differences were small from November to March, except when snow deposition increased the reflectivity of fallow land. The albedo of fallow changed little throughout the year under snow-free conditions. Seasonal variation was stronger at the willow site. Albedo increased with foliage expansion in spring, reached its snow-free maximum in summer and decreased quickly when the trees shed their leaves. Harvesting willow in April every third year affected albedo only during the first month after cutting. The variation in daily albedo was only high in months with snow.

The clear-cut had higher monthly albedo than the forest throughout the year, with the largest differences resulting from snow deposition. At the clear-cut site, albedo increased slightly in summer months, similar to observations for willow. The forest had the lowest albedo of all sites and the value remained almost constant throughout the year.

Monthly mean surface irradiance and atmospheric transmittance exhibited a clear seasonal cycle (Fig. 1b). Irregularities and day-to-day variability resulted mainly from clouds. Clear-sky values for a cloud-free atmosphere had a smoother seasonal cycle. Monthly clear-sky values were the upper limit to daily means, confirming the importance of clouds for day-to-day variability.

Monthly mean diurnal patterns of albedo confirmed the earlier observations of higher seasonal variation for willow compared with fallow (Fig. 2a,b), and for clear-cut compared with forest (Fig. 2e,f). At all sites, albedo exhibited a minimum around local noon and increased with SZA towards sunrise or sunset. Solar zenith angle at local noon was 49°, 36° and 56° in the selected spring, summer and autumn months, respectively. Between local noon and the cut-off at 85° in the evening,
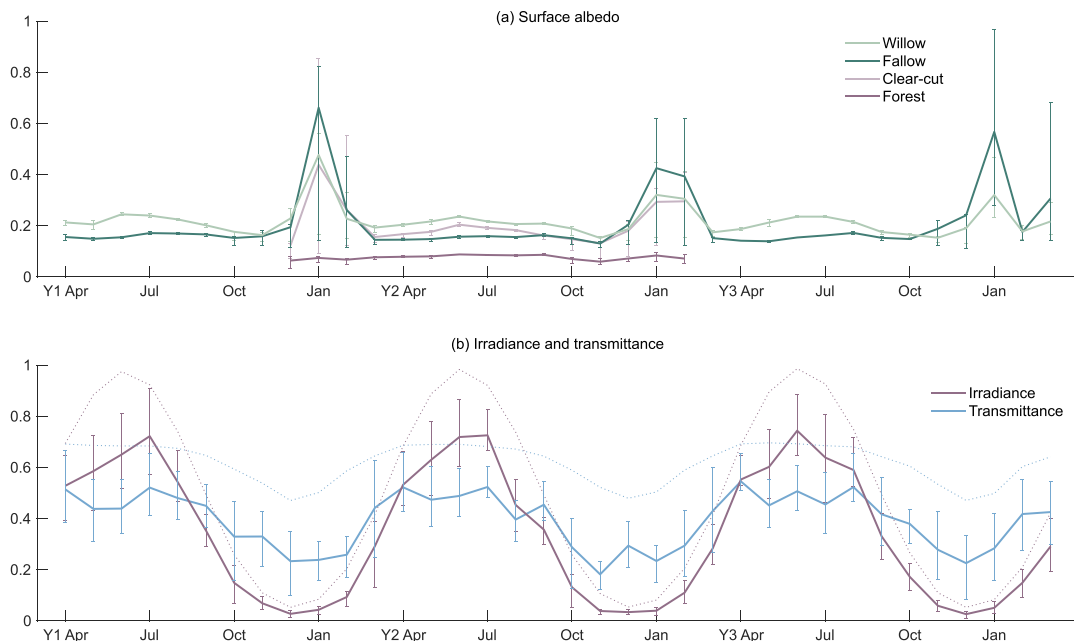

Fig. 1. Seasonal variation in (a) albedo and (b) surface irradiance (normalised by the maximum monthly mean clear-sky irradiance of 332 Wm^{-2}) and atmospheric transmittance. Solid lines are monthly values; vertical bars denote the dispersion of daily values between the first and third quartile. Dotted lines show clear-sky conditions.
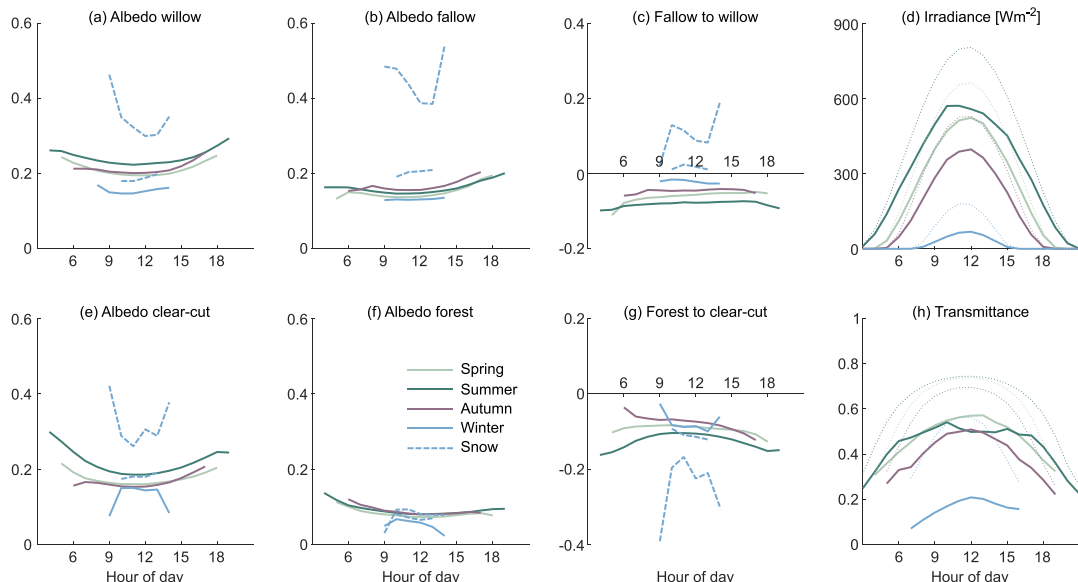
Fig. 2. Mean diurnal variation in selected months of year 2, representing different seasons and snow conditions: (a–c) albedo of willow and fallow, and albedo change in case 1 ($\Delta\alpha_S = \alpha_{S,fallow} - \alpha_{S,willow}$); (d) surface irradiance; (e–g) albedo of clear-cut and forest, and albedo change in case 2 ($\Delta\alpha_S = \alpha_{S,forest} - \alpha_{S,clear-cut}$); (h) atmospheric transmittance. Dotted lines show clear-sky conditions. Hour of day marks the beginning of the interval, i.e. hour 12 is 12:00 to 13:00 local standard time.

albedo increased by 30–60%. The pattern was not symmetrical around local noon in all months. The dependence of albedo on SZA differed by land cover type. Willow and clear-cut showed a stronger absolute increase in albedo between local noon and 85˚. Consequently, the difference in albedo from land use change was larger at high SZA in both cases (Fig. 2c,g).

Albedo at local noon is often used as a proxy for daily albedo. The potential effect of this simplification was evaluated for two sites. Hourly albedo at local noon was lower than daily albedo on 80% of measurement days at each site. Common deviations (Q1–Q3) were −0.5 to −5% for willow and −0.3 to −6% for fallow, with larger differences in summer due to greater SZA variation.

Mean diurnal patterns of surface irradiance and atmospheric transmittance were of the same order of magnitude as the seasonal cycle (Fig. 2d,h). The difference between all-sky and clear-sky values revealed the effect of clouds in each month. All-sky transmittance was higher in spring than in summer, due to lower effective cloud amount.

Irradiance and transmittance determine the ability of albedo change to cause radiative forcing. The largest albedo change due to snow in winter produced less RF_α than smaller changes in months with higher irradiance and transmittance. The same was true for diurnal time scales. Albedo change was higher in morning and evening hours, but less

effective in terms of radiative forcing. Diurnal peaks in RF_α were between 10:00 and 13:00 local standard time.

4.2. Radiative forcing and effect of aggregation

Land use change from fallow to willow gave a mean RF_α of −6.3·10^{-15} Wm^{-2}, using hourly time steps (benchmark model). RF_α differed between years as a result of changes in albedo at both sites, as well as differences in cloudiness (Table 2). These changes occurred on seasonal time scales. Clear-cutting gave an annual mean RF_α of −11.7·10^{-15} Wm^{-2}. Irradiance and transmittance were similar in all years. Effective atmospheric transmittance was calculated for comparison with methods that use an annual mean transmittance factor ($\tau_{eff} = RF_\alpha/RF_S$, where RF_S is radiative forcing from albedo change at the surface, i.e. RF_α with $\tau = 1$).

Models with reduced resolution were used to calculate annual mean RF_α (Table 3) and were evaluated against the benchmark model. An error in in RF_α (eRF_α) results from the dependence of three variables, i.e. albedo change, irradiance and transmittance. The effect of aggregation was broken down into two components. First, RF_S was calculated include only the dependence of albedo change and irradiance. Second, τ_{eff} was used as a measure for the relationship of transmittance

Table 2
Results of the benchmark model: annual mean radiative forcing from albedo change (RF_α) in case 1 and case 2. α_S denotes surface albedo, where ref is the reference and new is the new land cover. $R_{S\downarrow}$ is mean solar irradiance at the surface, τ is annual atmospheric transmittance and τ_{eff} is effective atmospheric transmittance.

Year	RF_α [10^{-15} Wm^{-2}]	α_{Sref} [−]	α_{Snew} [−]	$R_{S\downarrow}$ [Wm^{-2}]	τ [−]	τ_{eff} [−]
Case 1: Fallow to willow						
1	−6.7	0.165	0.222	114	0.45	0.55
2	−6.5	0.160	0.215	114	0.44	0.55
3	−5.7	0.168	0.212	118	0.46	0.60
Case 2: Forest to clear-cut						
–	−11.7	0.082	0.184	114	0.44	0.52

Table 3

Results of the models with reduced resolution: RF_α is radiative forcing from albedo change on $1\,m^2$ of land; τ_{eff} is effective atmospheric transmittance; eRF_α and eRF_S give the relative error in radiative forcing at the TOA and at the surface compared with the benchmark model. For case 1 results are shown for year 2 only, but discussed for all years.

Model	Case 1: Fallow to willow				Case 2: Forest to clear-cut			
	RF_α [$10^{-15}\,Wm^{-2}$]	eRF_α [%]	eRF_S [%]	τ_{eff} [−]	RF_α [$10^{-15}\,Wm^{-2}$]	eRF_α [%]	eRF_S [%]	τ_{eff} [−]
Method 1: Total fluxes								
D	−6.3	−3	0	0.53	−11.4	−2	1	0.50
M	−5.7	−13	−3	0.49	−10.4	−11	1	0.45
Y	−5.4	−17	2	0.44	−10.1	−13	1	0.44
Method 2: Monthly mean diurnal cycles								
MH filled	−5.9	−9	1	0.49	−10.2	−12	−1	0.46
MH gaps	−5.9	−8	1	0.49	−10.3	−12	−1	0.46
Method 3: Clear-sky days								
Mc	−5.7	−13	−4	0.50	−10.1	−13	−4	0.47
Mnc	−5.5	−15	−6	0.50	−9.0	−23	−15	0.47
Method 4: Local noon albedo								
Dn	−6.1	−5	−1	0.52	−10.6	−9	−5	0.49
Mn	−5.8	−11	0	0.49	−9.7	−17	−5	0.45
Yn	−2.4	−63	−55	0.44	−11.6	−1	16	0.44

with RF_S. The smaller the deviation of RF_S and τ_{eff} from the benchmark, the better the representation of the surface energy budget and of atmospheric transmittance, respectively. A good model of RF_α should be accurate in the individual components, so that an underestimation of RF_S cannot be compensated by an overestimation of τ_{eff}, or vice versa.

The error in RF_S was within ± 5% in both cases when seasonal and diurnal variations in albedo were taken into account (Table 3). This was accomplished by correct weighting in method 1 and by nested aggregation in method 2. Monthly mean diurnal cycles were robust despite data gaps (MH gaps). In method 3, the selective use of clear-sky days (Mc) and clear-sky albedo at local noon (Mnc) led to an underestimation of 4–16%. As these models rely on a single day per month, the effect of aggregation differed between years and cases due to interday variability.

Method 4 does not consider the co-variation of albedo change with irradiance and transmittance. Using method Yn in case 1, aggregation of local noon albedo to the annual arithmetic mean gave an error of −63% in year 2 (Table 3). The error was even larger in year 3, resulting in positive rather than negative RF_α. This was due to high albedo change in winter, which is not appropriately weighted by low irradiance in method Yn. The error was smaller in case 2 because albedo change was high throughout the year (see Fig. 1). Using methods Dn and Mn, the difference in all-sky albedo at local noon was a good proxy for time-dependent albedo change on daily or monthly time scales. Diurnal variation in $\Delta\alpha_S$ was weak in case 1, due to similar SZA dependence of albedo for willow and fallow. Albedo change had a stronger diurnal cycle in case 2 (see Fig. 2c,g), leading to a 5% underestimation of RF_α.

Calculations with a single transmittance factor did not give the same result as using site- and time-dependent transmittance. Using the global constant $T_c = 0.854$ led to an overestimation of RF_α for two reasons. First, the global mean is not appropriate for the high-latitude case study location with an average SZA of 68°. For comparison, local effective clear-sky transmittance was calculated to be 67–70%. Second, T_c does not account for the attenuation of upwelling radiation by clouds. Local effective all-sky transmittance was significantly lower with 55% in case 1 and 52% in case 2.

Effective transmittance was highest in the benchmark model (52–55%) and decreased with aggregation using daily (50–53%) monthly (45–50%) or yearly (44%) time steps in different models with reduced resolution. This was due to differences in implicit weighting. In the benchmark model, hourly transmittance is weighted by $R_{S\uparrow}$ during RF_α calculations, whereas in the simplified models it is weighted by $R_{TOA\downarrow}^2 \cdot R_{S\uparrow}^2$ during aggregation in the single-layer model. Weighting by

upwelling shortwave irradiance favours observations under low optical thickness (i.e. clear-sky or small SZA) relatively more. Consequently, the effect of aggregation is negligible for clear-sky transmittance, and it is particularly high in cloudy periods.

5. Discussion and implications for Life Cycle Assessment

The analysis of albedo at four sites in south-western Sweden revealed clear differences between land cover types and consistent diurnal and seasonal patterns. Albedo was highest for willow (0.216) and lowest for coniferous forest (0.082). Fallow and clear-cut had albedo of 0.165 and 0.184, respectively. The diurnal variation in albedo with SZA was stronger at sites with higher albedo. The seasonal variation was strong at sites where plant phenology or snow deposition changed the surface properties. Inter-annual variation resulted mainly from snowfall, whereas harvesting affected the albedo of willow only during the first month after cutting.

These findings agree with previous studies (e.g. Hollinger et al., 2010; Schaeffer et al., 2006). The albedo of fallow was on the low end of values reported for grassland, which is due to the high water table at the fallow site. For coniferous forests, similar albedos have been observed at northerly sites. The albedo of willow was on the high end of values reported for deciduous broadleaf species and our result is slightly higher than other measurements on willow (Levy et al., 2018). This may stem from differences in local climate, soil, management, species composition and SZA. These factors make it difficult to predict albedo by vegetation type. Generic parameterisations of albedo may lead to misconceptions about the magnitude and direction of albedo change. For instance, generic values for deciduous broadleaf trees and grassland suggest decreasing albedo due to willow cultivation, whereas our data showed an increase in each of 3 years.

The strength of albedo change as a climate forcer depends on where and when it occurs, as solar irradiance and atmospheric transmittance vary with SZA and atmospheric composition. Analysing geographical and seasonal variations in albedo, irradiance and transmittance helps to understand the potential climate impact of land cover change due to differences in albedo. This can be used to guide mitigation efforts through land cover management (Carrer et al., 2018) or to direct modelling efforts in LCA. For instance, albedo change resulting from the snow-masking effect of trees has received much attention (Betts, 2000). However, this has minor relevance in areas where snowfall is limited to periods with low incoming radiation and atmospheric transmittance. In the case studies for instance, snowfall between November and February was largely ineffective in terms of RF_α whereas smaller differences in

albedo in summer had a higher impact.

Previous LCA studies have accounted for spatial and temporal variations in surface irradiance, but variations in all-sky atmospheric transmittance have not commonly been considered. In this study a single-layer radiative transfer model was used, which allowed to include spatio-temporal variations in transmittance in an analytical approach. The suggested methods account for multiple reflections between surface and atmosphere, are computationally inexpensive and rely on publicly available data. Using this model, effective atmospheric transmittance was found to be lower in the case study area (around 55%) than the global constant of 85%. Local transmittance varied from 30% in winter months to over 50% in spring and summer, and between 20 and 60% on diurnal time scales.

Radiative transfer in this study is contingent on the assumptions underlying the single-layer model. This formulation has primarily been used to study the Earth's radiation budget (Stephens et al., 2015), but also for climate feedback analysis (Taylor et al., 2007) and to quantify the atmospheric attenuation of surface albedo change (Donohoe and Battisti, 2011). Monthly transmittance has been obtained with satisfactory accuracy compared with complex radiation schemes (Taylor et al., 2007). Differences in weighting due to calculation from daily instead of monthly shortwave fluxes have previously been observed (Winton, 2005), but a discussion of appropriate temporal resolution is lacking.

The RF_α estimates based on Eq. (6) were compared to using radiative kernels from four general circulation models. The result for case 1, $-6.3 \cdot 10^{-15}$ Wm^{-2}, fell between $-5.6 \cdot 10^{-15}$ and $-11.0 \cdot 10^{-15}$ Wm^{-2} obtained with different kernels. In case 2, $-11.7 \cdot 10^{-15}$ Wm^{-2} was slightly lower than the range of $-13.2 \cdot 10^{-15}$ to $-23.9 \cdot 10^{-15}$ Wm^{-2}. A disadvantage of using radiative kernels for this purpose is that correlations between albedo change and the kernels on sub-monthly timescales cannot be considered (Soden et al., 2008). For a constant change in albedo, Eq. (6) underestimated RF_α compared to using kernels, yet a magnitude smaller than inter-model differences.

The performed model evaluation showed how different resolutions and aggregation methods may affect estimations of RF_α. Radiative forcing can be modelled at high accuracy by using small time steps, e.g. hourly as demonstrated in the benchmark model. However, time series data of albedo are costly and time-consuming to obtain and usually affected by errors and gaps. Therefore, three strategies were identified to model annual mean RF_α depending on data availability.

When continuous radiation measurements are available to determine surface albedo, RF_α can be modelled in annual time steps. To increase robustness, monthly time steps are recommended as a minimal resolution. The correlation of instantaneous albedo and surface irradiance can be addressed by calculating albedo from total shortwave fluxes. This was not the case for the correlation of transmittance and irradiance, because the single-layer model underestimated the relative contribution of observations with lower cloudiness. Correct weighting can be obtained by calculating effective all-sky transmittance from hourly fluxes.

When observations are discontinuous, the seasonal co-variation of albedo change, surface irradiance and atmospheric transmittance needs to be considered. This can be done by using monthly time steps to calculate RF_α, or by weighting instantaneous albedo values with solar irradiance to calculate annual albedo. Ignoring the seasonal co-variation led to errors in RF_α in the case studies, doubling the cooling from clear-cutting or giving a warming rather than cooling from willow cultivation in year 3. Large errors are consistent with findings by Bright (2015). Diurnal variations of albedo change had a small effect on RF_α in the cases considered, so that albedo at local noon could be used as a proxy for daily values. However, ignoring the diurnal cycle of albedo leads to systematic underestimation of RF_α. This might be important when assessing albedo change at lower latitudes with greater SZA variation, and when new and old land cover differ strongly in SZA dependence.

Primary data can be collected selectively on clear-sky days to approximate monthly or seasonal albedo. In the case studies, monthly albedo was stable when vegetation or precipitation was not subject to seasonal change. For some periods and land cover types, a lower resolution can thus be sufficient. Clear-sky observations around local noon were a robust estimate of monthly albedo, as they appeared to be least prone to measurement errors related to clouds or high SZA. The difference between monthly RF_α from clear-sky and all-sky albedo was minor. This is because the effect of atmospheric conditions on albedo is generally small (Lyapustin, 1999), and because clear-sky observations are weighted by higher irradiance and transmittance. Several measurements can be aggregated to increase the robustness.

Surface albedo change was included in an analytical approach as common for LCA. The RF concept can be used directly to compare the impact from albedo change and GHGs, or as a basis for other climate metrics such as GWP. A cooling effect was found in both case studies, amounting to mean RF_α of $-6.3 \cdot 10^{-15}$ Wm^{-2} (-69 g CO$_2$e m^{-2} yr^{-1}) for conversion of fallow to willow and $-11.7 \cdot 10^{-15}$ Wm^{-2} (-128 g CO$_2$e m^{-2} yr^{-1}) for clear-cutting. These results are of the same magnitude as values reported for land cover change from aspen to clear-cut in Northern Wisconsin and spruce to clear-cut in south-eastern Norway, respectively (Cherubini et al., 2012). However, opportunities for direct comparison are limited as the albedo effect is highly specific to location and vegetation characteristics (Cai et al., 2016).

Albedo change can make a substantial contribution to the life cycle climate impact of a product in relation to GHG emissions. The net impact of cultivating SRC willow on previously fallow land in Sweden with combustion for energy has been estimated between -110 and $+108$ g CO$_2$e m^{-2} yr^{-1}, depending on yield levels (Hammar et al., 2014). In this system, an annual "offset" of 69 g CO$_2$e m^{-2} due to albedo change can improve the climate impact of willow bioenergy and potentially turn a net warming effect into net cooling. Due to the similar magnitude of net GHG and albedo impact in this system, the choice of modelling method for RF_α may be significant for the estimated total climate impact.

LCAs commonly use single-score metrics such as GWP to facilitate communication of results and comparisons between products or impacts. Single-score metrics require choosing a time horizon or time of evaluation, which leads to unequal weighting of short-term and long-term impacts. Employing this approach for joint assessments of long-lived GHGs and short-lived climate forcers, including albedo change, has thus been questioned (Peters et al., 2011). Methods to express impacts as a function of time have been suggested, using a time distributed inventory and global mean surface temperature change as an indicator (Ericsson et al., 2013). The temporal information included in such a result might better reflect the climate impact of albedo change compared with GHGs.

Further research is needed to improve understanding of albedo across a wider range of land cover types, locations and management practices. The climate impact of albedo change can strengthen or offset the effects of carbon sequestration or GHGs. Therefore, albedo should be considered when land use leads to a significant change in surface properties. Potential applications in LCA range from bioenergy systems to crop, harvest and residue management, building materials and paving of surfaces.

Declarations of interest

None.

Acknowledgements

References

Arora, V.K., Montenegro, A., 2011. Small temperature benefits provided by realistic afforestation efforts. Nat. Geosci. 4, 514. https://doi.org/10.1038/ngeo1182.

Betts, R.A., 2000. Offset of the potential carbon sink from boreal forestation by decreases in surface albedo. Nature 408 (6809), 187–190. https://doi.org/10.1038/35041545.

Betts, R.A., 2001. Biogeophysical impacts of land use on present-day climate: near-surface temperature change and radiative forcing. Atmos. Sci. Lett. 2 (1-4), 39–51. https://doi.org/10.1006/asle.2001.0023.

Block, K., Mauritsen, T., 2013. Forcing and feedback in the MPI-ESM-LR coupled model under abruptly quadrupled CO₂. J. Adv. Model. Earth Syst. 5 (4), 676–691. https://doi.org/10.1002/jame.20041.

Brieglib, B.P., Minnis, P., Ramanathan, V., Harrison, E., 1986. Comparison of regional clear-sky albedos inferred from satellite observations and model computations. J. Clim. Appl. Meteorol. 25 (2), 214–226. https://doi.org/10.1175/1520-0450(1986)025<0214:corcsa>2.0.co;2.

Bright, R.M., 2015. Metrics for biogeophysical climate forcings from land use and land cover changes and their inclusion in Life Cycle Assessment: a critical review. Environ. Sci. Technol. 49 (6), 3291–3303. https://doi.org/10.1021/es505465t.

Bright, R.M., Cherubini, F., Stromman, A.H., 2012. Climate impacts of bioenergy: inclusion of carbon cycle and albedo dynamics in life cycle impact assessment. Environ. Impact Assess. Rev. 37, 2–11. https://doi.org/10.1016/j.eiar.2012.01.002.

Bright, R.M., Zhao, K.G., Jackson, R.B., Cherubini, F., 2015. Quantifying surface albedo and other direct biogeophysical climate forcings of forestry activities. Glob. Chang. Biol. 21 (9), 3246–3266. https://doi.org/10.1111/gcb.12951.

Cai, H., Wang, J., Feng, Y., Wang, M., Qin, Z., Dunn, J.B., 2016. Consideration of land use change-induced surface albedo effects in life-cycle analysis of biofuels. Energy Environ. Sci. 9 (9), 2855–2867. https://doi.org/10.1039/c6ee01728b.

Caiazzo, F., Malina, R., Staples, M.D., Wolfe, P.J., Yim, S.H.L., Barrett, S.R.H., 2014. Quantifying the climate impacts of albedo changes due to biofuel production: a comparison with biogeochemical effects. Environ. Res. Lett. 9 (2). https://doi.org/10.1088/1748-9326/9/2/024015.

Carrer, D., Pique, G., Ferlicoq, M., Ceamanos, X., Ceschia, E., 2018. What is the potential of cropland albedo management in the fight against global warming? A case study based on the use of cover crops. Environ. Res. Lett. 13 (4). https://doi.org/10.1088/1748-9326/aab650.

Cherubini, F., Bright, R.M., Stromman, A.H., 2012. Site-specific global warming potentials of biogenic CO₂ for bioenergy: contributions from carbon fluxes and albedo dynamics. Environ. Res. Lett. 7 (4). https://doi.org/10.1088/1748-9326/7/4/045902.

Creutzig, F., Ravindranath, N.H., Berndes, G., Bolwig, S., Bright, R., Cherubini, F., Chum, H., Corbera, E., Delucchi, M., Faaij, A., Fargione, J., Haberl, H., Heath, G., Lucon, O., Plevin, R., Popp, A., Robledo-Abad, C., Rose, S., Smith, P., Stromman, A., Suh, S., Masera, O., 2015. Bioenergy and climate change mitigation: an assessment. Glob. Chang. Biol. Bioenergy 7 (5), 916–944. https://doi.org/10.1111/gcbb.12205.

Dickinson, R.E., 1983. Land surface processes and climate – surface albedo and energy balance. Adv. Geophys. 25, 305–353. https://doi.org/10.1016/S0065-2687(08)60176-4.

Donohoe, A., Battisti, D.S., 2011. Atmospheric and surface contributions to planetary albedo. J. Clim. 24 (16), 4402–4418. https://doi.org/10.1175/2011jcli3946.1.

ECMWF, 2018. ERA5 Hourly Data on Single Levels from 2000 to 2017. Generated Using Copernicus Climate Change Service Information. Retrieved 18/09/2018, from European Centre for Medium-Range Weather Forecasts (ECMWF) at. https://cds.climate.copernicus.eu.

Ericsson, N., Porsö, C., Ahlgren, S., Nordberg, A., Sundberg, C., Hansson, P.-A., 2013. Time-dependent climate impact of a bioenergy system – methodology development and application to Swedish conditions. Glob. Chang. Biol. Bioenergy 5 (5), 580–590. https://doi.org/10.1111/gcbb.12031.

Finnveden, G., Hauschild, M.Z., Ekvall, T., Guinee, J., Heijungs, R., Hellweg, S., Koehler, A., Pennington, D., Suh, S., 2009. Recent developments in Life Cycle Assessment. J. Environ. Manag. 91 (1), 1–21. https://doi.org/10.1016/j.jenvman.2009.06.018.

Ghimire, B., Williams, C.A., Masek, J., Gao, F., Wang, Z., Schaaf, C., He, T., 2014. Global albedo change and radiative cooling from anthropogenic land cover change, 1700 to 2005 based on MODIS, land use harmonization, radiative kernels, and reanalysis. Geophys. Res. Lett. 41 (24), 9087–9096. https://doi.org/10.1002/2014GL061671.

Hammar, T., Ericsson, N., Sundberg, C., Hansson, P.-A., 2014. Climate impact of willow grown for bioenergy in Sweden. Bioenergy Res. 7 (4), 1529–1540. https://doi.org/10.1007/s12155-014-9490-0.

Hellweg, S., Milà i Canals, L., 2014. Emerging approaches, challenges and opportunities in Life Cycle Assessment. Science 344 (6188), 1109–1113. https://doi.org/10.1126/science.1248361.

Hollinger, D.Y., Ollinger, S.V., Richardson, A.D., Meyers, T.P., Dail, D.B., Martin, M.E., Scott, N.A., Arkebauer, T.J., Baldocchi, D.D., Clark, K.L., Curtis, P.S., Davis, K.J., Desai, A.R., Dragoni, D., Goulden, M.L., Gu, L., Katul, G.G., Pallardy, S.G., Paw, K.T., Schmid, H.P., Stoy, P.C., Suyker, A.E., Verma, S.B., 2010. Albedo estimates for land surface models and support for a new paradigm based on foliage nitrogen concentration. Glob. Chang. Biol. 16 (2), 696–710. https://doi.org/10.1111/j.1365-2486.2009.02028.x.

Lenton, T.M., Vaughan, N.E., 2009. The radiative forcing potential of different climate geoengineering options. Atmos. Chem. Phys. 9 (15), 5539–5561. https://doi.org/10.5194/acp-9-5539-2009.

Levasseur, A., Lesage, P., Margni, M., Deschenes, L., Samson, R., 2010. Considering time in LCA: dynamic LCA and its application to global warming impact assessments. Environ. Sci. Technol. 44 (8), 3169–3174. https://doi.org/10.1021/es9030003.

Levy, C.R., Burakowski, E., Richardson, A.D., 2018. Novel measurements of fine-scale albedo: using a commercial quadcopter to measure radiation fluxes. Remote Sens. 10 (8). https://doi.org/10.3390/rs10081303.

Lyapustin, A.I., 1999. Atmospheric and geometrical effects on land surface albedo. J. Geophys. Res.-Atmos. 104 (D4), 4127–4143. https://doi.org/10.1029/1998jd200064.

Milà i Canals, L., Bauer, C., Depestele, J., Dubreuil, A., Freiermuth Knuchel, R., Gaillard, G., Michelsen, O., Müller-Wenk, R., Rydgren, B., 2007. Key elements in a framework for land use impact assessment within LCA. Int. J. Life Cycle Assess. 12 (1), 5–15. https://doi.org/10.1065/lca2006.05.250.

Muñoz, I., Campra, P., Fernández-Alba, A.R., 2010. Including CO₂-emission equivalence of changes in land surface albedo in Life Cycle Assessment. Methodology and case study on greenhouse agriculture. Int. J. Life Cycle Assess. 15 (7), 672–681. https://doi.org/10.1007/s11367-010-0202-5.

Myhre, G., Shindell, D., Breón, F.-M., Collins, W., Fuglestvedt, J., Huang, J., Koch, D., Lamarque, J., Lee, D., Mendoza, B., Nakajima, T., Robock, A., Stephens, G., Takemura, T., Zhang, H., 2013. Anthropogenic and natural radiative forcing. In: Stocker, T.F., Qin, D., Plattner, G.-K., Tignor, M., Allen, S.K., Boschung, J., Nauels, A., Xia, Y., Bex, V., Midgley, P.M. (Eds.), Climate Change 2013: The Physical Science Basis. Contribution of Working Group I to the Fifth Assessment Report of the Intergovernmental Panel on Climate Change. Cambridge University Press, Cambridge and New York, NY, pp. 659–740.

Pendergrass, A.G., Conley, A., Vitt, F.M., 2018. Surface and top-of-atmosphere radiative feedback kernels for CESM-CAM5. Earth Syst. Sci. Data 10 (1), 317–324. https://doi.org/10.5194/essd-10-317-2018.

Peters, G.P., Aamaas, B., Lund, M.T., Solli, C., Fuglestvedt, J.S., 2011. Alternative "Global Warming" metrics in Life Cycle Assessment: a case study with existing transportation data. Environ. Sci. Technol. 45 (20), 8633–8641. https://doi.org/10.1021/es200627s.

Pielke, R.A., Avissar, R., Raupach, M., Dolman, A.J., Zeng, X.B., Denning, A.S., 1998. Interactions between the atmosphere and terrestrial ecosystems: influence on weather and climate. Global Change Biology 4 (5), 461–475. https://doi.org/10.1046/j.1365-2486.1998.t01-1-00176.x.

Roesch, A., Wild, M., Ohmura, A., Dutton, E.G., Long, C.N., Zhang, T., 2011. Assessment of BSRN radiation records for the computation of monthly means. Atmos. Meas. Tech. 4 (2), 339–354. https://doi.org/10.5194/amt-4-339-2011.

Roy, P.O., Azevedo, L.B., Margni, M., van Zelm, R., Deschenes, L., Huijbregts, M.A.J., 2014. Characterization factors for terrestrial acidification at the global scale: a systematic analysis of spatial variability and uncertainty. Sci. Total Environ. 500, 270–276. https://doi.org/10.1016/j.scitotenv.2014.08.099.

Schaeffer, M., Eickhout, B., Hoogwijk, M., Strengers, B., Vuuren, D.v., Leemans, R., Opsteegh, T., 2006. CO₂ and albedo climate impacts of extratropical carbon and biomass plantations. Glob. Biogeochem. Cycles 20 (2). https://doi.org/10.1029/2005GB002581.

Schwaiger, H.P., Bird, D.N., 2010. Integration of albedo effects caused by land use change into the climate balance: should we still account in greenhouse gas units? For. Ecol. Manag. 260 (3), 278–286. https://doi.org/10.1016/j.foreco.2009.12.002.

Shell, K.M., Kiehl, J.T., Shields, C.A., 2008. Using the radiative kernel technique to calculate climate feedbacks in NCAR's community atmospheric model. J. Clim. 21 (10), 2269–2282. https://doi.org/10.1175/2007jcli2044.1.

Smith, P., Bustamante, M., Ahammad, H., Clark, H., Dong, H., Elsiddig, E.A., Haberl, H., Harper, R., House, J., Jafari, M., Masera, O., Mbow, C., Ravindranath, N.H., Rice, C.W., Robledo Abad, C., Romanovskaya, A., Sperling, F., Tubiello, F., 2014. Agriculture, forestry and other land use (AFOLU). In: Edenhofer, O., Pichs-Madruga, R., Sokona, Y., Farahani, E., Kadner, S., Seyboth, K., Adler, A., Baum, I., Brunner, S., Eickemeier, P., Kriemann, B., Savolainen, J., Schlömer, S., von Stechow, C., Zwickel, T., Minx, J.C. (Eds.), Climate Change 2014: Mitigation of Climate Change. Contribution of Working Group III to the Fifth Assessment Report of the Intergovernmental Panel on Climate Change. Cambridge University Press, Cambridge, United Kingdom and New York, NY, USA.

Smith, C.J., Kramer, R.J., Myhre, G., Forster, P.M., Soden, B.J., Andrews, T., Boucher, O., Faluvegi, G., Fläschner, D., Hodnebrog, Ø., Kasoar, M., Kharin, V., Kirkevåg, A., Lamarque, J.-F., Mülmenstädt, J., Olivié, D., Richardson, T., Samset, B.H., Shindell, D., Stier, D., Takemura, T., Voulgarakis, A., Watson-Parris, D., 2018. Understanding rapid adjustments to diverse climate forcings. Geophys. Res. Lett. 45 (21). https://doi.org/10.1029/2018GL079826. 12023-012031.

Soden, B.J., Held, I.M., Colman, R., Shell, K.M., Kiehl, J.T., Shields, C.A., 2008. Quantifying climate feedbacks using radiative kernels. J. Clim. 21 (14), 3504–3520. https://doi.org/10.1175/2007jcli2110.1.

Stephens, G.L., O'Brien, D., Webster, P.J., Pilewski, P., Kato, S., Li, J.L., 2015. The albedo of Earth. Rev. Geophys. 53 (1), 141–163. https://doi.org/10.1002/2014rg000449.

Taylor, K.E., Crucifix, M., Braconnot, P., Hewitt, C.D., Doutriaux, C., Broccoli, A.J., Mitchell, J.F.B., Webb, M.J., 2007. Estimating shortwave radiative forcing and response in climate models. J. Clim. 20 (11), 2530–2543. https://doi.org/10.1175/jcli4143.1.

Wang, Z., Zeng, X., Barlage, M., 2007. Moderate Resolution Imaging Spectroradiometer bidirectional reflectance distribution function-based albedo parameterization for weather and climate models. J. Geophys. Res.-Atmos. 112 (D2). https://doi.org/10.1029/2005jd006736.

Wang, D., Liang, S., He, T., Yu, Y., Schaaf, C., Wang, Z., 2015. Estimating daily mean land surface albedo from MODIS data. J. Geophys. Res.-Atmos. 120 (10), 4825–4841. https://doi.org/10.1002/2015jd023178.

Winton, M., 2005. Simple optical models for diagnosing surface-atmosphere shortwave interactions. J. Clim. 18 (18), 3796–3805. https://doi.org/10.1175/jcli3502.1.

Yang, F., Mitchell, K., Hou, Y.-T., Dai, Y., Zeng, X., Wang, Z., Liang, X.-Z., 2008. Dependence of land surface albedo on solar zenith angle: observations and model parameterization. J. Appl. Meteorol. Climatol. 47 (11), 2963–2982. https://doi.org/10.1175/2008jamc1843.1.

Petra Sieber is a doctoral candidate at the Department of Energy and Technology, Swedish University of Agricultural Sciences (SLU). Her research concerns the development of LCA methodology for assessing the climate impact of land use and renewable energy systems, with particular focus on surface albedo change.

Niclas Ericsson is a researcher at the Department of Energy and Technology, Swedish University of Agricultural Sciences (SLU). His main research area is the sustainability of bio-based products and systems, with special focus on LCA and time-dependent climate impact of agricultural and forestry based energy systems.

Per-Anders Hansson is a professor at the Department of Energy and Technology, Swedish University of Agricultural Sciences (SLU). His main research area is the sustainability of agriculturally based products and systems. LCA is the main methodology used to evaluate food, energy and biomaterials.

II

GLOBAL CHANGE BIOLOGY
BIOENERGY   WILEY

Including albedo in time-dependent LCA of bioenergy

Petra Sieber [ID] | Niclas Ericsson [ID] | Torun Hammar [ID] | Per-Anders Hansson

Department of Energy and Technology, Swedish University of Agricultural Sciences (SLU), Uppsala, Sweden

Correspondence
Petra Sieber, Department of Energy and Technology, Swedish University of Agricultural Sciences (SLU), Uppsala SE750 07, Sweden.
Email: petra.sieber@slu.se

Funding information
Swedish Government

Abstract

Albedo change during feedstock production can substantially alter the life cycle climate impact of bioenergy. Life cycle assessment (LCA) studies have compared the effects of albedo and greenhouse gases (GHGs) based on global warming potential (GWP). However, using GWP leads to unequal weighting of climate forcers that act on different timescales. In this study, albedo was included in the time-dependent LCA, which accounts for the timing of emissions and their impacts. We employed field-measured albedo and life cycle emissions data along with time-dependent models of radiative transfer, biogenic carbon fluxes and nitrous oxide emissions from soil. Climate impacts were expressed as global mean surface temperature change over time (ΔT) and as GWP. The bioenergy system analysed was heat and power production from short-rotation willow grown on former fallow land in Sweden. We found a net cooling effect in terms of ΔT per hectare (-3.8×10^{-11} K in year 100) and GWP_{100} per MJ fuel (-12.2 g CO_2e), as a result of soil carbon sequestration via high inputs of carbon from willow roots and litter. Albedo was higher under willow than fallow, contributing to the cooling effect and accounting for 34% of GWP_{100}, 36% of ΔT in year 50 and 6% of ΔT in year 100. Albedo dominated the short-term temperature response (10–20 years) but became, in relative terms, less important over time, owing to accumulation of soil carbon under sustained production and the longer perturbation lifetime of GHGs. The timing of impacts was explicit with ΔT, which improves the relevance of LCA results to climate targets. Our method can be used to quantify the first-order radiative effect of albedo change on the global climate and relate it to the climate impact of GHG emissions in LCA of bioenergy, alternative energy sources or land uses.

KEYWORDS
albedo, bioenergy, climate impact, greenhouse gases, land use change, LCA, life cycle assessment, willow

1 | INTRODUCTION

Biomass as a source of renewable energy can decrease dependency on fossil fuels and contribute to climate change mitigation by storing carbon in biomass and soil

(Creutzig et al., 2015). For bioenergy to generate negative carbon emissions, more carbon has to be sequestered during feedstock production than is released along the life cycle (Searchinger et al., 2008; Tilman, Hill, & Lehman, 2006). The greenhouse gas (GHG) balance of bioenergy is

commonly determined using life cycle assessment (LCA), a standardized method for evaluating potential environmental impacts (Cherubini et al., 2009; Creutzig et al., 2015; Hellweg & Milà i Canals, 2014). All direct and indirect sources of GHG emissions need to be considered, including production of inputs, field operations, land use, transport, processing and energy conversion.

Land management and land use change (direct or indirect) can dominate the GHG balance of bioenergy systems due to changes in carbon stocks (Searchinger et al., 2008) and nitrous oxide emissions from nitrogen application (Cherubini et al., 2009). Compared to annual crops, perennial grasses and short-rotation coppice (SRC) species are associated with lower land-related emissions as they require less fertilization and have the potential to sequester additional carbon in soil (Don et al., 2012). Cultivation of perennial crops on marginal lands has been suggested to minimize competition with other agricultural uses and increase the potential for soil carbon sequestration (Gelfand et al., 2013; Whitaker et al., 2018).

Land use further affects the climate by modifying the biophysical properties of the land surface, including albedo, evapotranspiration efficiency and surface roughness (Pielke et al., 2002). These properties regulate fluxes of energy, water and momentum between the surface and the atmosphere and influence climate variables on local, regional and global scale (Pielke et al., 1998). Albedo, the share of solar flux reflected back from the ground, directly impacts the Earth's energy budget. The more reflective a surface, the higher its albedo and the greater the potential for radiative cooling and eventually temperature change. Through this mechanism, land use over time has led to substantial radiative cooling (Betts, Falloon, Goldewijk, & Ramankutty, 2007; Ghimire et al., 2014) and resulted in lower temperatures (Betts et al., 2007). This is because most historical land cover change to date has been agricultural expansion in temperate regions, where the shift from forests to more reflective croplands has increased albedo and primarily caused albedo-related cooling (Betts et al., 2007). There is concern that albedo change today could offset the cooling achieved by emissions reduction measures that affect surface properties, such as afforestation (Arora & Montenegro, 2011), biomass plantation (Schaeffer et al., 2006) and biochar application (Smith, 2016). It has also been suggested that land could be managed proactively towards higher albedo to mitigate global warming, for example, by introducing cover crops (Carrer, Pique, Ferlicoq, Ceamanos, & Ceschia, 2018) or by using reflective materials on urban surfaces (Akbari, Menon, & Rosenfeld, 2009).

Albedo can be an important contributor to the life cycle climate impact of bioenergy. LCA studies show that changes in albedo may cause radiative forcing (RF) of similar magnitude to the RF of net GHG emissions in a bioenergy system (Cai et al., 2016; Caiazzo et al., 2014; Cherubini, Bright, & Stromman, 2012). However, the importance of albedo depends on a range of case-specific factors such as local climate, insolation, soil type, vegetation, management and yield. Therefore, additional research is needed to understand when, where and at which scale surface albedo should be considered in the planning and assessment of bioenergy systems.

The relative importance of albedo for the life cycle climate impact depends on the time perspective chosen for the assessment. Albedo change leads to RF that persists only as long as surface properties are modified, while the RF of GHGs decays gradually after emission and may persist for decades or centuries. Metrics commonly used in LCA, such as global warming potential (GWP), are calculated for a single time horizon. This results in unequal weighting of short-term and long-term climate forcers, which may be inappropriate in joint assessments of well-mixed GHGs, short-lived climate forcers and albedo effects (Peters, Aamaas, Lund, Solli, & Fuglestvedt, 2011; Tanaka, Peters, & Fuglestvedt, 2010). Methods have been developed to express climate impacts as a function of time (Levasseur et al., 2016), based on annual emission inventories and metrics such as instantaneous RF (Levasseur, Lesage, Margni, & Samson, 2013; Pourhashem, Adler, & Spatari, 2016), cumulative RF (Levasseur et al., 2013) or global mean surface temperature change (Ericsson et al., 2013). These time-dependent LCA methods have been used to compare the impact of GHGs with different lifetimes, account for the timing of emissions and include temporary storage of biogenic carbon. To our knowledge, few LCA studies have applied time-dependent methods to albedo using RF as a metric (Bright, Stromman, & Peters, 2011; Cherubini et al., 2012; Jørgensen, Cherubini, & Michelsen, 2014), whereas the majority has used GWP (Arvesen et al., 2018; Cai et al., 2016; Caiazzo et al., 2014; Meyer, Bright, Fischer, Schulz, & Glaser, 2012).

The aim of this study was to improve understanding of how albedo affects the life cycle climate impact of bioenergy. Specific objectives were (a) to include albedo in time-dependent LCA; and (b) to evaluate the magnitude of the life cycle climate impact due to albedo change and compare it with carbon sequestration and GHG emissions in a bioenergy system. For this purpose, LCA methodology was combined with time-dependent models of the production chain, biogenic carbon fluxes, nitrous oxide emissions from soil and radiative transfer. Climate impacts were expressed as global mean surface temperature change, which is a function of time, and as GWP using a 100 year time horizon.

The system analysed was production of heat and power from SRC willow cultivated on former long-term fallow land for 50 years. The study site was located in Västra Götaland County in south-western Sweden (58.2667, 12.7667). About 8% (36,000 ha) of the county's arable land area was under fallow between 2015 and 2019 (Swedish Board of Agriculture, 2019), whereof more than half was fallow for 3 years or

longer (Statistics Sweden, 2017). Hence, there is potential to cultivate perennial energy crops with a low risk of displacing food or feed production. Willow is a perennial energy crop that can provide rapid growth and high yields at low levels of agronomic inputs and management. Studies have shown good potential of SRC willow bioenergy systems to generate low (Heller, Keoleian, & Volk, 2003) or negative emissions (Ericsson et al., 2013; Hammar, Hansson, & Sundberg, 2017; Hillier et al., 2009).

2 | MATERIALS AND METHODS

2.1 | Goal and scope of the LCA

Life cycle assessment was used to analyse cultivation of SRC willow on former fallow in south-western Sweden for 50 years, supplying wood chips to a local energy plant for combined heat and power (CHP) production. The goal was to determine the climate impact of SRC willow bioenergy, including the three major GHGs (carbon dioxide [CO_2], methane [CH_4], and nitrous oxide [N_2O]) and albedo. Results are presented per hectare of land and per MJ fuel energy content, based on the lower heating value (LHV).

The willow scenario included production of inputs, field operations, transport and combustion of wood chips (Figure 1). Transformation and distribution losses of heat and electricity were not included. Direct effects of land use were accounted for, comprising the initial transformation of fallow land and the change in occupation during 50 years of

willow production. The production period consisted of two consecutive 25-year rotations of SRC willow. Each rotation started with soil preparation in autumn and establishment of a new plantation in the following spring. The rotation then consisted of eight 3-year cutting cycles, followed by one fallow year between termination of the old plantation and establishment of a new plantation. The crop was assumed to be harvested in spring every third year, yielding 20 Mg DM/ha in the first cutting cycle of each rotation and 30 Mg DM/ha in cutting cycles 2–8 (Hollsten, Arkelöv, & Ingelman, 2013).

The reference scenario included natural gas as a fuel combusted in the CHP plant. The land remained fallow for the duration of the study period, resulting in no transformation or change in occupation. Fallow was defined as set-aside land vegetated by grass with annual productivity of 3 Mg DM/ha. The management of green fallow was identical in the reference scenario and before the study period (i.e. when fallow was the former land use).

Time-dependent LCA methodology (Ericsson et al., 2013) was used to quantify the climate impact due to annual GHG emissions and albedo changes. Emissions of CO_2, CH_4 and N_2O were recorded for each year of the study period, in a time-distributed life cycle inventory. Upstream emissions from production of inputs were assigned to the year in which the inputs were used. CO_2 from the decay of methane was recorded as an emission in the year following the decay. Changes in annual carbon stocks were recorded as positive or negative CO_2 emissions. Surface albedo change was converted to the corresponding change in shortwave fluxes at the top of the atmosphere (TOA) and recorded in the inventory
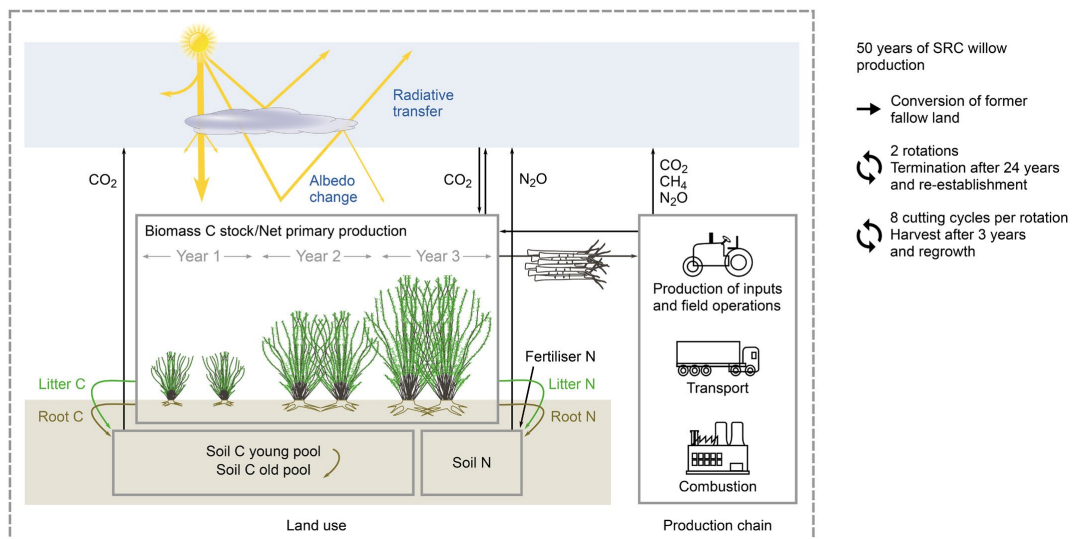

FIGURE 1 System components and life cycle inventory flows in the willow scenario. SRC, short-rotation coppice

as annual mean RF. Climate impacts were assessed as global mean surface temperature change over time up to year 100, and as CO_2-equivalents using GWP_{100}.

2.2 | Production chain

In the willow scenario, the production chain (production of inputs, field operations, transport and combustion) was based on Hammar, Ericsson, Sundberg, and Hansson (2014), using data from previous studies of SRC willow in Sweden. Data and references for activities, inputs and emissions are provided in Tables S1–S3. Management operations in the establishment phase included soil preparation by ploughing and harrowing, chemical and mechanical weed control, and planting of willow seedlings. Fertilizer was applied repeatedly during the rotation, following recommendations for the expected yield and net primary production (NPP; Aronsson, Rosenqvist, & Dimitriou, 2014; Börjesson, 2006). Harvesting using direct chipping, field transport and road transport took place in the third year of each cutting cycle. After the last harvest in each rotation, the plantation was terminated by mechanical destruction of plant residues and rootstocks.

The wood chips were transported 40 km to the CHP plant. Storage losses were considered assuming 3% dry matter loss during an average storage period of 60 days (Elinder, Almquist, & Jirjis, 1995). An LHV of 15.8 MJ/kg DM was used for the willow fuel (Hammar et al., 2017). Combustion emissions of N_2O and CH_4 were calculated based on the LHV (Table S2). Remaining fuel carbon that was not emitted as CH_4 was converted to CO_2 and considered under biogenic carbon fluxes.

In the reference scenario, the usage of natural gas was equivalent to the amount of willow fuel supplied per year in terms of the LHV. Emissions from production, distribution and combustion were calculated based on the LHV (Table S2). Green fallow was cut every autumn to avoid the growth of shrubs. Biomass was left in the field to decompose, providing input to the soil carbon pool. Activity data and emissions are presented in Table S4.

2.3 | Biogenic carbon fluxes

Carbon stocks in living biomass and soil were determined for each year and used to calculate annual net carbon fluxes to the atmosphere. Carbon in biomass was modelled based on annual NPP in different plant compartments (Tables S5 and S6). Willow stem NPP was calculated according to expected yield per cutting cycle and growth rates of 25%, 40% and 35%, respectively, in years 1, 2 and 3 of each cutting cycle (Ericsson et al., 2013). Quantities of willow leaves, fine roots and coarse roots were derived from NPP allocation in willow relative to stem growth (Rytter, 2001). Fallow NPP was based on annual productivity. Quantities of fallow fine roots and coarse roots were calculated based on carbon allocation in grassland (Bolinder, Janzen, Gregorich, Angers, & VandenBygaart, 2007).

A carbon content of 50% DM was assumed for willow stems and coarse roots (including stumps) and 45% DM for willow leaves and fine roots and for fallow grass leaves, fine roots and coarse roots (Table S7). Willow stems accumulated carbon until harvest and combustion after 3 years. Coarse roots accumulated under continued production until the willow plantation was terminated or the fallow was discontinued. Fine roots (including root exudates), willow litter and fallow grass leaves were recorded as annual turnover. The carbon in different crop residue fractions, that is, willow litter and roots, and fallow grass leaves and roots, was recorded as input to the soil pool in the year following the biomass stock change.

Carbon in soil was modelled using ICBMr, a version of the Introductory Carbon Balance Model (Andrén & Kätterer, 1997) adapted for use of annual inputs per production region, soil type and crop type (Andrén, Kätterer, & Karlsson, 2004). The model consists of two carbon pools, young (Y) for fresh organic matter and old (O) for stabilized material. Annual carbon inputs (i) enter Y and are transferred to O according to the humification coefficient (h), defining the substrate fraction stabilized. This fraction is about 2.3-fold higher for root-derived carbon than for litter and other above-ground crop residues (Kätterer, Bolinder, Andrén, Kirchmann, & Menichetti, 2011). Therefore, above-ground and below-ground carbon were modelled separately as inputs i_a and i_b, with humification coefficient h_a and h_b respectively (Ericsson et al., 2013; Table S8). Carbon in the young and old pools was calculated using Equations (1) and (2), respectively, and annual time steps:

$$Y_{[a,b]}[t] = \left(Y_{[a,b]_{t-1}} + i_{[a,b]_{t-1}} \right) \exp^{-k_Y r_e}, \quad (1)$$

$$O[t] = \left(O_{t-1} - \left(\frac{h_a k_Y}{k_O - k_Y} \left(Y_{a_{t-1}} + i_{a_{t-1}} \right) + \frac{h_b k_Y}{k_O - k_Y} \left(Y_{b_{t-1}} + i_{b_{t-1}} \right) \right) \right) \exp^{-k_O r_e}$$
$$+ \left(\frac{h_a k_Y}{k_O - k_Y} \left(Y_{a_{t-1}} + i_{a_{t-1}} \right) + \frac{h_b k_Y}{k_O - k_Y} \left(Y_{b_{t-1}} + i_{b_{t-1}} \right) \right) \exp^{-k_Y r_e}, \quad (2)$$

where k_Y and k_O are decomposition constants per pool and r_e is an external decomposition control affecting carbon losses from both pools. The external factor accounts for the effect of soil temperature, soil water content and degree of cultivation on decomposer activity (Andrén et al., 2004). A value of 0.95 and 1.03 was calculated for willow and green fallow, respectively, accounting for climate and soil types in Västra Götaland, crop type, and management intensity and frequency.

Soil carbon stocks were assumed to be in equilibrium under the long-term fallow preceding the willow. This means that annual inputs and losses were equal, resulting in constant stocks. Equilibrium values for Y_a, Y_b and O were computed through a 1,000 year spin-up simulation and used as starting values in year 0 when running ICBMr for willow and fallow respectively (see Table S8). Total soil carbon per year was calculated as the sum of the pools, that is, $C_{soil}[t] = Y_a[t] + Y_b[t] + O[t]$.

2.4 | Nitrous oxide emissions from soil

Microbial activity leads to formation of N_2O from nitrogen added with synthetic fertilizer or present in above-ground and below-ground crop residues (Table S9). Three emissions pathways were considered for synthetic and biogenic nitrogen inputs to soil: (1) direct N_2O emissions; (2) indirect N_2O emissions following volatilization and subsequent redeposition; and (3) indirect N_2O emissions following leaching and runoff.

Emissions were calculated following the IPCC Guidelines for National Greenhouse Gas Inventories, using disaggregated values from the 2019 refinement (IPCC, 2019). Volatilization of nitrogen in above-ground crop residues is not included in the IPCC default values. Therefore, a volatilization factor (f) was calculated based on nitrogen content (N_{bio}, g/kg DM) in litter and grass leaves respectively (de Ruijter & Huijsmans, 2012; Equation 3). Emissions factors are summarized in Table S10.

$$f = 0.4 \times N_{bio} - 5.08. \quad (3)$$

2.5 | Surface albedo and radiative transfer

Downwelling and reflected shortwave irradiance were measured with pyranometer pairs (Hukseflux NR-1, 285–3,000 nm) at two sites in south-western Sweden. Measurements from April 2013 to March 2016 covered a full 3-year cutting cycle of SRC willow (*Salix viminalis* L.). A nearby mire vegetated by grasses and sedges was used as a proxy for long-term fallow. Irradiance was sampled at 30 min intervals and processed according to Sieber, Ericsson, and Hansson (2019) to obtain corrected and gap-filled time series.

Albedo change increases or decreases the solar flux leaving the Earth's surface. The radiation is absorbed and scattered by clouds, aerosols and gases on its way to the top of the atmosphere (TOA), where a change in the upwelling shortwave flux eventually causes RF. Upwelling irradiance at the TOA in W/m^2 is given by (Winton, 2005):

$$R_{TOA\uparrow} = R_{TOA\downarrow} \frac{\tau_\downarrow \tau_\uparrow}{1 - \alpha r_\uparrow} \alpha, \quad (4)$$

where τ is transmittance during a single downward or upward pass through the atmosphere. The denominator represents an infinite number of reflections between the surface with albedo α and the atmosphere with reflectivity r. RF from albedo change (RF$_\alpha$, W/m^2) can then be expressed using the partial derivative of Equation (4) in relation to α (Equation 5; Bright & O'Halloran, 2019). The effect of multiple reflection, which increases solar irradiance at surfaces with higher albedo and reinforces RF$_\alpha$, is thereby included:

$$RF_\alpha = -\frac{\partial R_{TOA\uparrow}}{\partial \alpha} \Delta \alpha = -R_{TOA\downarrow} \frac{\tau_\downarrow \tau_\uparrow}{(1 - \alpha r_\uparrow)^2} \Delta \alpha. \quad (5)$$

A single atmospheric layer with isotropic properties was assumed to simplify radiative transfer (Stephens et al., 2015). By taking τ and r as directionally independent, atmospheric transmittance and reflectivity can be calculated from four shortwave fluxes according to Equations (6) and (7) (Winton, 2005):

$$\tau = \frac{R_{TOA\downarrow} R_{S\downarrow} - R_{TOA\uparrow} R_{S\uparrow}}{R_{TOA\downarrow}^2 - R_{S\uparrow}^2}, \quad (6)$$

$$r = \frac{R_{TOA\downarrow} R_{TOA\uparrow} - R_{S\downarrow} R_{S\uparrow}}{R_{TOA\downarrow}^2 - R_{S\uparrow}^2}, \quad (7)$$

where $R_{TOA\uparrow}$ and $R_{TOA\downarrow}$ are upwelling and downwelling irradiance at the TOA and $R_{S\uparrow}$ and $R_{S\downarrow}$ are upwelling and downwelling irradiance at the surface. Here we used variables from the ERA5 global reanalysis dataset at a resolution of 31 km and 1 hr (Copernicus Climate Change Service [C3S], 2017). The data were averaged across 15 years (2004–2018) to generate standard atmospheric conditions, which were used in all years of the study period.

Using Equations (6)–(8), annual mean albedo RF can be calculated for each year of the study period and recorded as inventory vector $I_\alpha[t]$:

$$I_\alpha[t] = \frac{A}{A_E} \frac{1}{N} \sum_{s=1}^{N} -R_{TOA\downarrow t,s} \frac{\tau_{t,s}^2}{(1 - \alpha_{t,s} r_{t,s})^2} \Delta \alpha_{t,s}, \quad (8)$$

where A is the affected area in relation to the Earth's total surface area ($A_E = 5.1 \times 10^{14}$ m^2) and N is the number of sub-annual time steps s. The time step has to be chosen sufficiently small to account for the seasonal covariation of albedo change with irradiance (Bright, Zhao, Jackson, & Cherubini, 2015) and radiative transfer (Sieber et al., 2019). Here surface and atmospheric properties (α, τ, r) were calculated from 5-day-average irradiances to smoothen variability in the temporally decoupled data sets (i.e. measured albedo from 2013 to 2016 and climatological shortwave fluxes from 2004 to 2018). This is in contrast
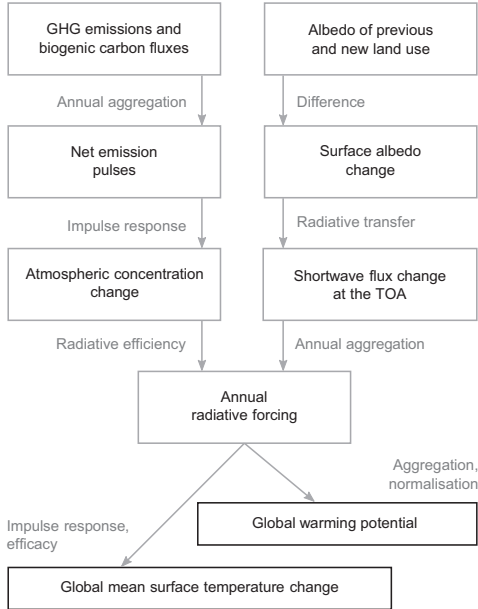
FIGURE 2 Modelling steps from input data for greenhouse gases (GHGs) and albedo to climate impact using time-dependent life cycle assessment methodology. TOA, top of the atmosphere
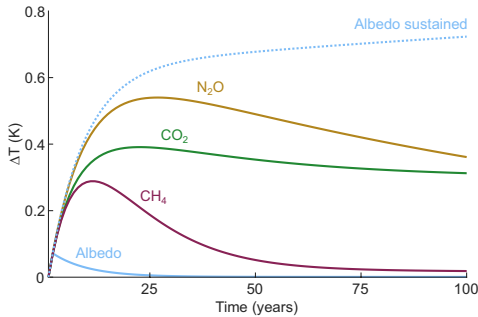

FIGURE 3 Annual temperature response to radiative forcing of 1 W/m² in year 0, resulting from emission pulses of 570 Pg CO_2, 2.8 Pg N_2O or 4.7 Pg fossil CH_4 in year 0; from temporary albedo change in year 0; or from sustained albedo change in years 0–100. Metric values taken from Myhre et al. (2013)

to Sieber et al. (2019), who matched hourly albedo change, irradiance and radiative transfer during the same 3 years.

2.6 | Climate impact assessment

The time-dependent characterization model was taken from the methodology for GHGs in Ericsson et al. (2013) and

expanded for albedo (Figure 2). Annual GHG emissions and albedo RF were converted to global mean surface temperature change (ΔT). Impacts were expressed as a function of time from the start of the study period up to year 100. Including the timing of impacts can better reflect the relative contribution of climate forcers with different perturbation lifetimes (Aamaas, Peters, & Fuglestvedt, 2013; Boucher & Reddy, 2008). Perturbation lifetimes of climate forcers included in this study range from instantaneous for albedo change up to centuries for CO_2. Implications for the temperature response are illustrated in Figure 3.

The time-dependent characterization model can be written as a convolution sum (here square brackets denote discrete vectors, whereas round brackets denote continuous functions):

$$\Delta T_x[H] = \sum_{t=0}^{H} I_x[t] \mathrm{AGTP}_x[H - t], \quad (9)$$

where $I_x[t]$ in kg is a vector with annual inventory results for forcing agent x, and $\mathrm{AGTP}_x[t]$ is the absolute global temperature potential of x at the same time step. $\mathrm{AGTP}_x(t)$ in K/kg is defined as the change in global mean surface temperature over time, following a pulse release of x in year 0. By performing the convolution in Equation (9), $\Delta T_x[H]$ gives the response to emissions and forcings in different years up to evaluation time H.

The AGTP of GHGs is determined as the convolution integral of two impulse response functions (IRF; Boucher & Reddy, 2008; Fuglestvedt et al., 2010):

$$\mathrm{AGTP}_x(H) = e_x \int_{t=0}^{H} \mathrm{IRF}_x(t) \mathrm{IRF}_T(H - t) \mathrm{d}t, \quad (10)$$

where e_x is radiative efficiency of GHGs, that is, the additional RF per unit mass increase of gas x in the atmosphere, $\mathrm{IRF}_x(t)$ is the fraction of a gas remaining in the atmosphere after a pulse emission and $\mathrm{IRF}_T(t)$ is the temperature response of the climate system to a unit RF. Here we used $\mathrm{IRF}_x(t)$ for CO_2 based on the Bern Carbon Cycle Model (Joos et al., 2013), $\mathrm{IRF}_x(t)$ for CH_4 and N_2O based on simple exponential decay (Prather, 2007) and $\mathrm{IRF}_T(t)$ based on simulations with the HadCM3 climate model (Boucher & Reddy, 2008). The functions and metric values used are those summarized in the Supporting Information to the IPCC Fifth Assessment Report (Myhre et al., 2013).

Solving the convolution integral in Equation (10) and using the analytical solution of AGTP to calculate ΔT allows handling the characterization in LCA in discrete time steps according to Equation (9), without generating errors from numerical approximation (as it would happen if the convolution integral in Equation 10 was approximated by a convolution sum using discrete time steps). The analytical solution of AGTP is provided for CO_2, CH_4 and N_2O in Myhre et al. (2013).

Here we used the same approach for albedo and formulated $\text{AGTP}_\alpha(H)$ as the convolution integral of two IRFs, analogously to Equation (10). $\text{IRF}_\alpha(t)$ was written as a boxcar function that is 1 for $0 \leq t < 1$. $\text{IRF}_T(t)$ is commonly used independently of the emitted species (Aamaas, Berntsen, Fuglestvedt, Shine, & Bellouin, 2016) and was therefore assumed identical with GHGs (Boucher & Reddy, 2008):

$$\text{IRF}_T(t) = \sum_{j=1}^{2} \frac{c_j}{d_j} \exp\left(\frac{-t}{d_j}\right), \quad (11)$$

where c_j are components of climate sensitivity and d_j a short and a long response timescale. The solution of AGTP for albedo RF was found by analytical integration and is given by (in $\text{K (W m}^{-2})^{-1}$):

$$\text{AGTP}_\alpha(H) = \sum_{j=1}^{2} c_j \left(\left(1 - \exp^{\frac{-H}{d_j}}\right) - \left(1 - \exp^{\frac{-(H-a)}{d_j}}\right) u(H-a) \right), \quad (12)$$

where the first exponential term is the response to a constant sustained forcing and the second one removes the response in $H \geq a$. The Heaviside step function $u(t)$ was defined to return 1 for $t \geq 0$ and 0 otherwise. Consequently, removal starts at a, which can be interpreted as the perturbation lifetime in years. For RF_α it corresponds to the aggregation interval chosen in the inventory, here $a = 1$. The same method can be used at any temporal resolution, for example, with a monthly inventory and $a = 1/12$. Combining Equations (9) and (12), the inventory vector of annual mean RF from albedo change, $I_\alpha[t]$, can be converted to $\Delta T_\alpha[H]$.

The metric values for c_j and d_j used in Equation (11) were derived from simulations with increased CO_2 concentration in a climate model with an equilibrium climate sensitivity of $\lambda_{CO_2} = \sum c_j = 1.06 \text{ K (W m}^{-2})^{-1}$ (Boucher & Reddy, 2008). Using the same parameters to model the response to albedo RF (Equation 12) assumes the same climate sensitivity and response timescales, despite differences in the vertical (surface vs. troposphere) and horizontal (global vs. local) distribution of the physical perturbation (Bright et al., 2015). Methods have been developed to account for differences in climate sensitivity by forcing agent (Hansen et al., 2005), which could be used to linearly scale $\text{AGTP}_\alpha(H)$. Here we assumed $\lambda_\alpha/\lambda_{CO_2} = 1$. Potentially lower or higher efficacy is addressed in Section 4.

Climate impacts were also assessed using GWP with a 100 year time horizon (GWP_{100}), a common climate metric in LCA. Characterization factors for GHGs including climate carbon cycle feedbacks were taken from Myhre et al. (2013). The corresponding characterization factor for annual mean albedo RF is $1/\text{AGWP}_{CO_2}(100) = 10.9 \times 10^{12} \text{ kg } CO_2\text{e (W m}^{-2})^{-1}$, using $\text{AGWP}_{CO_2}(100) = 91.7 \times 10^{-15} \text{ W m}^{-2} \text{ year kg}^{-1}$ from Myhre et al. (2013). Consequently, the GWP_{100} of albedo RF can be calculated as:

$$\text{GWP}_\alpha^{100} = \frac{\sum_{t=0}^{100} I_\alpha[t]}{\text{AGWP}_{CO_2}^{100}}. \quad (13)$$

2.7 | Sensitivity analysis

A sensitivity analysis was performed to address uncertainty and variability associated with parameters, choices and the characterization model. The yields of SRC willow and fallow were reduced while keeping the original rates of fertilizer application. Soil carbon stocks were assumed to be lower than the equilibrium values in year 0. Potential feedback effects between yield and soil carbon were not considered. Fallow albedo was approximated using measured data for 2014 from an alternative site, a fresh clear-cut vegetated by grass in southern Sweden. Albedo RF calculated using Equation (8) was compared with that calculated using an alternative method (Ghimire et al., 2014; Sieber et al., 2019) based on monthly radiative kernels from global climate models (Table S13a).

3 | RESULTS

3.1 | Inventory analysis

The SRC willow plantation captured up to 18.7 Mg C/ha in biomass carbon stocks, with an average of 11.6 Mg C/ha during the study period (Figure 4a). Soil carbon stocks increased by 41.4 Mg C compared with the former fallow, which is equivalent to an average sequestration rate of 0.83 Mg C ha^{-1} year^{-1} over 50 years. Nitrogen inputs varied with NPP and fertilization in each cutting cycle (Figure 4b). In the reference scenario, soil carbon stocks remained nearly stable at the equilibrium value of 57.9 Mg C/ha. Biomass carbon stocks did not change compared with the former land use (3.1 Mg C/ha). Nitrogen inputs were from biomass only and remained constant over the study period. Activity data and annual GHG emissions from the production chain can be found in Tables S2–S4.

In the willow scenario, annual albedo was elevated in every year of the cutting cycle (0.222, 0.215 and 0.212, compared with 0.165, 0.161 and 0.168 under fallow). On sub-annual timescales, 5 day albedo was mostly higher for willow than for fallow (Figure 5). Summer albedo increased by 0.05–0.1 under willow and led to peaks in negative RF between May and July. Winter albedo decreased by 0.3–0.6, because willow was less well covered by snow than fallow. However, the resulting positive RF was low as snowfall occurred only between November and March, when solar irradiance and atmospheric transmittance were low. Albedo RF in the willow scenario was -5.3×10^{-11} W/m^2 on average during the study period, including one fallow year per rotation with no albedo
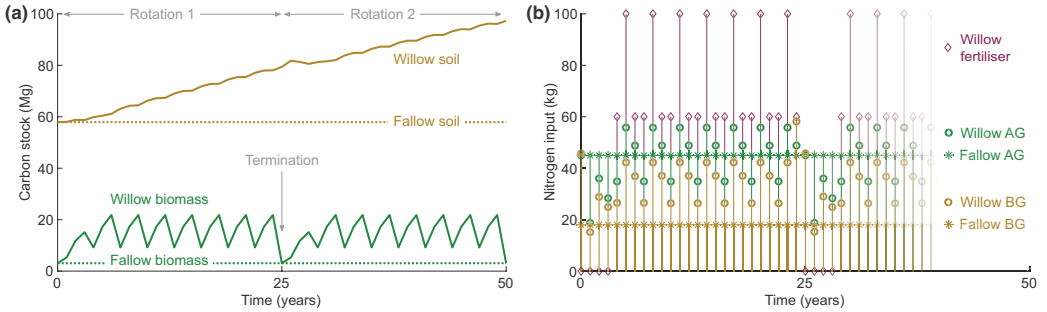
FIGURE 4 (a) Carbon stocks in biomass and soil and (b) annual nitrogen inputs from crop residues and mineral fertiliser, shown per hectare land use in the willow scenario (willow) and in the reference scenario (fallow) during the study period (50 years). Biomass includes all plant compartments; crop residues aboveground (AG) include willow leaves and fallow grass leaves; crop residues belowground (BG) include fine roots and coarse roots
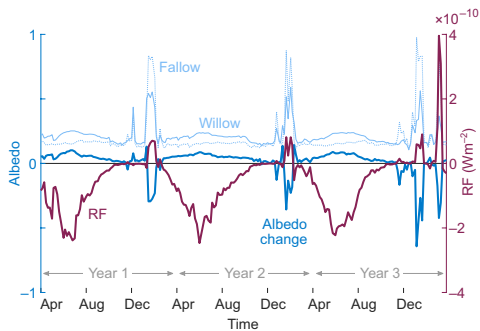

FIGURE 5 Willow albedo, fallow albedo and albedo change under willow relative to fallow (left axis) and radiative forcing (RF) from albedo change on 1 ha (right axis) during a 3-year cutting cycle of willow, using 5-day resolution

change (Table S11). Albedo did not change outside the study period or in the reference scenario.

Net inventory results for the entire study period are summarized in Table 1 and will be used to calculate GWP. Wood fuel produced during two rotations of SRC willow had a total energy content of 7,072 GJ/ha, corresponding to an annual average yield of 141 GJ/ha during the study period.

3.2 | Climate impact

The willow scenario had a net cooling effect on global mean surface temperature. The maximum effect, -10.1×10^{-11} K/ha, was reached at the end of the study period (year 50; Figure 6a). The main cooling resulted from increased soil carbon stocks under willow. Soil carbon sequestration alone

was sufficient to offset positive emissions from the production chain (i.e. production of inputs, field operations, transport and combustion) and synthetic and biogenic N_2O from soil. Albedo change led to additional cooling, which was of similar magnitude to the warming effect of production emissions during the study period. The relative importance of albedo RF decreased over time as soil carbon accumulated under sustained production. After the study period, the temperature effect of albedo change was shorter than that of the GHGs, which remained in the atmosphere for decades to centuries (see Figure 3). Another consequence of CO_2 lifetime and gradual decay was that the sudden release of biomass carbon that had been sequestered throughout the production period led to 'overshoot warming' from year 60 onward.

The reference scenario had a warming effect over time, reaching a maximum of 38.4×10^{-11} K/ha in year 56 (Figure 6b). The main contributor was CO_2 from the use of natural gas as an alternative fuel. The reference land use led to a positive temperature response, mainly due to N_2O emissions from the application of biomass to soil.

Using GWP_{100} per MJ fuel energy content, the willow scenario had a climate impact of -12.2 g CO_2e (Table 2). Albedo was responsible for 34% of GWP_{100}, but only 6% of $\Delta T[100]$. The reference scenario had GWP_{100} of 81.9 g CO_2e/MJ fuel, which is of opposite sign and nearly sevenfold higher than that of the willow scenario. Natural gas was the single largest source of GHG emissions.

The differences between results with GWP_{100} and $\Delta T[100]$ stemmed from how the two climate metrics treat the timing of forcings (i.e. GHG emissions and albedo RF) and of impacts. The GWP metric applies the same time horizon to all forcings within the study period, whereas $\Delta T[H]$ applies the same evaluation time to all forcings, but a moving time horizon $H - t$ that becomes shorter the closer a forcing

TABLE 1 Inventory results for the willow and reference scenarios aggregated over the study period, presented per system component and climate forcer. Production chain includes production of inputs, field operations, transport and combustion; biomass includes willow stems, leaves and roots and fallow grass leaves and roots; nitrous oxide emissions from soil (soil N_2O) include direct and indirect emissions due to addition of synthetic and biogenic nitrogen; albedo change refers to the difference between land use in the respective scenario and the former land use (i.e. fallow)

	CO_2 (kg/ha)	CH_4 (kg/ha)	N_2O (kg/ha)	Albedo RF $(10^{-9}$ W m^{-2} ha$^{-1})$
Willow scenario	−128,000	96.4	227	−2.65
Production chain	23,400	96.4	78.0	
Biomass carbon	0			
Soil carbon	−152,000			
Soil N_2O			149	
Albedo change				−2.65
Reference scenario	488,000	2,160	44.9	0
Production chain	875	0.380	0.000624	
Biomass carbon	0			
Soil carbon	0			
Soil N_2O			44.1	
Albedo change				0
Natural gas	487,000	2,160	0.782	

Abbreviation: RF, radiative forcing.

FIGURE 6 Climate impact of (a) the willow scenario and (b) the reference scenario expressed as global mean surface temperature change per hectare. Willow total includes albedo change and greenhouse gas (GHG) emissions from the production chain (production of inputs, field operations, transport and combustion), from carbon stock change in biomass (biomass C) and soil (soil C) and from addition of synthetic and biogenic nitrogen to soil (soil N_2O). Reference total includes GHG emissions from land use (production of inputs, field operations and soil N_2O) and from natural gas (production, distribution and combustion)

TABLE 2 Climate impact in the willow and reference scenarios using alternative functional units, metrics and evaluation times. The relative importance of albedo change in the willow scenario is highlighted. Land use emissions in the reference scenario (production chain and soil N_2O) are summarized. Results can be converted between functional units based on total energy production (7,072 GJ/ha)

	GWP$_{100}$ (g CO$_2$e/MJ)	$\Delta T[100]$ $(10^{-11}$ K/ha)	$\Delta T[50]$ $(10^{-11}$ K/ha)
Willow system	−12.2	−3.8	−10.1
Production chain	7.1	2.6	3.0
Biomass carbon	0	0.3	−3.2
Soil carbon	−21.5	−8.7	−8.7
Soil N_2O	6.3	2.2	2.4
Albedo change	−4.1 (34%)	−0.2 (6%)	−3.7 (36%)
Reference system	81.9	30.0	37.3
Land use	2.0	0.7	0.8
Natural gas	79.9	29.3	36.5
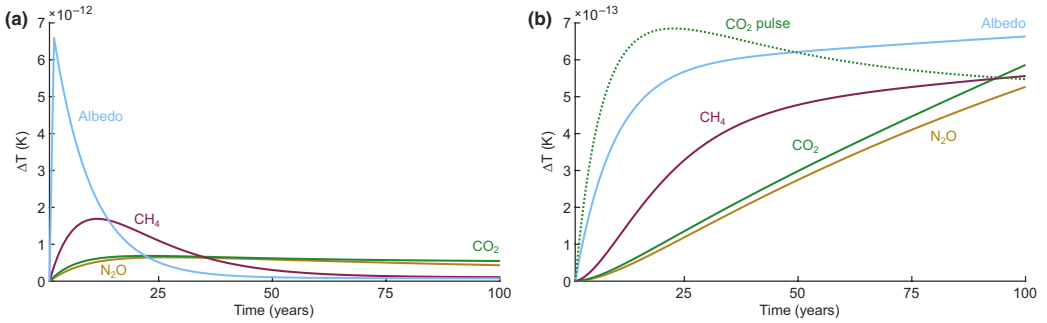
FIGURE 7 Annual temperature response to GWP_{100} of 1 Mg CO_2e resulting from (a) emission pulses of 1 Mg CO_2, 27.8 kg N_2O or 3.4 kg fossil CH_4, or from annual mean albedo RF of 9.2×10^{-11} W/m^2 during 1 year; and (b) from sustained emissions or albedo RF at constant rate over 100 years; the response to the CO_2 pulse is reproduced from (a) for comparison. GWP, global warming potential; RF, radiative forcing. Metric values taken from Myhre et al. (2013)

appears to the evaluation time. In other words, GWP gives the same weight to inventory elements regardless of their timing, whereas $\Delta T[H]$ gives forcings different weights depending on when they appear with respect to H. The weighting over time is specific for each forcing agent and given by its AGTP (see Equations 9–11). Consequently, the same result in terms of GWP_{100} (e.g. 1 kg CO_2e) can imply substantially different temperature responses over time depending on (a) the perturbation lifetime and decay timescales of the climate forcers involved (Figure 7); and (b) the distribution of emissions and albedo RF throughout the study period. For reason (a), albedo RF in years 1–49 was relatively more important for the climate impact using GWP_{100} than using $\Delta T[100]$. For reason (b), temporary carbon storage in biomass was 'climate neutral' with GWP_{100}, but gave a cooling or warming temperature response at different points in time (see Table 2).

3.3 | Sensitivity analysis

A 20% reduction in yields mainly affected the result of the willow scenario due to lower soil carbon sequestration (0.59 Mg C ha^{-1} $year^{-1}$ on average during the study period, i.e. −30% compared with the baseline). Yield-induced changes in biomass carbon stocks, production chain (e.g. harvesting, transport and combustion) and N_2O emissions from soil had smaller effects on the results. In total, the cooling effect of the willow system was reduced by 55% using $\Delta T[100]$ per hectare and by 29% using GWP_{100} per MJ fuel. The reference scenario was primarily affected due to reduced demand for natural gas, resulting in 17% lower climate impact with $\Delta T[100]$ per hectare (Table S12, including figures).

A 20% reduction in initial soil carbon stocks led to a higher net gain in the willow scenario (0.91 Mg C ha^{-1} $year^{-1}$ on
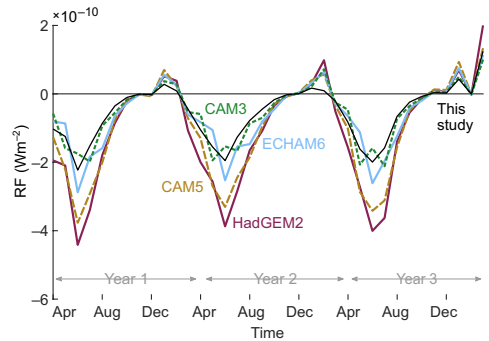

FIGURE 8 Monthly radiative forcing (RF) from albedo change during a 3-year cutting cycle of willow, calculated using monthly radiative kernels from global climate models; albedo RF using the method in this study with 5-day resolution is shown for comparison

average during the study period, i.e. +10% compared with the baseline). The cooling effect of the willow scenario increased by 22% using $\Delta T[100]$ per hectare and by 17% using GWP_{100} per MJ fuel (Table S12). The net gain was a result of smaller losses from the initial soil carbon stock, while the inputs from plant residues remained the same as in the baseline. Consequently, the absolute difference to the baseline was almost identical in both scenarios. A slightly higher loss of initial soil carbon under fallow was due to higher decomposer activity (see Equations 1 and 2).

Using an alternative site as a proxy for the albedo of fallow (0.184), smaller albedo change in the willow scenario resulted in 36% lower RF on average over each cutting cycle (Table S11). The GWP_{100} and the temperature response scaled linearly to RF.

Using monthly radiative kernels from CAM3, ECHAM6, CAM6 and HadGEM2 to calculate RF from albedo change

in the willow scenario resulted in 2%, 15%, 78% and 100% higher albedo RF on average over the cutting cycle, respectively, compared with the method used in this study with 5 day resolution (Table S13b). The kernels from global climate models were higher in most months than the equivalent calculated with our data (Table S13a). Consequently, albedo RF was more strongly negative in summer and more strongly positive in winter in every year of the cutting cycle (Figure 8).

4 | DISCUSSION

4.1 | Climate impact of willow bioenergy

A net cooling effect of SRC willow bioenergy was found in terms of global mean surface temperature change per hectare (-10.1×10^{-11} K in year 50, -3.8×10^{-11} K in year 100) and GWP_{100} per MJ fuel energy content (-12.2 g CO_2e), even when replacement of fossil fuels was not considered. The main cooling in the willow scenario was a result of soil carbon sequestration, thanks to high inputs of carbon from root and leaf biomass. Soil carbon stock change was sensitive to yield levels and may be lower or potentially negative on land with high initial carbon stocks (Hillier et al., 2009). Net carbon sequestration relative to the reference land use was positive and not affected by the initial carbon stock. Our findings are consistent with yields, carbon sequestration, soil N_2O and life cycle GHG emissions reported elsewhere for SRC cultivated on former cropland (as opposed to native vegetation or perennial grasslands; Creutzig et al., 2015; Don et al., 2012; Whitaker et al., 2018). The SRC willow system has been shown to be carbon-negative despite uncertainties associated with management and biological parameters such as yield, litterfall and soil carbon sequestration (Caputo et al., 2014).

Natural gas in the reference scenario was the single largest source of emissions and thus substitution of this fossil fuel gave the greatest potential for climate change mitigation in the case study. Substituting bioenergy for natural gas over the production period could avoid a maximum warming of 38.4×10^{-11} K/ha in year 56, or emissions of 79.9 g CO_2e/MJ fuel, adding to the climate change mitigation potential of the willow scenario alone.

Albedo increased under willow relative to the former fallow and hence contributed to the cooling effect. Albedo RF accounted for 34% of GWP_{100}, 36% of $\Delta T[50]$ and 6% of $\Delta T[100]$ in the willow scenario. The albedo effect dominated on short timescales of 10–20 years and offset the warming from production chain emissions during the study period. Its relative importance decreased over time, owing to accumulation of soil carbon under sustained production (a property of the chosen scenario) and the longer perturbation lifetime of GHGs (a property of the climate system). This relationship

would be the reverse in a scenario of permanent land use change where soil carbon stocks have reached a new equilibrium. Sustained albedo change leads to constant RF and a stabilizing temperature response, whereas the effect of elevated yet stable soil carbon stocks decays according to the removal rate of CO_2 from the atmosphere. This difference can be observed in the willow scenario by comparing the effect of albedo change and elevated yet stable biomass carbon stocks under sustained production (see Figure 6a).

4.2 | Importance of albedo and uncertainties

The results demonstrated the potential importance of albedo change for the life cycle climate impact of bioenergy from SRC willow. The relative importance of albedo change as a climate forcer varies over time and depends on case-specific factors such as local climate, insolation, soil type, management, yield, reference land use and study period duration. Understanding the potential magnitude of the albedo effect can help decide whether to include albedo in future assessments of bioenergy. Once fossil fuel emissions have been cut, the next challenge is to mitigate impacts of bioenergy feedstock production and to foster potential climate benefits by carbon sequestration and higher albedo. Willow as a perennial energy crop is known for low emissions from feedstock production and high carbon sequestration potential (Don et al., 2012). Annual energy crops are more resource-intensive and usually reduce soil carbon stocks (Hillier et al., 2009), so albedo change could act as an important cooling factor in annual cropping systems, especially in regions with higher solar irradiance than in Sweden (Cai et al., 2016; Caiazzo et al., 2014).

Albedo of the reference land use was an important variable in the assessment. Albedo is often considered per land cover type, although there can be substantial variation. Ranges of 0.16–0.26 have been reported for grassland and 0.15–0.20 for deciduous forest (Bonan, 2015). Assuming grass as a proxy for green fallow and deciduous trees as a proxy for SRC willow, a warming effect could be expected from albedo change in our scenario, and a cooling effect from any reduction in tree cover. Indeed, albedo RF of 0 to -0.71×10^{-11} W m^{-2} ha^{-1} has been found for generic (non-species specific) conversion of woody vegetation (forest and shrubland) to non-woody vegetation (crops and grassland) in different world regions (Jones, Calvin, Collins, & Edmonds, 2015), although that study also included non-radiative effects. Our data and other studies suggest that SRC willow is more reflective than most broadleaf species (Levy, Burakowski, & Richardson, 2018), and that the vegetation typically found on fallow land has lower albedo than productive and potentially fertilized grasslands (Hollinger et al., 2010). Moreover, we found smaller effects due to reduced snow cover than suggested by global modelling studies on shifting grassland to forest in the

northern mid-latitudes (Arora & Montenegro, 2011; Betts, 2000), confirming similar findings for a plantation of hybrid poplar (Cai, Price, Orchansky, & Thomas, 2011).

Albedo RF calculated with the isotropic single-layer radiative transfer model was lower than that obtained with monthly radiative kernels mimicking sophisticated radiative transfer schemes, indicating that our model underestimated upward transmittance of reflected radiation through the atmosphere. However, the spread of the four sets of kernels considered was larger than the difference between the lowest kernels and our values. The kernels are associated with other uncertainties, for example, the atmospheric state climatology of a climate model might not be representative of current conditions (Bright & O'Halloran, 2019) or interactions between albedo and clouds on submonthly timescales may be omitted (Soden et al., 2008).

Climate sensitivity to albedo RF relative to CO_2 forcing is a remaining source of uncertainty. The literature is inconclusive, suggesting that RF from land cover change may have a weaker or stronger effect on global mean surface temperature change than the same amount of CO_2 forcing. Values of 0.50, 0.78, 0.79 and 1.02 for $\lambda_\alpha / \lambda_{CO_2}$ have been estimated for global-scale land use change based on experiments with different climate models (Davin & de Noblet-Ducoudré, 2010; Davin, de Noblet-Ducoudré, & Friedlingstein, 2007; Hansen et al., 2005; Jones, Collins, & Torn, 2013). The variation stems from factors related to the model used (parameterization, processes and feedbacks included) and the experiment performed (vegetation types and surface variables modified jointly with albedo; Bright et al., 2015). Laguë, Bonan, and Swann (2019) disentangled temperature effects by surface variable (albedo, evaporative resistance and surface roughness) and mechanism (surface effects and atmospheric feedbacks). However, applying an efficacy factor on albedo RF may still not result in the same global temperature change as an equivalent amount of CO_2 forcing, a limitation of the RF concept in capturing land use change effects (Jones et al., 2013).

4.3 | Climate metrics for albedo

The timing of emissions and forcings was reflected in the results for the time-dependent metric ΔT, but not for GWP_{100} (Ericsson et al., 2013). GWP_{100} was easy to use once albedo change had been converted to RF using a (simplified) radiative transfer model, but it obscured that only 1% of the initial temperature effect of albedo change lasts for 100 years (see Equation 11). GWP_{100} is frequently used to express albedo RF in carbon or CO_2 equivalents to make it comparable to the impact of GHGs (Betts, 2000; Caiazzo et al., 2014; Cherubini et al., 2012; Muñoz, Campra, & Fernández-Alba, 2010; Schwaiger & Bird, 2010; Zhao & Jackson, 2014). We developed a theoretical GWP_{100} characterization factor for albedo

RF (10.9×10^{12} kg CO_2e (W m^{-2})$^{-1}$) and demonstrated that using it as a time-independent metric can bias LCA results.

When using GWP_{100}, the climate change mitigation potential of temporary carbon storage was overlooked and the importance of albedo relative to CO_2 was understated on short timescales and overstated on timescales longer than 22 years after emission or albedo change. This agrees with previous findings that GWP_{100} effectively measures the relative impact of long-lived and short-lived pollutants on temperatures 20–40 years after emission and thus overstates the role of cutting current emissions of short-lived pollutants if the goal is to limit peak warming (Allen et al., 2016). This was shown to be also true for albedo in our study, with GWP_{100} indicating the temperature impact of an equivalent CO_2 pulse 22 and 50 years after emission, under temporary and sustained albedo change respectively (see Figure 7). A similar observation has been made for afforestation, where the short- to medium-term nature of the albedo effect (here warming) might hamper the option to 'buy time' until transformations in the energy sector come into effect (Schaeffer et al., 2006). Including the timing of impacts in LCA results can significantly improve their relevance to climate targets, since albedo change and GHGs act on different timescales.

4.4 | Areas of application

The method presented in this study can be used to estimate the effect of albedo change on the global climate and relate it to that of GHG emissions in LCA. It includes first-order radiative effects of albedo change, but not the fate of the absorbed energy in latent heat, sensible heat and outgoing longwave radiation. Moreover, changes in evapotranspiration efficiency and aerodynamic roughness are not considered. These initially non-radiative processes can lead to atmospheric feedbacks that affect shortwave or longwave fluxes locally or remotely (Devaraju, de Noblet-Ducoudré, Quesada, & Bala, 2018; Laguë et al., 2019). In terms of their effect on surface temperature, non-radiative processes are reported to be comparable in magnitude and opposite in sign to radiative processes (Burakowski et al., 2018). However, capturing such processes requires complex climate models, which are less suited to answer the questions usually dealt with in LCA studies. In temperate regions where radiative processes dominate the land cover change effects, the RF concept can be acceptable to quantify impacts on the global climate (Davin & de Noblet-Ducoudré, 2010; Pielke et al., 2002).

There is still a need for methods to account for the climate impact of land use in a comprehensive manner (Bernier et al., 2011). Different methods have been used for local effects, but for global climate impacts comparable

to GHGs there are few alternatives to RF (Bright et al., 2015). In this study we demonstrated how to quantify the magnitude and uncertainties of the albedo effect in LCA in relation to that of GHGs emitted along the supply chain of bioenergy and compared the climate impact of bioenergy due to albedo and GHGs with that of alternative energy sources and land uses.

ORCID

Petra Sieber https://orcid.org/0000-0003-2626-9502
Niclas Ericsson https://orcid.org/0000-0002-3057-1563
Torun Hammar https://orcid.org/0000-0003-2961-5933

REFERENCES

Aamaas, B., Berntsen, T. K., Fuglestvedt, J. S., Shine, K. P., & Bellouin, N. (2016). Regional emission metrics for short-lived climate forcers from multiple models. *Atmospheric Chemistry and Physics*, *16*(11), 7451–7468. https://doi.org/10.5194/acp-16-7451-2016

Aamaas, B., Peters, G. P., & Fuglestvedt, J. S. (2013). Simple emission metrics for climate impacts. *Earth System Dynamics*, *4*(1), 145–170. https://doi.org/10.5194/esd-4-145-2013

Akbari, H., Menon, S., & Rosenfeld, A. (2009). Global cooling: Increasing world-wide urban albedos to offset CO_2. *Climatic Change*, *94*(3–4), 275–286. https://doi.org/10.1007/s10584-008-9515-9

Allen, M. R., Fuglestvedt, J. S., Shine, K. P., Reisinger, A., Pierrehumbert, R. T., & Forster, P. M. (2016). New use of global warming potentials to compare cumulative and short-lived climate pollutants. *Nature Climate Change*, *6*(8), 773–776. https://doi.org/10.1038/nclimate2998

Andrén, O., & Kätterer, T. (1997). ICBM: The introductory carbon balance model for exploration of soil carbon balances. *Ecological Applications*, *7*(4), 1226–1236. https://doi.org/10.1890/1051-0761(1997)007[1226:ITICBM]2.0.CO;2

Andrén, O., Kätterer, T., & Karlsson, T. (2004). ICBM regional model for estimations of dynamics of agricultural soil carbon pools. *Nutrient Cycling in Agroecosystems*, *70*(2), 231–239. https://doi.org/10.1023/B:FRES.0000048471.59164.ff

Aronsson, P., Rosenqvist, H., & Dimitriou, I. (2014). Impact of nitrogen fertilization to short-rotation willow coppice plantations grown in Sweden on yield and economy. *BioEnergy Research*, *7*(3), 993–1001. https://doi.org/10.1007/s12155-014-9435-7

Arora, V. K., & Montenegro, A. (2011). Small temperature benefits provided by realistic afforestation efforts. *Nature Geoscience*, *4*, 514–518. https://doi.org/10.1038/ngeo1182

Arvesen, A., Cherubini, F., del Alamo Serrano, G., Astrup, R., Becidan, M., Belbo, H., … Strømman, A. H. (2018). Cooling aerosols and changes in albedo counteract warming from CO_2 and black carbon from forest bioenergy in Norway. *Scientific Reports*, *8*(1), 3299. https://doi.org/10.1038/s41598-018-21559-8

Bernier, P. Y., Desjardins, R. L., Karimi-Zindashty, Y., Worth, D., Beaudoin, A., Luo, Y., & Wang, S. (2011). Boreal lichen woodlands: A possible negative feedback to climate change in eastern North America. *Agricultural and Forest Meteorology*, *151*(4), 521–528. https://doi.org/10.1016/j.agrformet.2010.12.013

Betts, R. A. (2000). Offset of the potential carbon sink from boreal forestation by decreases in surface albedo. *Nature*, *408*(6809), 187–190. https://doi.org/10.1038/35041545

Betts, R. A., Falloon, P. D., Goldewijk, K. K., & Ramankutty, N. (2007). Biogeophysical effects of land use on climate: Model simulations of radiative forcing and large-scale temperature change. *Agricultural and Forest Meteorology*, *142*(2–4), 216–233. https://doi.org/10.1016/j.agrformet.2006.08.021

Bolinder, M. A., Janzen, H. H., Gregorich, E. G., Angers, D. A., & VandenBygaart, A. J. (2007). An approach for estimating net primary productivity and annual carbon inputs to soil for common agricultural crops in Canada. *Agriculture, Ecosystems & Environment*, *118*(1), 29–42. https://doi.org/10.1016/j.agee.2006.05.013

Bonan, G. (2015). *Ecological climatology: Concepts and applications* (3rd ed.). Cambridge, UK: Cambridge University Press.

Börjesson, P. (2006). Livscykelanalys av Salixproduktion (Life cycle assessment of willow production) (Vol. 60). IMES/EESS report. Lund, Sweden: Department of Environmental and Energy Systems Studies, Lund University.

Boucher, O., & Reddy, M. S. (2008). Climate trade-off between black carbon and carbon dioxide emissions. *Energy Policy*, *36*(1), 193–200. https://doi.org/10.1016/j.enpol.2007.08.039

Bright, R. M., & O'Halloran, T. L. (2019). Developing a monthly radiative kernel for surface albedo change from satellite climatologies of Earth's shortwave radiation budget: CACK v1.0. *Geoscientific Model Development*, *12*(9), 3975–3990. https://doi.org/10.5194/gmd-12-3975-2019

Bright, R. M., Stromman, A. H., & Peters, G. P. (2011). Radiative forcing impacts of boreal forest biofuels: A scenario study for Norway in light of albedo. *Environmental Science & Technology*, *45*(17), 7570–7580. https://doi.org/10.1021/es201746b

Bright, R. M., Zhao, K. G., Jackson, R. B., & Cherubini, F. (2015). Quantifying surface albedo and other direct biogeophysical climate forcings of forestry activities. *Global Change Biology*, *21*(9), 3246–3266. https://doi.org/10.1111/gcb.12951

Burakowski, E., Tawfik, A., Ouimette, A., Lepine, L., Novick, K., Ollinger, S., … Bonan, G. (2018). The role of surface roughness, albedo, and Bowen ratio on ecosystem energy balance in the Eastern United States. *Agricultural and Forest Meteorology*, *249*, 367–376. https://doi.org/10.1016/j.agrformet.2017.11.030

Cai, H., Wang, J., Feng, Y., Wang, M., Qin, Z., & Dunn, J. B. (2016). Consideration of land use change-induced surface albedo effects in life-cycle analysis of biofuels. *Energy & Environmental Science*, *9*(9), 2855–2867. https://doi.org/10.1039/c6ee01728b

Cai, T., Price, D. T., Orchansky, A. L., & Thomas, B. R. (2011). Carbon, water, and energy exchanges of a hybrid poplar plantation during the first five years following planting. *Ecosystems*, *14*(4), 658–671. https://doi.org/10.1007/s10021-011-9436-8

Caiazzo, F., Malina, R., Staples, M. D., Wolfe, P. J., Yim, S. H. L., & Barrett, S. R. H. (2014). Quantifying the climate impacts of albedo changes due to biofuel production: A comparison with biogeochemical effects. *Environmental Research Letters*, *9*(2), 024015. https://doi.org/10.1088/1748-9326/9/2/024015

Caputo, J., Balogh, S. B., Volk, T. A., Johnson, L., Puettmann, M., Lippke, B., & Oneil, E. (2014). Incorporating uncertainty into a life

cycle assessment (LCA) model of short-rotation willow biomass (*Salix* spp.) crops. *BioEnergy Research*, 7(1), 48–59. https://doi.org/10.1007/s12155-013-9347-y

Carrer, D., Pique, G., Ferlicoq, M., Ceamanos, X., & Ceschia, E. (2018). What is the potential of cropland albedo management in the fight against global warming? A case study based on the use of cover crops. *Environmental Research Letters*, 13(4), 044030. https://doi.org/10.1088/1748-9326/aab650

Cherubini, F., Bird, N. D., Cowie, A., Jungmeier, G., Schlamadinger, B., & Woess-Gallasch, S. (2009). Energy- and greenhouse gas-based LCA of biofuel and bioenergy systems: Key issues, ranges and recommendations. *Resources Conservation and Recycling*, 53(8), 434–447. https://doi.org/10.1016/j.resconrec.2009.03.013

Cherubini, F., Bright, R. M., & Stromman, A. H. (2012). Site-specific global warming potentials of biogenic CO_2 for bioenergy: Contributions from carbon fluxes and albedo dynamics. *Environmental Research Letters*, 7(4). https://doi.org/10.1088/1748-9326/7/4/045902

Copernicus Climate Change Service (C3S). (2017). *ERA5: Fifth generation of ECMWF atmospheric reanalyses of the global climate*. Retrieved from https://cds.climate.copernicus.eu/

Creutzig, F., Ravindranath, N. H., Berndes, G., Bolwig, S., Bright, R., Cherubini, F., … Masera, O. (2015). Bioenergy and climate change mitigation: An assessment. *GCB Bioenergy*, 7(5), 916–944. https://doi.org/10.1111/gcbb.12205

Davin, E. L., & de Noblet-Ducoudré, N. (2010). Climatic impact of global-scale deforestation: Radiative versus nonradiative processes. *Journal of Climate*, 23(1), 97–112. https://doi.org/10.1175/2009JCLI3102.1

Davin, E. L., de Noblet-Ducoudré, N., & Friedlingstein, P. (2007). Impact of land cover change on surface climate: Relevance of the radiative forcing concept. *Geophysical Research Letters*, 34(13). https://doi.org/10.1029/2007gl029678

de Ruijter, F. J., & Huijsmans, J. F. M. (2012). *Ammonia emissions from crop residues*. Wageningen, The Netherlands: Plant Reserach International, Wageningen University and Reserach.

Devaraju, N., de Noblet-Ducoudré, N., Quesada, B., & Bala, G. (2018). Quantifying the relative importance of direct and indirect biophysical effects of deforestation on surface temperature and teleconnections. *Journal of Climate*, 31(10), 3811–3829. https://doi.org/10.1175/jcli-d-17-0563.1

Don, A., Osborne, B., Hastings, A., Skiba, U., Carter, M. S., Drewer, J., … Zenone, T. (2012). Land-use change to bioenergy production in Europe: Implications for the greenhouse gas balance and soil carbon. *GCB Bioenergy*, 4(4), 372–391. https://doi.org/10.1111/j.1757-1707.2011.01116.x

Elinder, M., Almquist, A., & Jirjis, R. (1995). *Kyllagring av salixflis ventilerad med kall uteluft (Cold air ventilated storage of Salix chips)*. SLF report 18. Stockholm, Sweden: Stiftelsen Lantbruksforskning.

Ericsson, N., Porsö, C., Ahlgren, S., Nordberg, A., Sundberg, C., & Hansson, P.-A. (2013). Time-dependent climate impact of a bioenergy system – Methodology development and application to Swedish conditions. *GCB Bioenergy*, 5(5), 580–590. https://doi.org/10.1111/gcbb.12031

Fuglestvedt, J. S., Shine, K. P., Berntsen, T., Cook, J., Lee, D. S., Stenke, A., … Waitz, I. A. (2010). Transport impacts on atmosphere and climate: Metrics. *Atmospheric Environment*, 44(37), 4648–4677. https://doi.org/10.1016/j.atmosenv.2009.04.044

Gelfand, I., Sahajpal, R., Zhang, X., Izaurralde, R. C., Gross, K. L., & Robertson, G. P. (2013). Sustainable bioenergy production from marginal lands in the US Midwest. *Nature*, 493(7433), 514–517. https://doi.org/10.1038/nature11811

Ghimire, B., Williams, C. A., Masek, J., Gao, F., Wang, Z., Schaaf, C., & He, T. (2014). Global albedo change and radiative cooling from anthropogenic land cover change, 1700 to 2005 based on MODIS, land use harmonization, radiative kernels, and reanalysis. *Geophysical Research Letters*, 41(24), 9087–9096. https://doi.org/10.1002/2014GL061671

Hammar, T., Ericsson, N., Sundberg, C., & Hansson, P.-A. (2014). Climate impact of willow grown for bioenergy in Sweden. *BioEnergy Research*, 7(4), 1529–1540. https://doi.org/10.1007/s12155-014-9490-0

Hammar, T., Hansson, P.-A., & Sundberg, C. (2017). Climate impact assessment of willow energy from a landscape perspective: A Swedish case study. *GCB Bioenergy*, 9(5), 973–985. https://doi.org/10.1111/gcbb.12399

Hansen, J., Sato, M., Ruedy, R., Nazarenko, L., Lacis, A., Schmidt, G. A., … Zhang, S. (2005). Efficacy of climate forcings. *Journal of Geophysical Research: Atmospheres*, 110(D18). https://doi.org/10.1029/2005JD005776

Heller, M. C., Keoleian, G. A., & Volk, T. A. (2003). Life cycle assessment of a willow bioenergy cropping system. *Biomass and Bioenergy*, 25(2), 147–165. https://doi.org/10.1016/S0961-9534(02)00190-3

Hellweg, S., & Milà i Canals, L. (2014). Emerging approaches, challenges and opportunities in life cycle assessment. *Science*, 344(6188), 1109–1113. https://doi.org/10.1126/science.1248361

Hillier, J., Whittaker, C., Dailey, G., Aylott, M., Casella, E., Richter, G. M., … Smith, P. (2009). Greenhouse gas emissions from four bioenergy crops in England and Wales: Integrating spatial estimates of yield and soil carbon balance in life cycle analyses. *Global Change Biology Bioenergy*, 1(4), 267–281. https://doi.org/10.1111/j.1757-1707.2009.01021.x

Hollinger, D. Y., Ollinger, S. V., Richardson, A. D., Meyers, T. P., Dail, D. B., Martin, M. E., … Verma, S. B. (2010). Albedo estimates for land surface models and support for a new paradigm based on foliage nitrogen concentration. *Global Change Biology*, 16(2), 696–710. https://doi.org/10.1111/j.1365-2486.2009.02028.x

Hollsten, R., Arkelöv, O., & Ingelman, G. (2013). *Handbok för salixodlare (Manual for willow farmers)* (2nd ed.). Jönköping, Sweden: Swedish Board of Agriculture.

IPCC. (2019). *2019 Refinement to the 2006 IPCC Guidelines for National Greenhouse Gas Inventories*. Hayama, Japan: IGES.

Jones, A. D., Calvin, K. V., Collins, W. D., & Edmonds, J. (2015). Accounting for radiative forcing from albedo change in future global land-use scenarios. *Climatic Change*, 131(4), 691–703. https://doi.org/10.1007/s10584-015-1411-5

Jones, A. D., Collins, W. D., & Torn, M. S. (2013). On the additivity of radiative forcing between land use change and greenhouse gases. *Geophysical Research Letters*, 40(15), 4036–4041. https://doi.org/10.1002/grl.50754

Joos, F., Roth, R., Fuglestvedt, J. S., Peters, G. P., Enting, I. G., von Bloh, W., … Weaver, A. J. (2013). Carbon dioxide and climate impulse response functions for the computation of greenhouse gas metrics: A multi-model analysis. *Atmospheric Chemistry and Physics*, 13(5), 2793–2825. https://doi.org/10.5194/acp-13-2793-2013

Jørgensen, S. V., Cherubini, F., & Michelsen, O. (2014). Biogenic CO_2 fluxes, changes in surface albedo and biodiversity impacts from establishment of a miscanthus plantation. *Journal of Environmental Management*, 146, 346–354. https://doi.org/10.1016/j.jenvman.2014.06.033

Kätterer, T., Bolinder, M. A., Andrén, O., Kirchmann, H., & Menichetti, L. (2011). Roots contribute more to refractory soil organic matter than above-ground crop residues, as revealed by a long-term field experiment. *Agriculture, Ecosystems & Environment*, *141*(1), 184–192. https://doi.org/10.1016/j.agee.2011.02.029

Laguë, M. M., Bonan, G. B., & Swann, A. L. S. (2019). Separating the impact of individual land surface properties on the terrestrial surface energy budget in both the coupled and uncoupled land-atmosphere system. *Journal of Climate*, *32*(18), 5725–5744. https://doi.org/10.1175/jcli-d-18-0812.1

Levasseur, A., Cavalett, O., Fuglestvedt, J. S., Gasser, T., Johansson, D. J. A., Jørgensen, S. V., … Cherubini, F. (2016). Enhancing life cycle impact assessment from climate science: Review of recent findings and recommendations for application to LCA. *Ecological Indicators*, *71*, 163–174. https://doi.org/10.1016/j.ecolind.2016.06.049

Levasseur, A., Lesage, P., Margni, M., & Samson, R. (2013). Biogenic carbon and temporary storage addressed with dynamic life cycle assessment. *Journal of Industrial Ecology*, *17*(1), 117–128. https://doi.org/10.1111/j.1530-9290.2012.00503.x

Levy, C. R., Burakowski, E., & Richardson, A. D. (2018). Novel measurements of fine-scale albedo: Using a commercial quadcopter to measure radiation fluxes. *Remote Sensing*, *10*(8), 1303. https://doi.org/10.3390/rs10081303

Meyer, S., Bright, R. M., Fischer, D., Schulz, H., & Glaser, B. (2012). Albedo impact on the suitability of biochar systems to mitigate global warming. *Environmental Science & Technology*, *46*(22), 12726–12734. https://doi.org/10.1021/es302302g

Muñoz, I., Campra, P., & Fernández-Alba, A. R. (2010). Including CO_2-emission equivalence of changes in land surface albedo in life cycle assessment. Methodology and case study on greenhouse agriculture. *The International Journal of Life Cycle Assessment*, *15*(7), 672–681. https://doi.org/10.1007/s11367-010-0202-5

Myhre, G., Shindell, D., Bréon, F.-M., Collins, W., Fuglestvedt, J., Huang, J., … Zhang, H. (2013). Anthropogenic and natural radiative forcing supplementary material. In T. F. Stocker, D. Qin, G.-K. Plattner, M. Tignor, S. K. Allen, J. Boschung, A. Nauels, Y. Xia, V. Bex, & P. M. Midgley (Eds.), *Climate change 2013: The physical science basis. Contribution of working group I to the fifth assessment report of the Intergovernmental Panel on Climate Change* (pp. 659–740). Cambridge and New York, NY: Cambridge University Press.

Peters, G. P., Aamaas, B., Lund, M. T., Solli, C., & Fuglestvedt, J. S. (2011). Alternative "global warming" metrics in life cycle assessment: A case study with existing transportation data. *Environmental Science & Technology*, *45*(20), 8633–8641. https://doi.org/10.1021/es200627s

Pielke, R. A., Avissar, R. I., Raupach, M., Dolman, A. J., Zeng, X., & Denning, A. S. (1998). Interactions between the atmosphere and terrestrial ecosystems: Influence on weather and climate. *Global Change Biology*, *4*(5), 461–475. https://doi.org/10.1046/j.1365-2486.1998.t01-1-00176.x

Pielke, R. A., Marland, G., Betts, R. A., Chase, T. N., Eastman, J. L., Niles, J. O., … Running, S. W. (2002). The influence of land-use change and landscape dynamics on the climate system: Relevance to climate-change policy beyond the radiative effect of greenhouse gases. *Philosophical Transactions of the Royal Society of London. Series A: Mathematical, Physical and Engineering Sciences*, *360*(1797), 1705–1719. https://doi.org/10.1098/rsta.2002.1027

Pourhashem, G., Adler, P. R., & Spatari, S. (2016). Time effects of climate change mitigation strategies for second generation biofuels and co-products with temporary carbon storage. *Journal of Cleaner Production*, *112*, 2642–2653. https://doi.org/10.1016/j.jclepro.2015.09.135

Prather, M. J. (2007). Lifetimes and time scales in atmospheric chemistry. *Philosophical Transactions of the Royal Society A: Mathematical, Physical and Engineering Sciences*, *365*(1856), 1705–1726. https://doi.org/10.1098/rsta.2007.2040

Rytter, R.-M. (2001). Biomass production and allocation, including fine-root turnover, and annual N uptake in lysimeter-grown basket willows. *Forest Ecology and Management*, *140*(2), 177–192. https://doi.org/10.1016/S0378-1127(00)00319-4

Schaeffer, M., Eickhout, B., Hoogwijk, M., Strengers, B., Vuuren, D. V., Leemans, R., & Opsteegh, T. (2006). CO_2 and albedo climate impacts of extratropical carbon and biomass plantations. *Global Biogeochemical Cycles*, *20*(2). https://doi.org/10.1029/2005GB002581

Schwaiger, H. P., & Bird, D. N. (2010). Integration of albedo effects caused by land use change into the climate balance: Should we still account in greenhouse gas units? *Forest Ecology and Management*, *260*(3), 278–286. https://doi.org/10.1016/j.foreco.2009.12.002

Searchinger, T., Heimlich, R., Houghton, R. A., Dong, F. X., Elobeid, A., Fabiosa, J., … Yu, T. H. (2008). Use of US croplands for biofuels increases greenhouse gases through emissions from land-use change. *Science*, *319*(5867), 1238–1240. https://doi.org/10.1126/science.1151861

Sieber, P., Ericsson, N., & Hansson, P.-A. (2019). Climate impact of surface albedo change in life cycle assessment: Implications of site and time dependence. *Environmental Impact Assessment Review*, *77*, 191–200. https://doi.org/10.1016/j.eiar.2019.04.003

Smith, P. (2016). Soil carbon sequestration and biochar as negative emission technologies. *Global Change Biology*, *22*(3), 1315–1324. https://doi.org/10.1111/gcb.13178

Soden, B. J., Held, I. M., Colman, R., Shell, K. M., Kiehl, J. T., & Shields, C. A. (2008). Quantifying climate feedbacks using radiative kernels. *Journal of Climate*, *21*(14), 3504–3520. https://doi.org/10.1175/2007jcli2110.1

Statistics Sweden. (2017). *Set-aside (Fallow) 2016 divided by short and long term set-aside*. Retrieved from https://www.scb.se/en/finding-statistics/statistics-by-subject-area/environment/fertilisers-and-lime/use-of-fertilisers-and-animal-manure-and-cultivation-measures-in-agriculture/pong/tables-and-graphs/cultivation-measures/set-aside-fallow-2016-divided-by-short-and-long-term-set-aside/

Stephens, G. L., O'Brien, D., Webster, P. J., Pilewski, P., Kato, S., & Li, J. L. (2015). The albedo of Earth. *Reviews of Geophysics*, *53*(1), 141–163. https://doi.org/10.1002/2014rg000449

Swedish Board of Agriculture. (2019). *Use of agricultural land*. Retrieved from http://www.scb.se/jo0104-en

Tanaka, K., Peters, G. P., & Fuglestvedt, J. S. (2010). Multicomponent climate policy: Why do emission metrics matter? *Carbon Management*, *1*(2), 191–197. https://doi.org/10.4155/cmt.10.28

Tilman, D., Hill, J., & Lehman, C. (2006). Carbon-negative biofuels from low-input high-diversity grassland biomass. *Science*, *314*(5805), 1598–1600. https://doi.org/10.1126/science.1133306

Whitaker, J., Field, J. L., Bernacchi, C. J., Cerri, C. E. P., Ceulemans, R., Davies, C. A., … McNamara, N. P. (2018). Consensus, uncertainties and challenges for perennial bioenergy crops and land use. *GCB Bioenergy*, *10*(3), 150–164. https://doi.org/10.1111/gcbb.12488

Winton, M. (2005). Simple optical models for diagnosing surface-atmosphere shortwave interactions. *Journal of Climate*, *18*(18), 3796–3805. https://doi.org/10.1175/jcli3502.1

Zhao, K., & Jackson, R. B. (2014). Biophysical forcings of land-use changes from potential forestry activities in North America. *Ecological Monographs*, *84*(2), 329–353. https://doi.org/10.1890/12-1705.1

SUPPORTING INFORMATION

Additional supporting information may be found online in the Supporting Information section.

Acta Universitatis Agriculturae Sueciae

Doctoral Thesis No. 2021:87

Agricultural land use affects the climate by changing land surface albedo (reflectivity). This thesis examines the effect of individual crops and cultivation practices on albedo under Swedish conditions and the importance of albedo change for the climate impact of agricultural systems. The time-dependent life cycle assessment performed on crop and bioenergy production provides new insights on the magnitude and timing of impacts from albedo change compared with those from life-cycle greenhouse gas emissions.

Petra Sieber received her postgraduate education at the Department of Energy and Technology, SLU, Uppsala, Sweden. She holds a Master of Science in Environment and Bio-Resources Management from the University of Natural Resources and Life Sciences, Vienna, Austria.

Acta Universitatis Agriculturae Sueciae presents doctoral theses from the Swedish University of Agricultural Sciences (SLU).

SLU generates knowledge for the sustainable use of biological natural resources. Research, education, extension, as well as environmental monitoring and assessment are used to achieve this goal.